URANIUM LUMINESCENCE

A thesis presented for the

degree of DOCTOR OF PHILOSOPHY in PHYSICS

in the University of Canterbury

Christchurch, New Zealand.

by

J.V. NICHOLAS

JUNE, 1966.

CONTENTS

CHAPTER I

INTRODUCTION

Luminescence of uranium compounds has been mostly due to the divalent uranyl ion UO_2^{++}. This ion, chemically, is very stable and takes part in chemical reactions in the same way as a normal metal ion. This stability of a metal oxide ion is one of the characteristic features of the chemistry of the actinide elements. Spectra of many salts of the uranyl ion have been investigated, e.g. for uranyl nitrates, sulphates, acetates etc. Though much has been found about the spectra, there is much left unexplained and will require considerable effort for a full interpretation.

When dissolved in some acidic (but not basic) glasses, the uranyl ion still gives an absorption and luminescent spectrum which is considered that of the uranyl ion isolated from a crystal lattice. Dissolving uranyl ions or uranium oxide in molten salts of the alkali and akaline earth metals (e.g. NaCl, KBr, Sr SO_4, phosphates) will also produce phosphors with absorption and luminescent spectra similar to that of the uranyl ion. However, many fluorides show sufficiently different spectra to suggest that it is due to a new luminescent centre formed around an uranium atom. Further investigation has shown that the spectra are not over-much different from that of the uranyl ion when account is taken of the surroundings of the ion in the crystal lattice. More work is required to determine what the nature of the centre is.

To further the work on uranium as an activator of luminescence this thesis was undertaken on uranium in fluorite type lattices and especially that of calcium fluorides. (this is a continuation of some work done on several different fluoride crystals by the author in his M.Sc thesis, University of Canterbury 1963).

Interpretation of the spectral results can give some clarification of the two main points of interest for the uranium centres:-

1. The nature of the electronic structure.

This is complicated by the presence of a strong uranium-oxygen bond for which no adequate theory has been given. Spectral data can give information on the symmetry of the centres from selection rules with the vibronic side bands and polarization experiments. Symmetry of the luminescent centre can be important in deciding bonding arrangements of the uranium with surrounding oxygens.

2. Interactions with vibrations.

From the temperature dependence of the vibronic spectra, it should be possible to determine how the vibrational modes of the host lattice and those of the centre itself interact with the electronic transition. Alternatively, from the vibronic spectra, it may be possible to infer information about the vibrational modes of the lattice, depending on which is more unknown. Here the uranium luminescent centre system seems quite promising in determining information about the lattice dynamics of many crystal structures which give rise to, with uranium, luminescent and absorption spectra containing a wealth of vibrational data (see author's M.Sc. thesis for examples).

This thesis has been mainly concerned with the vibrational interaction which has been looked at in light of current theories on electron-phonon interactions and it has been possible to show that the vibronic spectra is closely related to the vibrational spectra in the case of calcium fluoride.

URANYL SPECTRA

Since the spectra of uranium in fluoride crystals has similar characteristics to that of the uranyl ion

an outline is given below of aspects of the uranyl ion and spectra that appear relevant. Fuller information can be obtained from the following references:-

E. Rabinowitch and R.L. Belford "Spectroscopy and Photochemistry of Uranyl Compounds" - Pergamon 1964.

G.H. Dieke and A.B.F. Duncan "Spectroscopic Properties of Uranium Compounds" - McGraw Hill 1949.

G.T. Seaborg and J.J. Katz "The chemistry of Actinide Elements" Methuen 1957.

STRUCTURE OF URANYL CRYSTALS: All structure data indicate that the uranyl ion ($O - U - O^{++}$) is linear and that there is no bend in it. In solution, a bent structure has been postulated to explain some phenomena but there is an alternative explanation using a linear ion. Therefore the uranyl ion is considered linear as there is no real evidence to suggest that it is not.

Bond lengths for the U - O bond in uranyl salts vary. In the orthourarates $(UO_2)O_2C_a$, $(UO_2)O_2Sr$, it is 1.91Å with the secondary oxygen atoms at 2.3Å from the uranium atom all lying in approximately the equatorial plane of the uranyl ion (three oxygens above, and three below, as shown in Fig. 1.1).

The tendency for the uranyl ion to have ions (usually O^2 or F^- ions) surrounding it in the equatorial plane is quite general. In $K_3UO_2F_5$ crystals the $UO_2F_5^{3-}$ group is a pentagonal bipyramid (i.e. fluorines are symmetrically placed in the equatorial plane) with the U - O distance 1.76A°, and the U - F distance 2.24A°. Nitrates and carbonates such as $RbUO_2(NO_3)_3$ and UO_2CO_3 have a planar arrangement of six NO_3^- or CO_3'' oxygens in the equatorial plane. Fig. 1.2 shows this for UO_2CO_3 where U - O is 1.67A° with the secondary U - O distances 2.5A°.

The co-ordination number of uranium besides that due to the two uranyl oxygens can vary from four to six and perhaps even up to eight, and for a given co-ordination number, the ligard arrangement is not fixed. (Compare

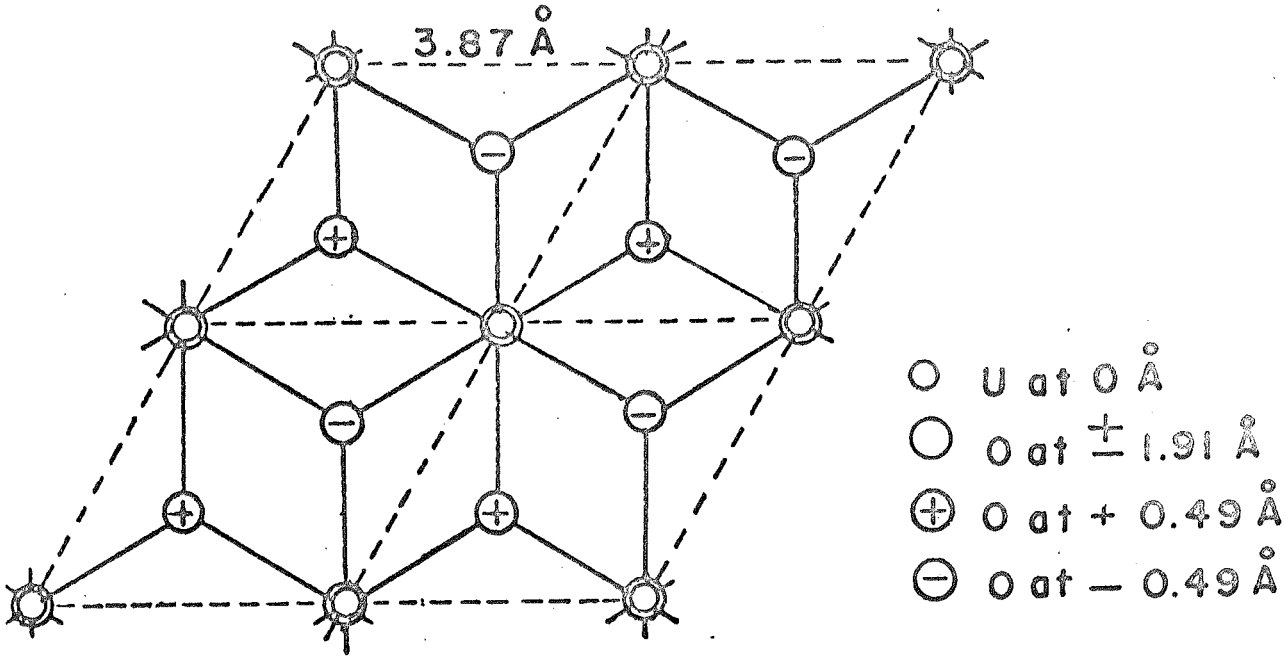

Figure 1.1 Crystal Structure of Calcium Uranate

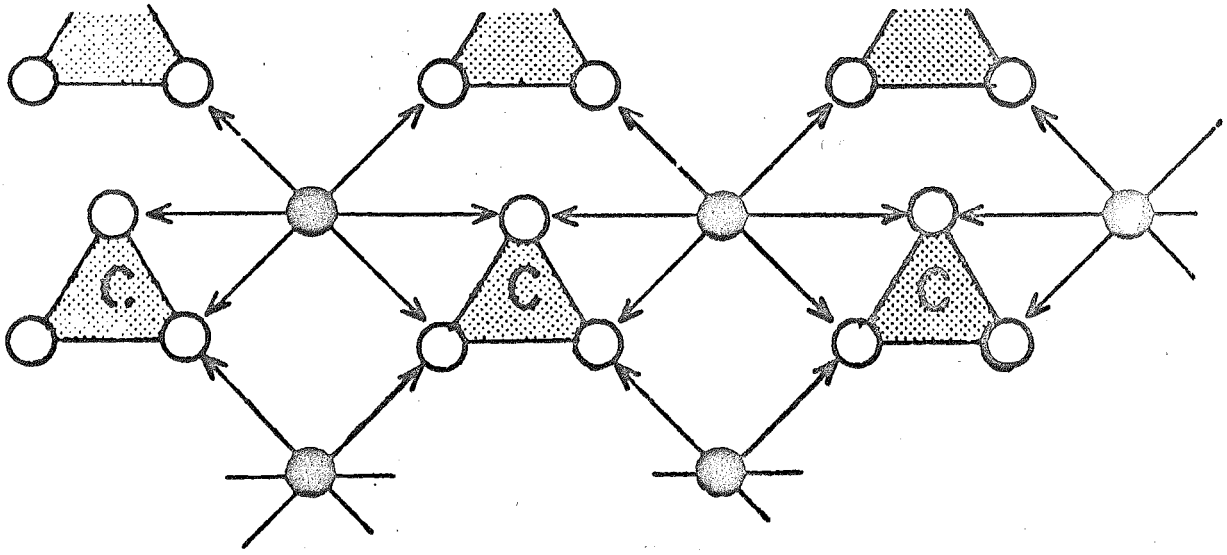

Figure 1.2 Crystal Structure of Uranyl Carbonate

black circle - uranyl ions
shaded triangle with white circles - carbonate ions

Figs 1.1 and 1.2). This, together with the relative constancy of the geometry of the uranyl group itself, suggests that strong directed valence bonds join the uranyl atoms but that electrostatic forces and packing conditions play the important roles in secondary uranium ligand bonds, though, of course, some directed covalency may occur.

URANYL CRYSTAL SPECTRA. At room temperature the luminescent spectra of uranyl compounds consists of several bands approximately equally spaced (in terms of energy) spreading from about the blue-green to the red region of the visible spectrum. The absorption spectra can be considered as consisting of three parts (see Fig. 1.3) one of which is an approximate mirror image of the luminescent spectra.

On cooling to 77°K, most of the spectra are groups of lines with quite definite energy differences between lines. Most of the lines are vibronic. (i.e. due to an electronic and a vibrational transition). Many of these lines can be interpreted as arising from vibrations of the uranyl group itself and also some of its neighbouring ligands (i.e. NO_3^- group vibrations occur and have been identified by isotope shift experiments).

A linear group such as $O\text{-}U\text{-}O^{++}$ has three fundamental vibrations:-

ν_s A symmetric bond vibration which is Raman active

$O \rightarrow U \leftarrow O$ or $\overleftarrow{O} - U - \overrightarrow{O}$

ν_a An antisymmetric bond vibration which is infra red active.

$O \rightarrow U \rightarrow O$ or $\overrightarrow{O} - \overleftarrow{U} - \overrightarrow{O}$

ν_b A bending vibration which is infra red active.

$O \searrow - U - \swarrow O$ or $\overset{\uparrow}{O} - \underset{\downarrow}{U} - \overset{\uparrow}{O}$

This is doubly degenerate (since it can occur in

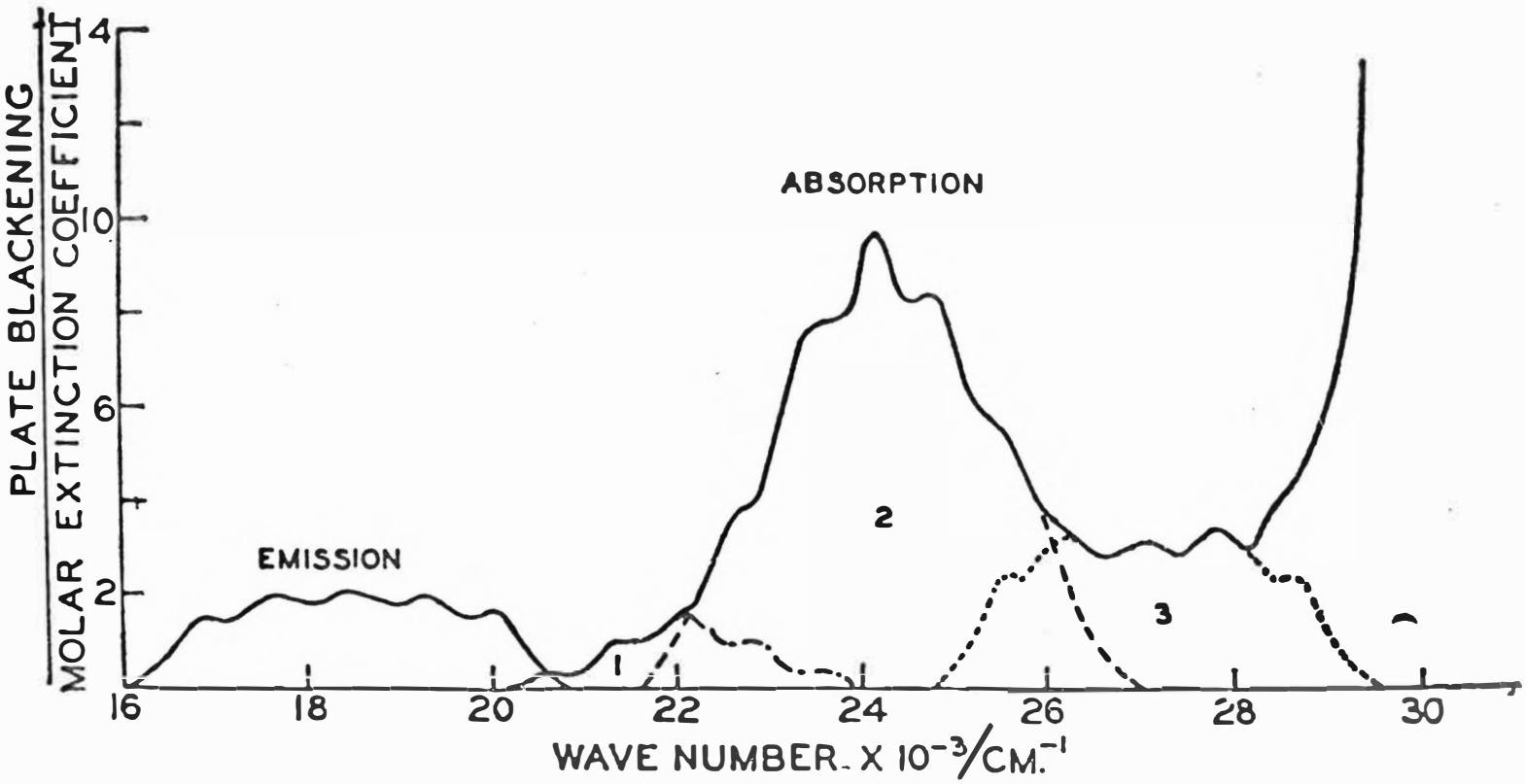

Figure 1.3 Spectra of uranyl nitrate, showing different regions. Region 1 is an approximate mirror image of the emission spectra.

two mutually perpendicular planes) and should split into two components when the ion is in an external field of force.

It is possible to determine these frequencies from infra red absorption and Raman work for different uranyl crystals. Fig. 1.4 gives the measured frequencies collected from Raman and infra red studies for three uranyl compounds and compares them with values from their luminescent spectra.

Figure 1.4*

	$UO_2(NO_3)_2$		Na UO_2(Acetate)$_3$		Rb $UO_2(NO_3)_3$	
	Infra red & Raman cm^{-1}	Luminescent cm^{-1}	Infra red & Raman cm^{-1}	Luminescent cm^{-1}	Infra red & Raman cm^{-1}	Luminescent cm^{-1}
ν_s	865	874	856	855	883	888
ν_a	941	948	931	927	960	962
ν_b	210	220(?)			213	

(* some values could not be measured directly and have been inferred from overtones)

Because the uranyl ion has an external field on it (due to the crystal) rigid selection rules are not followed and it is possible to obtain the Raman active vibration ν_s weakly in infra-red spectra, and conversely for ν_a All three vibrations are permitted in combination with an electronic transition and they do occur. The ν_b value is normally hard to assign since it is generally split.

If the three vibrations are assumed to be harmonic with the elastic force constants f (in the direction of

the U - O bond) and d (in the direction perpendicular to this bond), their frequencies can be given by:-

$$\nu_s = \sqrt{\frac{f}{M_o}}$$

$$\nu_a = \nu_s \sqrt{1 + \frac{2M_o}{M_u}}$$

$$\nu_b = \nu_a \sqrt{\frac{2d}{f}}$$

where M_o = mass of an atom of oxygen
and M_u = mass of an atom of uranium

In the electronic spectra, several quanta of can occur giving the repetitive band or line structure common to all uranyl luminescence. Other vibrations occur with only one quanta or coupled to several quanta of ν_s. It is possible to represent the low temperature luminescent spectra of the uranyl ion by the equation:-

$$\nu_{fl} = \nu_F - n_s\nu_s - n_a\nu_a - n_b\nu_b - \sum_i n_i\nu_i$$

where ν_F is the pure electronic transition (resonance transition since it also occurs in absorption, i.e. $X_o \rightleftharpoons F_o$ in Fig. 1.5).

n_s = 0 to 8 i.e. number of quanta of ν_s

Similarly for n_a & n_b = 0 or 1.

$\sum_i n_i\nu_i$ refers to the vibrations of associated ligands or crystal as a whole.

Identification of these vibrations has been made by known infra red and Raman spectra of the ligands and also by isotope substitution.

Figure 1.5 Typical energy levels and transitions for the uranyl ion. M is a second electronic level.

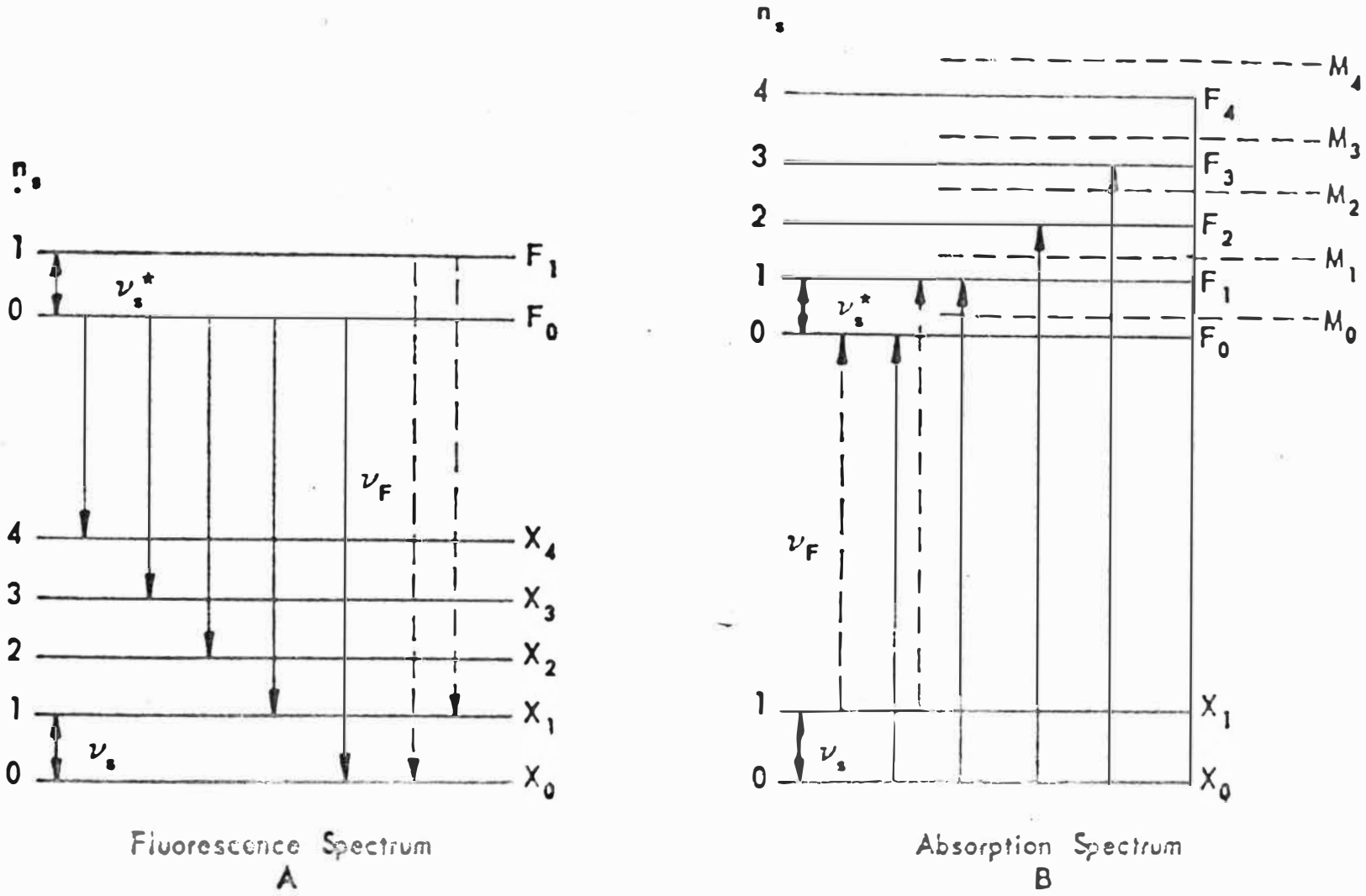

Generally as n_s increases the values of ν_s, ν_a and ν_b change slightly due to unharmonic effects.

Above zero temperature there is a chance that lines on the high energy side of ν_E can occur (anti-Stokes' lines, i.e. emission lines occuring at higher energy than the exciting absorption line) due to the thermal excitation to a higher vibrational state (e.g. $X_0 \rightarrow F_1$ in Fig. 1.5).

In absorption the frequencies ν_s , ν_a , ν_b are changed to ν_s^* , ν_a^* , ν_b^* and are found to be smaller. (Typically $\nu_s \sim 880 cm^{-1}$ and $\nu_s^* \sim 700 cm^{-1}$). The low temperature absorption spectrum can be represented by the equation:-

$$\nu_{abs} = \nu_E + n_s \nu_s^* + n_a \nu_a^* + n_b \nu_b^* + \sum_i n_i \nu_i$$

where $\nu_E = \nu_E$ or may be some higher electronic term of the uranyl ion. (There appears to be at least two others though identification is uncertain).

$$n_s = 0 \text{ to } 8$$

$$n_a, n_b = 0, 1 \text{ or } 2.$$

Fig. 1.5 shows the energy level scheme with a second electronic level M which is considered "magnetic" since it shows Zeeman splitting. At higher temperatures absorption lines on the low energy side of ν_E are possible due to the thermal excitation of vibrational energy on the ground state.

In Fig. 1.5 sublevels are not shown for ν_a , ν_b or ν_i , but they will also occur, and it is to be noted that since $\nu_a > \nu_s$ that there will be overlapping of the band groups.

It is possible to get up to four band groups of luminescence and absorption overlapping due to anti-

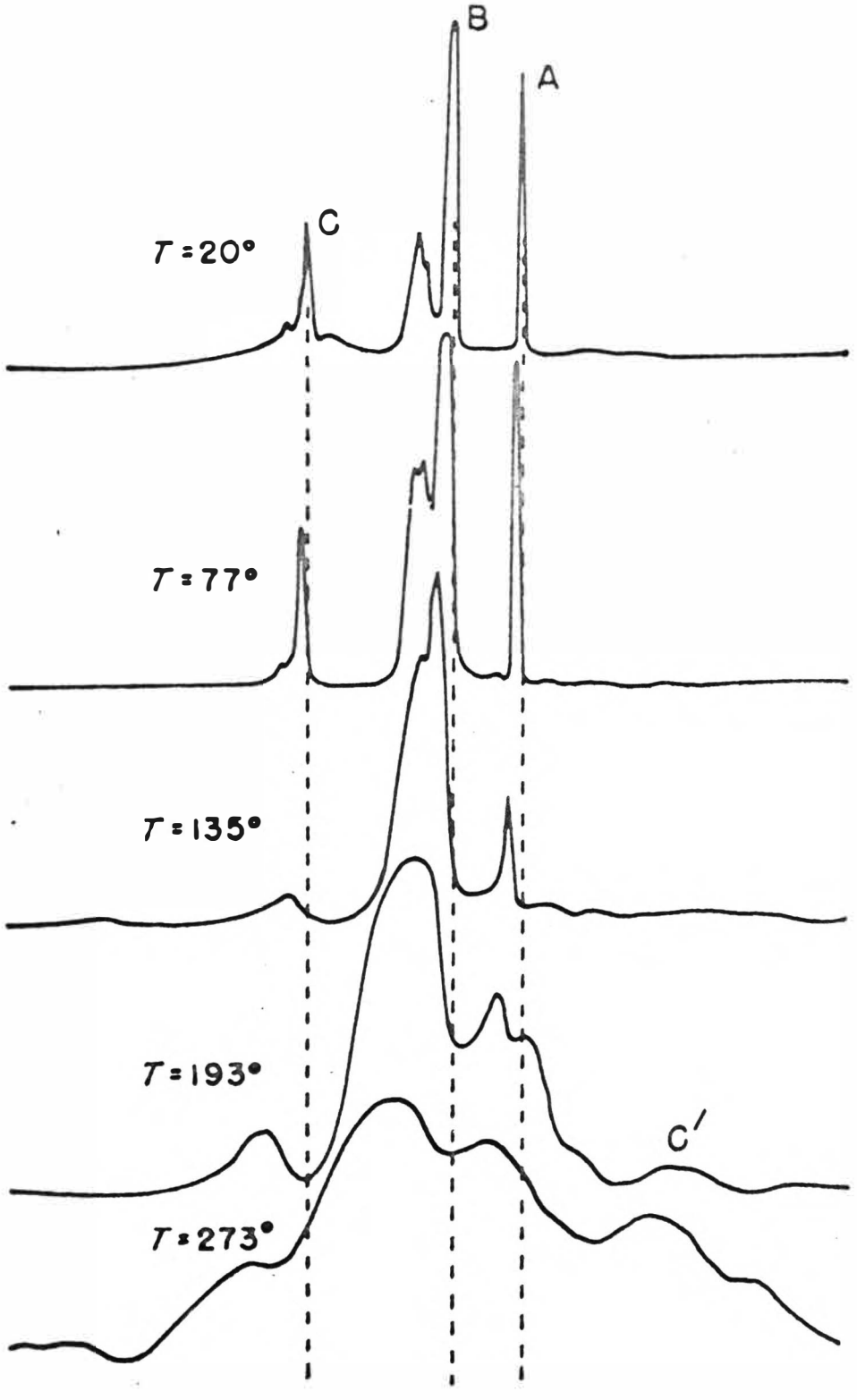

Figure 1.6 Temperature dependence of the third group in the luminescence spectra of uranyl chloride.

Stokes vibrations. These do not appear to be due to the upper level M which could give rise to apparent anti-Stokes' lines. All the luminescence is assumed to come from only one electronic transition though there have been suggestions (which remain to be properly tested) that there is a second electronic level separated from X_o or F_o by 50 cm^{-1} to 250 cm^{-1} that gives some of the luminescent lines.

TEMPERATURE EFFECTS: Little experimental work has been done on this. The main observations have been taken at readily available temperatures such as 4.2°K, 20°K, 77°K, 193°K and room temperature. The spectra at room temperature show broad bands and these sharpen up as the temperature decreases to give lines at 77°K. Further cooling to 4.2°K causes the lines to become even sharper, often splitting into two components (see Fig. 1.6)

POLARIZATION: In properly orientated single crystals of uranyl double chlorides or nitrates it is found that the absorption spectra are different for light beams polarized in two mutually perpendicular planes. When the transmitted light is polarized parallel to the optical axis, little absorption occurs and the crystals appear whitish ("white" spectrum). Blue light polarized normally to the optical axis is absorbed much more strongly than blue light polarized parallel to the axis and in the so-polarized beam the crystals appear yellow ("yellow" spectrum). Also the luminescent spectra show a similar polarization effect.

The differences in the yellow and white spectra has been taken to indicate a further multiplicity of excited electronic states than those normally considered. However, since these effects occur only in low symmetry crystals (triclinic), whose detailed structures are not known, they could be accounted for on the basis of different local environments of the uranyl ion. Further work is required to clarify the origin of the polarization effects.

LIFETIMES: At room temperature the decay time of the uranyl luminescence is of the order of 3×10^{-4} sec. which lengthens to about 30×10^{-4} sec. at $4.2^{\circ}K$. The decay is exponential. This suggests, as is expected, that the luminescence is a transition from an excited upper state to a ground state with no metastable levels involved. (This would prolong the decay time and also give a non-exponential decay).

Vibrations would help towards non-radiative transitions and as the temperature increases the increase in vibrational levels will aid non-radiative transitions to these and hence the decay time is faster.

This time of the order of a milli second is typical of a magnetic dipole transition or a "forced" electric dipole transition (i.e. a forbidden electric dipole transition made allowed by vibrational interactions). Some work has suggested a quadrapole transition, but this is in doubt. Rare earth luminescent decay times are of the same order of magnitude and these are magnetic dipole or forced electric dipole transitions.

Some uranyl compounds show two luminescent decay times, and further work is required, especially in measuring decay times of individual lines or bands in the uranyl spectra. Any different electronic levels contributing to the luminescence would be expected to have different decay times.

VARIATIONS: The spectra of the uranyl ion can show many variations even for the same compound depending on impurities or degree of hydration of the crystal. This has often caused conflicting results and conclusions by different workers on the subject.

ACTINYL COMPOUNDS: The other actindes form an almost identical group to the uranyl ion, e.g. NpO_2^{++}, PuO_2^{++}, and AmO_2^{++}. These are also linear ions and form similar compounds, but they are non-luminescent and have their own absorption spectra. Their vibrational frequencies are

similar to that of the uranyl ion. Fig. 1.7 gives the values for the sodium actinyl acetate.

Figure 1.7

Actinyl ion	UO_2^{++}	NpO_2^{++}	PuO_2^{++}	AmO_2^{++}
ν_s in cm^{-1}	856	844	818	749
ν_u in cm^{-1}	931	934	930	914

These other actinyl groups are helpful in deciding the electronic structure of the uranyl group. The UO_2^{++} plays a similar role in relation to the actinyl ions as La^{3+} does to the other trivalent rare earth ions, in that there is no ground state paramagnetism.

ELECTRONIC STRUCTURE: While the electronic structure is not known fully, an outline is given of some recent work since it could have relevance to the uranium activated luminescence. References besides the book by Rabinowitch and Belford are:-

J.B. Newman, The Johns Hopkins University Caryle Barton Laboratory, Technical Report No. WR-AF-4, April 1964.

J.B. Newman, J. Chem. Phys. 43 1691 (1965)

From all the chemical evidence the actinyl ions are strongly covalent. To account for this a molecular orbital (MO) theory of the electronic structure is required. In the molecular orbital theory linear combinations of atomic orbitals (LCAO) are written to form the MO basis set, even for those that remain substantially unchanged on an atomic core when these cores are bound together to form molecules. The self-consistent field (SCF) solution is determined by varying the co-

efficients of the atomic orbitals (AO) in all the MO's. For the large number of electron (106) involved in the uranyl ion a rather lengthy calculation is needed. However, it is possible to consider the atoms as an electronic core surrounded by valence electrons which only take part in the bonding. For the uranyl ion the AO's required are the 5f, 6d, 7s, 7p from the uranium and the 2s, 2p from the oxygen. This leaves the cores $K^2\ L^8\ M^{18}\ N^{32}\ 5s^2\ 5p^6\ 5d^{10}\ 6s^2\ 6p^6$ for the uranium (U^{6+}) and K^2 for the oxygen.

Under the symmetry group $D_{\infty h}$ (∞/mm) for the free uranyl ion only those AO's with the same representation will combine to form MO's. Fig. 1.8 lists these with their representation labels. In the coordinate system used, the molecular axis is taken to coincide with the z axis of the (x, y, z) coordinate system. The uranium nucleus is located at z = o and the two oxygens nuclei for ground state equilibrium at $z = \pm R_o$. Primed and double primed z - coordinates are used to distinguish the two oxygen nuclei. The z and z' systems are parallel to each other and antiparallel to z".

Figure 1.8

Uranium Orbitals and Oxygen Group Orbitals in $D_{\infty h}$

Atomic Orbitals	Oxygen Group Orbitals	Representation in $D_{\infty h}$
p_z, f_{z^3} (f_o)	$\frac{1}{\sqrt{2}}(p_z' - p_z'')$, $\frac{1}{\sqrt{2}}(s' - s'')$	σ_u^+ (a_{2u})
s, d_{z^2} (d_o)	$\frac{1}{\sqrt{2}}(p_z' + p_z'')$, $\frac{1}{\sqrt{2}}(s' + s'')$	σ_g^+ (a_{1g})
p_x, f_{xz^2} p_y, f_{yz^2} $\}(p_{\pm1}, f_{\pm1})$	$\frac{1}{\sqrt{2}}(p_x' + p_x'')$ $\frac{1}{\sqrt{2}}(p_y' + p_y'')$	π_u (e_{1u})
d_{xz} d_{yz} $\}(d_{\pm1})$	$\frac{1}{\sqrt{2}}(p_x' - p_x'')$ $\frac{1}{\sqrt{2}}(p_y' - p_y'')$	π_g (e_{1g})
$f_{z(x^2-y^2)}$ f_{xyz} $\}(f_{\pm2})$		δ_u (e_{2u})
$d_{x^2-y^2}$ d_{xy} $\}(d_{\pm2})$		δ_g (e_{2g})
$f_{x(x^2-y^2)}$ $f_{y(x^2-y^2)}$ $\}f_{\pm3}$		ϕ_u (e_{3u})

From the AO's in Fig. 1.8 a MO set can be formed to give a possible ground state configuration for the uranyl ion. One way of doing this (at present the only quantitative way) is to consider overlap integrals to calculate bonding strengths. Newman has considered these for different radial functions for uranium and his results are given in Fig. 1.9 with a comparison.

Figure 1.9
URANYL OVERLAPS

Wave functions	U-O distance	σf	πf	σd	πd
Hartree-Fock-Slater	1.67Å	0.054	0.051	0.188	0.229
	1.92Å	0.038	0.029	0.185	0.157
Belford & Belford	1.67Å	0.066	0.075	0.175	1.269
	1.92Å	0.052	0.047	0.192	0.192
Hartree relativistic	1.67Å	0.081	0.133	0.132	0.315
	1.92Å	0.075	0.090	0.141	0.305

These considerations suggest the configuration $(\pi_g)^4 (\sigma_g^+)^2 (\pi_u)^4 (\sigma_u^+)^2$ as the most likely ground state of the free uranyl ion. There are two main features of this configuration which was not expected from earlier work:-

1. The strength of the π bonds. These were assumed to be weak but are in fact stronger than σ bonds.
2. The weakness of f orbital bonds. Nearly all bonding can be ascribed to d orbitals with little or no f electron contribution. It had been assumed that f orbital bonding was strong to explain the paramagnetic susceptibility. However, it is possible to explain it on mostly d - orbital contributions.

The above MO solution only gives consideration to a free uranyl ion. There are two other factors influencing the ion and its electronic state:-

1. The vibrational interaction of the uranyl ion with its electronic levels.
2. The interaction of the uranyl ion with surrounding ligands.

The uranyl ion never appears free but always co-ordinated with other ligands which for most cases reduces the symmetry from $D_{\infty h}$ to D_{3h} ($\bar{6}m2$)

To account for the effect of ligands using a MO theory becomes impossible due to the large number of nuclei and electrons involved. A simpler theoretical model is required and Newman has considered applying that of the Ligand Field Theory. He gives two lines of attack which seem promising and capable of quantitative investigations. These are given below to show how the problem can be handled, as an analogous situation could be set up for the uranium activated luminescence.

The first assumes that the excitation of the luminescent level takes place by electron transfer from some oxygen orbital (AO or group symmetry orbital) to an empty 5f orbital (or one of the $D_{\infty h}$ orbital base functions, presumably a component of a 5f uranium orbital). This gives a formal charge distribution ($O^{-\frac{1}{2}}$ U^{3+} $O^{-\frac{1}{2}}$). From chemical evidence the formal charge on the uranium atom is known to be between $+3$ and $+6$ and on each uranyl oxygen, between $-\frac{1}{2}$ and $+2$.

The second model is based on the formal charge distribution (O^- U^{4+} O^-) and has 5f orbitals occupied in the ground state. The spectra can therefore be discussed on the basis of an U^{4+} ion in a f^2 configuration, in the field of the two collinear O^- ions. An intermediate - to - strong field model appears to be required for this f^2 configuration in the uranyl ion.

CONCLUSION: As yet there is no satisfactory theory for the uranyl ion though a large amount of experimental data exist. However, it appears that not sufficient systematic measurements have been undertaken on the uranyl ion and the other actinyl ions. These experiments should follow up calculations or predictions from some theory.

URANIUM ACTIVATED LUMINESCENCE

The literature on this subject is not very large and the list of references given below covers almost all published papers in this field. (They represent all the papers consulted by the author. There are several early Russian papers (in Russian) not consulted or listed below). The papers are grouped together in terms of their age and continuity.

1926 E.L. Nichols and M.K. Slattery J. Opt. Soc. Am. 12 449

1928 M.K. Slattery Proc. Natl. Acad. Sci. U.S. 14 777

1929 M.K. Slattery J. Opt. Soc. Am. 19 175

1948 F.A. Krüger Physica 14 488

1953 G.R. Price B.J. Feretta and S. Schawarz. Analyt. Chem. 25 322

1959 H. Le Roux Nature 183 1180

1955 W.A. Runciman Brit. J. Appl. Phys. Supp. 4 S78

1955 W.A. Runciman Nature 75 1082

1955 W.A. Runciman Proc. Phys. Soc. A68 647

1956 W.A. Runciman Proc. Roy. Soc. A237 39

1959 J.E.A. Lys M.Sc. thesis University of Canterbury

1960 J.E.A. Lys and W.A. Runciman Proc. Phys. Soc. 76 158

1963 J.V. Nicholas M.Sc thesis University of Canterbury

1959 I.P. Shapiro Optics and Spectr. 7 78

1959 P.P. Feofilov Optics and Spectr. 7 493

1960 P.P. Feofilov Optics and Spectr. 8 433
1960 L.M. Belyaev, Z.B. Perekalina, V.N. Varfolmeeva, V.P. Panova, G.F. Dobrzhanskii, Soviet Physics-Crystallography 5 722
1961 P. Görlich, H. Karras, R. Lehmann, Phys. Stat. Sol. 1 525
1961 L.M. Belyaev, G.F. Dobrzhanskii, P.P. Feofilov. Bull. Acad. Sci. (U.S.S.R.) phys series 25 545
1961 E.P. Alekseeva Bull. Acad. Sci. (U.S.S.R.) phys series 25 541
1962 N.A. Tols'toi and Liu Shun-Fu Optics and Spectr. 13 59
1962 A.A. Kaplyanskii and N.A. Moskvin Optics and Spectr. 13 303
1962 P.P. Feofilov and A.A. Kaplyanskii Soviet Phys. Uspekhi 5 79
1963 A.A. Kaplyanskii and N.A. Moskvin Optics and Spectr. 14 357
1964 A.A. Kaplyanskii, N.A. Moskvin and P.P. Feofilov Optics and Spectr. 16 339

The review of the field given below is based on the more well established ideas concerning observations made on the activated luminescence. Nearly all the important work has been done on LiF and NaF crystals (since they are more easily grown than the other fluorides). These are therefore presented in some detail. How these fluoride phosphors are related to the others remains to be investigated.

MODEL OF LUMINESCENT CENTRE: As mentioned above, the uranyl ion can give rise to luminescence when it is an impurity in some crystal lattice or glass. Generally the luminescent spectra consists of equally spaced bands at almost the same repetitive frequency (860 cm^{-1}) of the uranyl spectra. Many fluoride lattices appeared to give

quite different spectra. On cooling, the spectra consists of many lines or sharp bands and the repetitive nature is not obvious. At room temperature there is only one broadish band and not several of approximately the same intensity.

It was suggested that a new luminescent centre was formed which was not just simply uranyl ion. The principle of charge compensation was used to build up a model of the centre. For LiF and NaF a uranium atom would replace the metal ion, e.g. a U^{6+} (radius 0.83Å) replaces a Na^{+} (radius 0.95Å), leaving five excess positive charges. To balance this charge five oxygen ions, O^{2-} (radius 1.40Å) were assumed to replace five fluorine ions F^{-} (radius 1.36Å), thus neutralizing the charge. (Feofilov's model Fig. 1.10). An alternative is one where 6 O^{2-} ions go in with a fluorine vacancy nearby. (Runciman's model Fig. 1.11). It is well established that oxygen is present at the centre from isotopic substitution effects on the spectra of NaF(u), and also by controlling the amount of oxygen present in making the phosphors.

These two possible centres have different symmetries. Feofilov's model is effectively orientated along the C_4 axis of the crystal (Fig. 1.10) while Runciman's of along the C_3 axis (Fig. 1.11). There are two experimental methods of distinguishing between them and both suggest that the centre is along the C_4 axis. The methods are polarization experiments and stress spectra. Both of these require clear single crystals and are taken on the luminescent spectra.

The two experimental methods depend on the fact that the centre is anisotropic even though it is in a cubic crystal lattice. In the polarization experiments the exciting light is polarized parallel to a crystal axis and the angle of polarization rotated. The resulting degree of polarization of the luminescence is observed as

FIG. 1.10

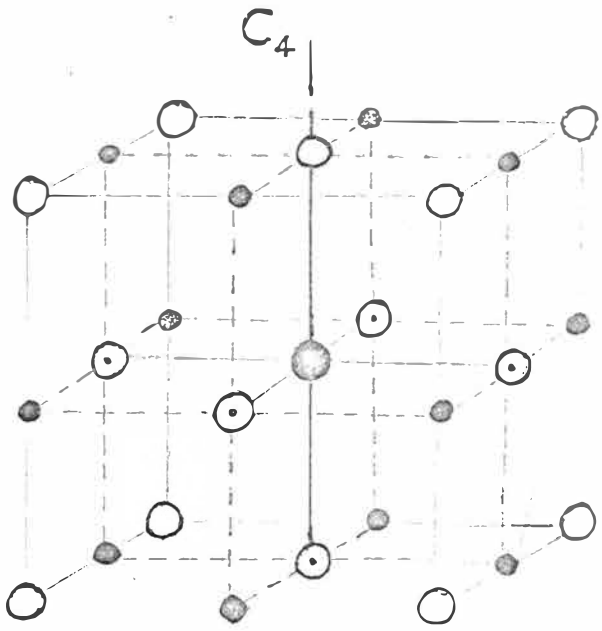

FEOFILOV

FIG. 1.11

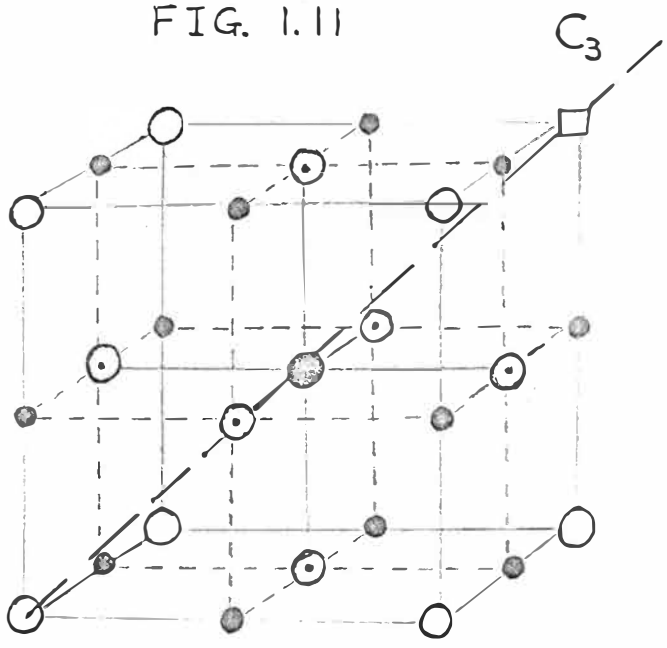

RUNCIMAN

● Na^+ ○ F^- ● U^{6+}

⊙ O^{2-} □ ANIONIC VACANCY

a function of the angle of rotation. From this theory it is possible to calculate the results for different orientations of the centre, and these are compared with those found experimentally. This method can also distinguish between magnetic and electric dipole transitions and this has been done for many lines in the luminescent spectra of LiF(U) and NaF(U) (see below).

When an unaxial stress is applied to a cubic crystal a shift in the position of an electronic transition of an anisotropic centre will occur. This gives the stress spectra of the crystal. The shift may be positive or negative (in energy) so that it generally would appear as if the line is split. (Actual line splitting may also occur if a degenerate electronic level is present). From the splitting pattern for stress along different axes, it is possible to determine the orientation of the centre. If in addition polarization experiments are carried out, and also the dependence of the splitting on various stresses noted, it is possible to say something about the actual symmetry of the luminescent centre.

All results show that the centre is orientated along the C_4 axis. However, several types of centres are present since different types of splittings (and polarizations) are found. An explanation for the various centres can be made on the basis of the uranyl ion. The linear uranyl ion is assumed to replace the metal cation and two fluorines and this forms the optical core of the centre along a C_4 axis. This is responsible for the optical emission and the different centres arise from the various methods of charge compensation. In the first approximation of a uranyl ion, only the ligands in the equatorial plane will effect it. (see above on crystal structure etc.). Figure 1.12 gives the first coordination sphere around the uranium and the resulting symmetry. Where the charge is not fully compensated, compensation is

FIGURE 1.12

(a)

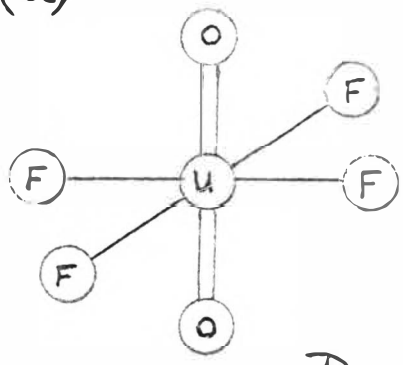

D_{4h}

(b)

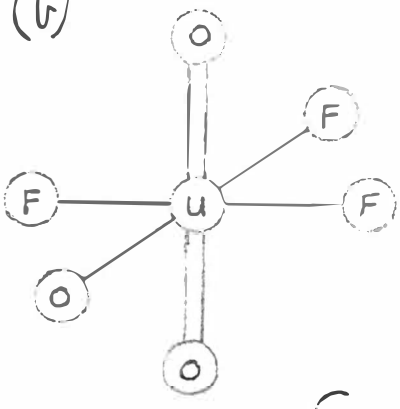

C_{2v}

(c)

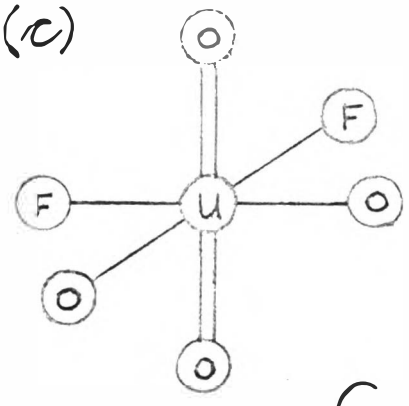

C_{2v}

(d)

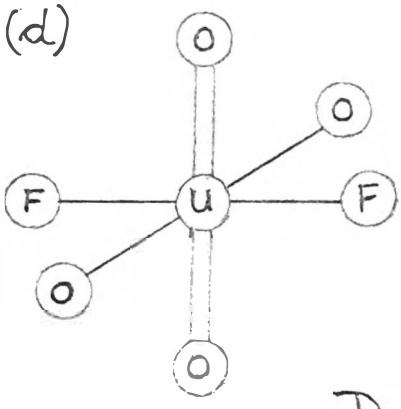

D_{2h}

(e)

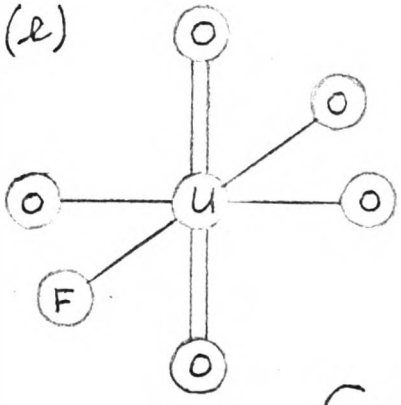

C_{2v}

(f)

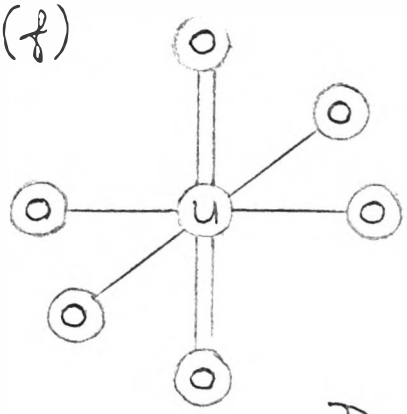

D_{4h}

assumed to occur further away and will have little effect on the spectra (may cause broadening due to unresolved splitting).

All the types of centres in Fig. 1.12 are required to explain the splittings observed. A tetragonal one can arise from case (a) and (f), and similarly, a rhombic one from (d). Splittings which require C_{2v} symmetry fall into two types, depending on the polarization. Centres (b) and (e) are similar while centre (c) will give a different polarization dependence. (N.B. a bent uranyl ion has symmetry C_{2v}). No assessment has been made on the importance of each model in contributing to the spectra.

LUMINESCENT SPECTRA: For Li F(U) and Na F(U) the luminescent spectra can be divided into two regions (not necessarily separate), a long wavelength region and a short wavelength region. The short wavelength region overlaps a part of the absorption spectra and contains several resonance lines. The long wavelength region has not any resonance lines (apart from the first) and forms a series of vibrational bands similar to uranyl spectra but with two types of electronic transitions, electric dipole and magnetic. The spectra can be described by the following equations.

for Li F(U)

$$\nu_{ek} = 19286 - 800\,k \ \text{cm}^{-1}$$

$$\nu_{mk} = 18947 - 800\,k \ \text{cm}^{-1}, \quad k = 0, 1, 2$$

and for Na F(U)

$$\nu_{ek} = 18093 - 708\,k \ \text{cm}^{-1}$$

$$\nu_{mk} = 17743 - 708k \ \text{cm}^{-1}, \quad k = 0,1,2,3.$$

There are several other lines and bands with the same repetitive frequency but no assignment of them has yet been given.

FIGURE 1.13 ENERGY LEVELS

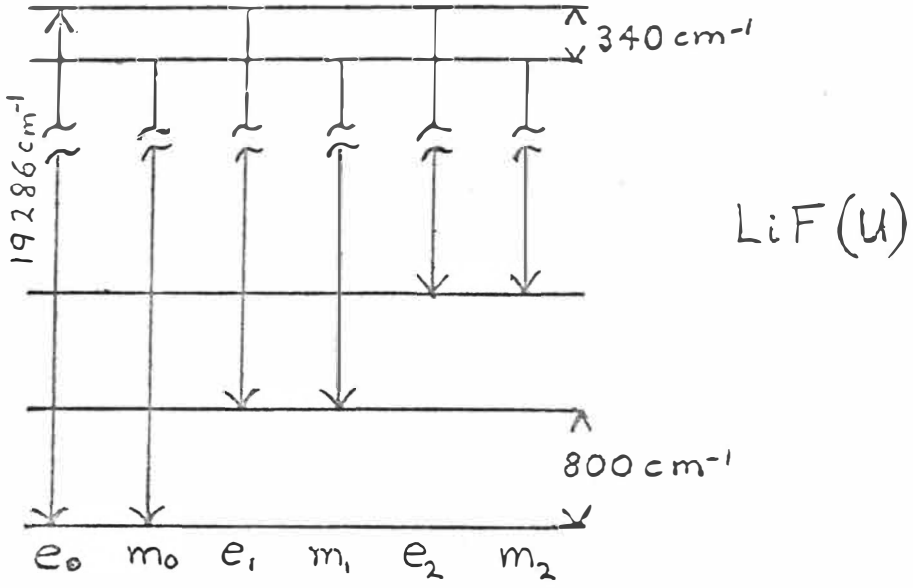

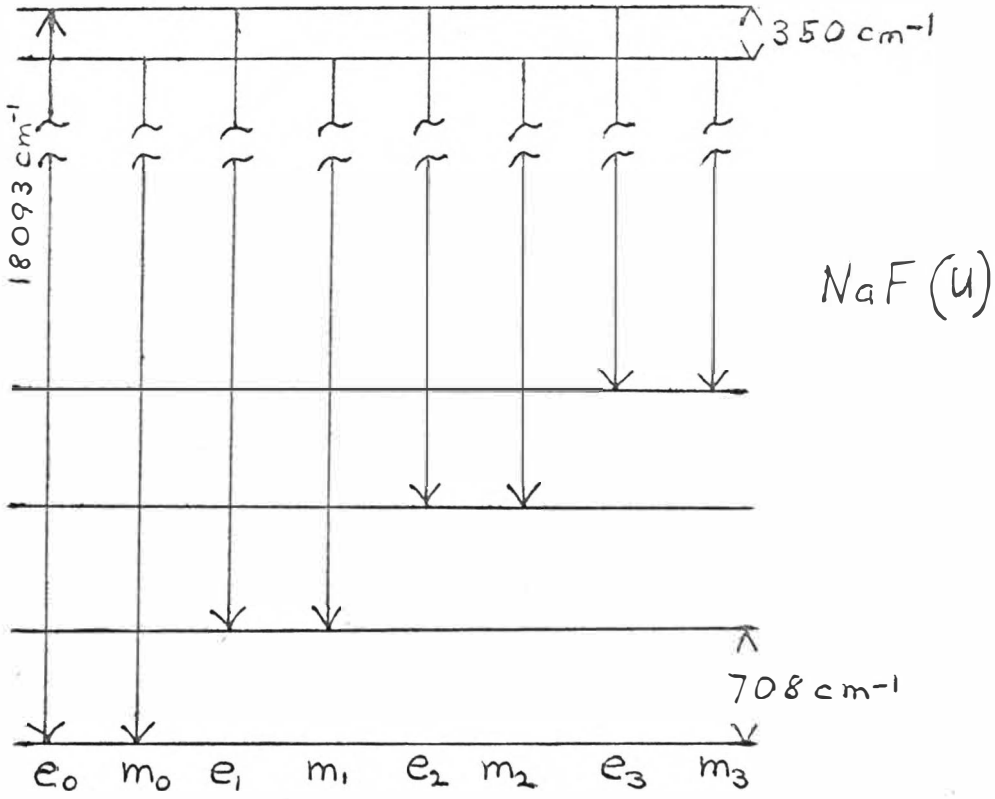

In Fig. 1.13 the energy level scheme is given for Li F(U) and Na F(U), showing two excited states from which the luminescence occurs. This has been shown from some simple temperature dependence work.

Variations occur in the short wavelength spectra according to the method of preparation of the phosphor. These variations can be quite marked and definite since it often means the appearance or non-appearance of some strong luminescent lines or bands (also of weak ones). An explanation for these can be based on several possibilities.

1. The effect of re-absorption.
2. A second electronic transition.
3. A different type of luminescent centre forming.

Effects 1 and 3 are the most likely on the evidence available, though 2 cannot be ruled out altogether.

ABSORPTION SPECTRA: The absorption spectra of Li F(U) shows no clear regularities and is unusual in that there are at least fifteen resonance lines. However, Na F(U) shows a vibrational structure of frequency 630 cm^{-1} (cf 708 cm^{-1} in luminescence) and also like Li F(U) has absorption bands in the ultra-violet. Many absorption lines may not belong to the luminescent centre as such things as colour centres etc. are likely to occur.

Many of the lines in absorption and in emission are very narrow (for solid state spectra) and are often less than 1 cm^{-1} wide.

DECAY TIMES: The decay is mostly exponential, and the decay time depends on the wavelength of the emitted light. For Na F(U) there are approximately three main decay times, 7.8×10^{-4} sec., 6.4×10^{-4} sec., and 5.5×10^{-4} sec. at 77°K (N.B.: Decay times depend on sample thickness and concentration and values given are for low concentrations and thin specimens). Similar values are found for Li F(U).

Ca F_2(U) and SrF_2(U) have decay times of about

2.5×10^{-4} sec., and show less variation with wavelength (only difference is at head of luminescent series where re-absorption may be important).

OTHER FLUORIDES: Fig. 1.14 gives a list of the uranium activated fluorides known to luminescence. They are listed under crystal structure type with a brief comment on their spectra. The metal ion radius is also given for a comparison with the uranium ion radius. Apart from reporting the spectra and occasional measurement of the wavelengths, not much work has been carried out on them apart from Na F(U) and Li F(U).

Figure 1.14

Luminescence of Uranium Activated Fluorides

Crystal Structure	Fluoride	Appearance at 4.2°K	Metal ion radius A°
rock salt	Li F	lines, strong	0.60
	Na F	Lines, very strong	0.95
	K F	Lines, strong	1.33
	CsF	Bands, medium	1.69
rutile	MgF_2	Lines, strong	0.65
	ZnF_2	Lines, weak	0.74
fluorite	CdF_2	Band, weak	0.99
	CaF_2	Lines, very strong	0.99
	SrF_2	Lines, strong	1.13
	BaF_2	Band, weak	1.35
perovskite	K ZnF_3	Band, weak	
	K MgF_3	Lines, medium	
double fluorides	Li_3AlF_6	Lines, strong	
	Na_3AlF_6	Band, weak	
	K_3AlF_6	Lines, medium	

Uranium ion radius is about 0.83Å to 0.97Å

CONCLUSION: A picture of the luminescence of Li F(U) and Na F(U) phosphors has now emerged based on experimental evidence. This is that the luminescence is due to a uranyl ion substituted into the crystal lattice. The spectra being modified by the various means of charge compensation. One type of centre predominates and its electronic level was given in Fig. 1.13. From the decay times and the approximately equal intensities of the electric and magnetic dipole transitions, it is evident that the transition is a "forbidden" one made allowed by some vibrational interaction. Further development of the centre awaits the solution of the electronic structure for the uranyl ion. This can then serve as a starting point for further work (or the spectra may serve as a test for the structure of the ion).

No work has been done to explain the origin and nature of the sharp lines and the many bands observed. These will belong to vibrations of the centre and the crystal lattice and could help to provide information about the lattice dynamics of several crystals. For Li F(U) and Na F(U) this is somewhat complicated due to several transitions occurring, but not so for CaF_2(U). Also since it is not possible to fit a uranyl ion totally into lattice sites in calcium fluoride, it is of interest to find out whether the uranyl ion is still responsible for the luminescence.

CHAPTER II
EXPERIMENTAL PROCEDURE

SAMPLE PREPARATION: Three methods were adopted for obtaining samples.

1. Powder samples were made by mixing uranyl nitrate and calcium fluoride powders together and heating to above 1000°C (melting point of calcium fluoride is 1400°C) in air. Both reagents were of "Analar" or higher grade purity. Several samples were made with various concentrations of uranium from about 0.01% to 10% (fraction of uranium atoms to calcium atoms). All of these were capable of luminescing (see Chapter III). The higher concentration samples were orange in colour, and sometimes a green (non-luminescing) powder was also formed.

Because the high concentration of uranium could possibly distort the lattice or cause new compound formation, X-ray powder diffraction photographs were taken. These showed that any distortion of the lattice was not detectable. However, some extra lines appeared. One group was due to calcium oxide, and appeared in some samples and not in others (see below). The other group of lines were that of a face centred cubic lattice with a lattice constant $a_o = 8.28\text{Å}$. These only occurred in some high concentration samples, and were very weak. E.G. Steward and W.A. Runciman, Nature 172 75 (1953), have shown that calcium oxide and uranium can form a compound Ca_3UO_6 which is face centred cubic with $a_o = 8.29\text{Å}$, and it seems most probable that it has formed here, using CaO formed from the hydrolysis of CaF_2.

Strontium fluoride powder samples were attempted but SrF_2 went to SrO far too readily to get suitable powders by this method.

2. Crystalline Samples. An attempt was made to see if crystal of calcium fluoride could be grown. The greatest difficulty with growing CaF_2 (or SrF_2 , BaF_2) is the strong tendency to hydrolyse to give the oxide with any moisture or

oxygen present (see for example D. Lewis and H. Pearson J. App. Phys. 35 1939 (1964). It should be grown in a hydrogen fluoride atmosphere to prevent this.

With the furnace available, it was possible only to use an inert atmosphere of nitrogen. The samples were heated above the melting point of CaF_2 and the temperature lowered slowly at a few tens of degrees an hour. This produced a crystalline lump of $CaF_2(U)$ which was greenish in colour (most probably due to U^{4+}) and which did not luminesce, until roasted in air at 700°C. The material then had a whitish appearance due to CaO precipitated in the CaF_2 lattice.

Several tries were made but it was not possible to get clear luminescing crystals suitable for obtaining absorption spectra by transmission methods. A fairly thick crystal would be required as the absorption from powders was very weak.

In attempting to make the higher concentration samples, a large amount of black material was produced. This could be due to some reaction of the uranium with the carbon crucibles used. Thus it was not possible to obtain crystalline samples with a high concentration of uranium.

3. Commercial Samples. Some crystals of CaF_2, SrF_2 and BaF_2 containing uranium were obtained from "Semi-Elements". These had a greenish colour and did not luminesce. They contained largely U^{4+} ions. Chips from these of CaF_2 and SrF_2 were heated to about 800°C. This caused them to luminesce and also to go milky due to the oxide forming. As the oxygen must diffuse in from the outside, the centre of the chip was not luminescent but was now a dark brown. The dark brown most probably due to U^{6+} ions without oxygen for charge compensation (see P. Görlich, H. Karras, R. Lehmann Phys. Stat. Sol. 1 389 (1961)).

Spectra of the samples is given in Chapter III and they are similar to the one reported by Görlich et al.

SPECTRA: The luminescence was excited by a black mercury lamp with ultra violet radiation of mainly 3650Å. Absorption spectra were taken by reflection or transmission methods using a tungaten filament lamp for the visible and a hydrogen discharge lamp for the ultra violet. The spectra were recorded on a prism spectrograph or a grating spectrograph.

PRISM SPECTROGRAPHS: Two Hilger instruments were used. A medium quartz spectrograph and an automatic large quartz and glass spectrograph. These were used for the general investigation of the spectra. The large glass spectrograph was mostly used having a dispersion of 9Å/mm at 5000Å compared to 65Å/mm for the medium instrument. Slit width of 20μ ($1\mu = 10^{-6}$ m) was typically used and the plates used were the Ilford R40 and Astra III for the ultra violet to visible region and Kodak II L for the near infra-red. The photographic process was very useful in finding weak emission lines and much structure of interest was found this way by taking very prolonged exposures.

For measuring wavelengths the medium spectrograph has an internal scale and wavelengths could generally be measured to within 10Å. For the large an iron arc calibration was required and lines fitted to a Hartman formula. This enabled lines to be measured to 1Å.

GRATING SPECTROGRAPH: A 3.4 metre Ebert spectrograph manufactured by the Jamel-Ash Company was used for photoelectric recording of the spectra, and for investigating the temperature dependence of line shapes and shifts.

Over various runs three photomultipliers were used.

1. RCAIP2I.
2. EMI 6255S.
3. EMI 9558Q.

These all gave satisfactory performances, the 9558 tube while slightly noisier was better for the red end of the spectrum. An electrometer amplifier was used to detect the signal which was then recorded by a chart recorder.

The grating used was a replica of a MIT grating with 7620 grooves per inch and blazed for 59°. This meant that the luminescent spectra being centred around 5200Å was taken in the sixth order. To prevent overlapping of orders, wide band interference filters were used in the entrance optics.

Entrance and exit slit widths of 30μ were used to give reasonable light intensity for the detecting system. This corresponds to a spectral slit width of 0.04Å for the sixth order. Since line widths of interest were not narrower than 0.4Å this gave quite adequate resolution. For this line the spectral slit width would cause an error of 0.5% in width using the formula.

$$\tilde{\delta}_T^2 + \tilde{\delta}_s^2 = \tilde{\delta}_{obs}^2$$

$\tilde{\delta}_{obs}$ = observed line width

$\tilde{\delta}_s$ = spectral slit width

δ_T = true line width

(This assumes a Gaussian line shape, see H.C. Vande Hulst and J.J.M. Reesinck Astrophys J. 106 121 (1947) for a discussion on the validity of the equation).

The absolute wavelength calibration for the spectrograph was checked using mercury lines and was found to be accurate to ± 0.2Å over the spectral range of interest.

Wavelength readings were taken off a counter which gave values of $n\lambda$ (n the order and λ the wavelength). This could be read to within one division, so that the errors in readings are ± 0.1Å or ± 0.5 cm^{-1}. So the error in taking the difference of two readings is ± 1cm^{-1}. This would represent the accuracy in considering line shifts. For line widths or separation of lines the accuracy can be higher, depending on the speed of scan, since the measurements are taken on the same record.

An intensity calibration was also carried out to find the wavelength response of the system (spectrograph, photo-

FIGURE 2.1

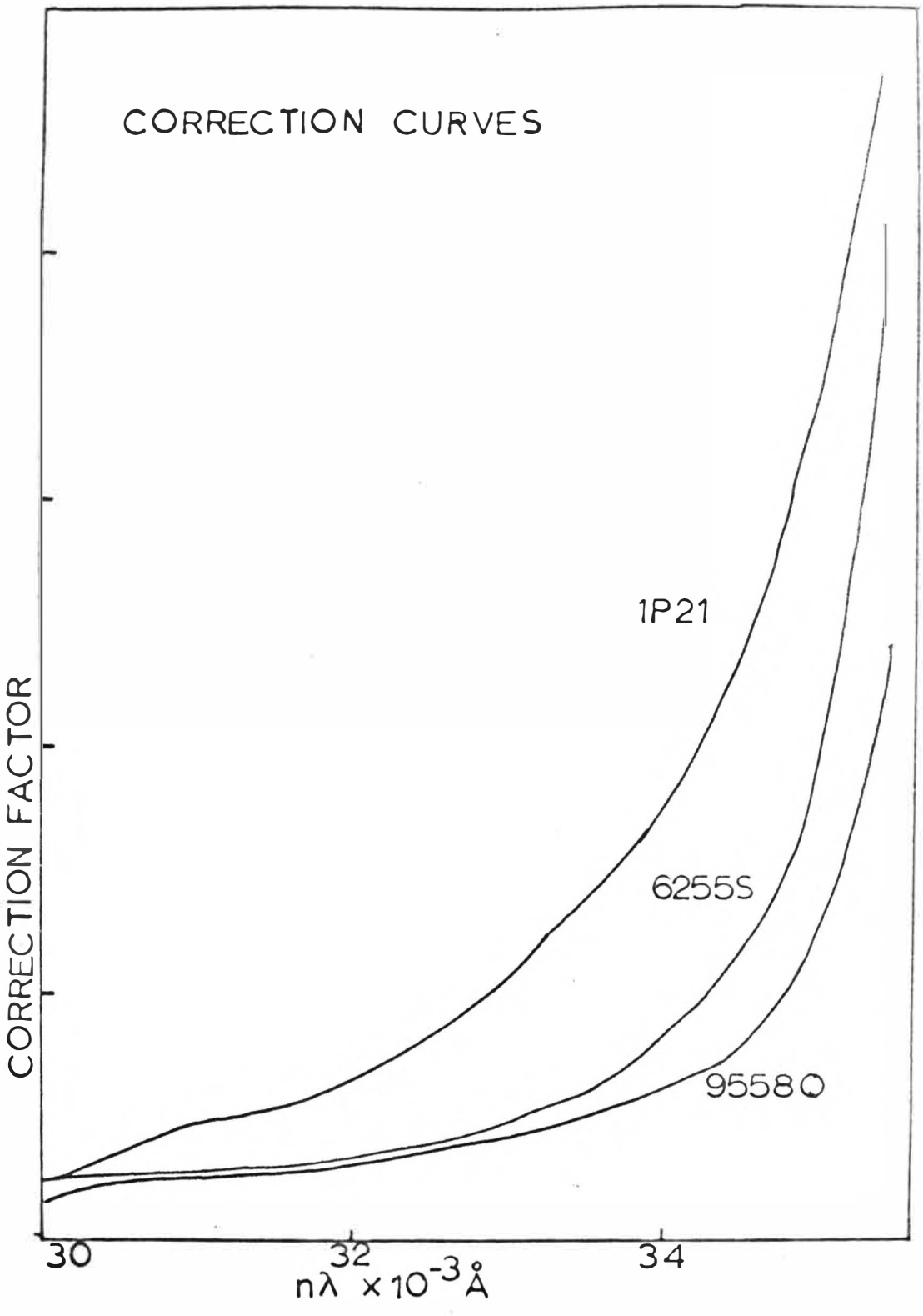
CORRECTION CURVES
1P21
6255S
9558O
CORRECTION FACTOR
30
32
34
nλ x 10⁻³ Å

multiplier and filters). To do this a calibrated tungsten strip lamp was put in place of the luminescent sample. The lamp had a calibration of colour (brightness) temperature versus current. This was converted into true temperature versus current by using tables in the American Institute of Physics Handbook 1957 (which also gives the blackbody radiation function). Thus, by using known values of the emissivity of tungsten as a function of wavelength (J.C. De Vos Physica 20 690 (1954) give most recent and accurate data) and the blackbody radiation function, the spectral output of the lamp can be calculated. From the response of the system to this spectra, it is quite simple to obtain a calibration curve to give correct relative intensities for emission spectra. (See Fig. 2.1 for typical correction curves by which spectra obtained should be multiplied. N.B. curves do not have the same normalization).

DEWARS: For spectra taken with photographic plates, the samples were immersed directly in liquid nitrogen ($77^{\circ}K$) or liquid helium ($4.2^{\circ}K$) by using suitable glass dewars. Before a metal dewar (see below) became available some photo-electric recording was made using these dewars. Providing the bubbles in the boiling liquid were kept small, the time constant in the recording system was sufficient to remove the noise caused by them.

For the variable temperature work, a metal dewar obtained from "Andonian Associates" was used. In this dewar the sample is mounted on a cold finger in vacuum and the temperature of the finger measured using a gold-cobalt or a copper-constantan thermocouple with a microvoltmeter.

To control the temperature, an electrical heater was wound around the sample holder (or cold finger) which was attached to the liquid helium tank by a hollow stainless steel tube. In the tube the gas pressure (helium or nitrogen) could be changed to vary the rate of heat flow from the sample to coolant. By suitably varying the heater current and the gas pressure, a wide range of temperatures could be obtained

and maintained. From 5 °K to 70°K liquid helium was used and from 65°K to nearly room temperature liquid nitrogen was used in the liquid helium tank instead. Temperatures below 77°K for liquid nitrogen were obtained by pumping on the tank to lower the pressure above the liquid nitrogen causing the temperature to drop.

The accuracy to which the temperature could be controlled depended on the temperature. Near the temperature of the reference junction (either 77°K or 4·2°K) the sample could be held within ± 0·5°K while for temperatures further away it could be held to ± 3°K at the worst. The temperature of the sample itself could be one or two degrees higher than that measured by the thermocouples due to local heating of the sample by the incoming radiation from the lamp.

Figure 2.2 gives a general view of the dewar mounted on the 3·4 m spectrograph with associated equipment.

E.S.R. SPECTRA: Using an X-band spectrometer a search at 77°K and room temperature was made for any possible resonances in the uranium activated crystals. No obvious spectra was found for the luminescent samples Li F(U), Na F(U) and Ca F_2(U). Though there were faint signs of some lines, these could be due to other impurities. Samples of Li F(U) which had been melted in a furnace with no oxygen gave a broad line at g = 2, but these samples did not give the normal luminescence. They gave instead a red luminescence typical of colour centres in LiF. (P. Görlich, H. Karras, G. Kötitz, Phys. Stat. Sol. 3 1803 (1963).

These results show that there are no free spins associated with the luminescent centre and that there are no colour centres present. Extension of the measurements to other frequencies and 4·2°K may give some resonances which would be helpful in determining the bonding arrangement of the centres.

POLARIZATION SPECTRA: Exciting light from a Bausch and Lomb high intensity monochromator was polarized by a

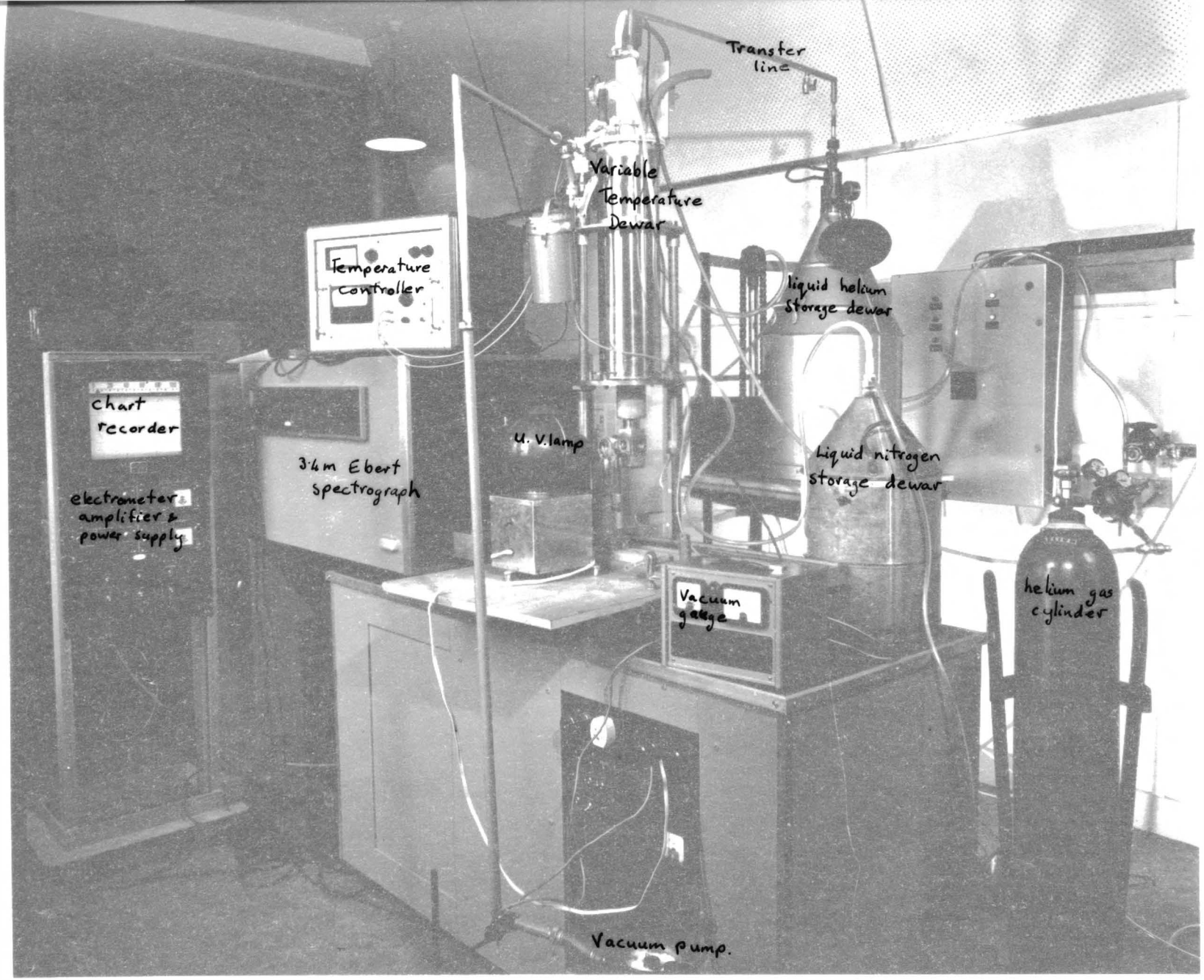
Transfer line
Variable Temperature Dewar
Temperature controller
liquid helium storage dewar
chart recorder
U. V. lamp
3·4m Ebert spectrograph
Liquid nitrogen storage dewar
electrometer amplifier & power supply
Vacuum gauge
helium gas cylinder
Vacuum pump.

Figure 2.2

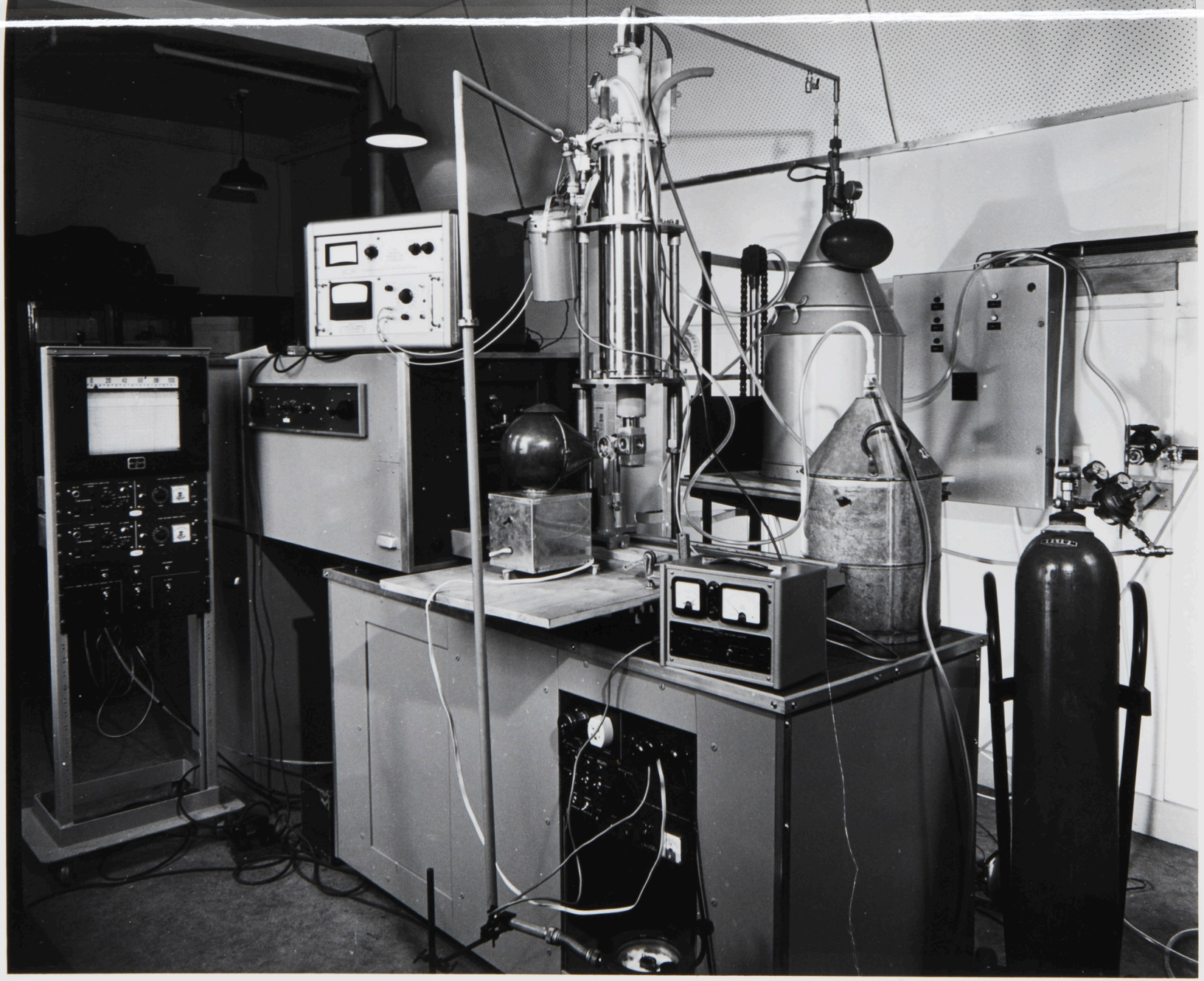

Glan-Thompson prism and focussed onto a single crystal. The resulting luminescence was analysed for any polarization by a Babinet compensator. Na F(U) crystals showed some degree of polarization, as expected from the work of Feofilov and others (see Chapter I). However, for Ca F_2(U) and Sr F_2(U) no obvious polarization was found (a degree of polarization greater than 2% can be detected with a Babinet compensator). The test was tried for both absorption bands, one in the near ultra-violet (3500Å) and the other near the luminescence (5000Å). This does not convincingly show that there is no polarization since the crystals were milky due to CaO precipitates and this would scatter the light causing depolarization.

CHAPTER III

RESULTS

ABSORPTION SPECTRA. Some small chips of the crystalline samples and the "Semi-Elements" crystal of $CaF_2(U)$ proved suitable for some absorption spectra by transmission.

Figure 3.1 summarizes the results for the ultra-violet absorption spectra.

Figure 3.1

Ultra-Violet Absorption Spectra for $CaF_2(U)$

λ* Å	COMMENT
2500	strong absorption for shorter wavelengths
2783 – 2789	broad lines
2900 – 3080	bands
3420	centre of a broad band

* wavelengths as from the medium spectrograph with an accuracy of ± 5Å.

Many of these bands will be due to oxygen in the CaF_2 crystal and also due to $Ca(OH)_2$ or $CaCO_3$ on the surfaces. (P. Görlich, H. Karras, R. Lehmann, Phys. Stat. Sol. 1 389 (1961)). The band centred at 3420 Å is very weak and broad but is the one used to excite the luminescence, and it seems likely that it belongs to the luminescent centre. However, it could be due to the oxygens used for charge compensation and the

absorbed energy is transferred from these to the electronic system (assumed on the uranium atom) responsible for the luminescence.

Several lines were found in the red and near infra-red region for many samples, but not all, possibly due to the weakness of some lines. These lines are at 9148Å, 7480Å, and 6055Å (these do not correspond to any lines of U^{3+} or U^{4+} in CaF_2). Some of the lines appear to have weak structure associated with them, but were beyond the limit of measurement for a photographic plate. Absorption bands in CaF_2 for regions near these lines have been reported (see Görlich et. at. above) as due to OH^- ions. The absorption line at 6055Å is possibly associated with secondary luminescent bands centred at 6049Å and 6521Å (see below under Secondary Luminescence). However, the absorption line can occur in samples which do not give the luminescence. No explanation has been found for the other two lines, 9148Å and 7480Å. The 9148Å line appears to be very sharp.

From the higher concentration powders, it was possible to obtain a very weak absorption spectra in the same region as the luminescent spectra. Filters were used to prevent any ultra-violet light from the tungsten lamp causing luminescence. The lines obtained are given in Figure 3.2. The values given may be in error since the lines were very weak and hard to locate.

Figure 3.2

Visible Absorption Spectra for $CaF_2(U)$

λ Å	ν cm^{-1}	$\Delta\nu$ cm^{-1}	COMMENT
5000.4	19992	824	
5035.6	19853	685	$\Delta\nu$ also in luminescence
5090.2	19640	472	
5127.9	19496	328	$\Delta\nu$ also in luminescence
5144.7	19432	264	$\Delta\nu$ also in luminescence
5158.2	19381	213	
5188.3	19269	101	
5215.5	19168	0	resonance line. Type I
5275.1	18952	- 216	resonance line. Type II

This spectra was obtained from a high concentration sample (0.3% U) and the lines can belong to either Type I or Type II centres (see below under Concentration Effects). The resonance lines are assumed as they are very close to lines found in luminescence. For Type I absorption spectra there are at least three lines corresponding to vibrational frequencies found in the luminescent spectra. Actual band intensities should be compared with the intensities for the luminescent spectra to see if the vibrational structure is similar. (This would, as mentioned in Chapter II, require clear thick crystals). Type II spectra has a resonance line at 5275.1Å and some of the absorption lines could belong to this spectra, but at present it is difficult to identify any. Both resonance lines appear as doublets, but were not well resolved due to the broadish nature of the lines.

CONCENTRATION EFFECTS: The luminescent spectra of the CaF_2 powders with varying concentrations of uranium showed differences. A description of the spectra can be based on considering that there are two types of spectra present, Type I and Type II. The origin of the two spectra is most probably due to two different luminescent centres. Explanations based on a single centre meet grave difficulties in postulating a likely energy level scheme, and also in explaining the observed temperature dependence.

For low concentrations the spectra is that of one centre only (see Figure 3.3). Figures 3.3 to 3.6 give the uncorrected chart recorder output from the Ebert spectrograph. The type of photomultiplier (P.M) tube used and the temperature of the sample are indicated. Since the spectra were taken under very similar conditions the area under the spectral curves gives some idea of the relative intensities of the luminescence for the different samples (e.g. that of Figure 3.5 is the most intense). Type I spectra is characterized by a sharp no-phonon line (see Chapter IV) at 5212.7Å with a vibrational structure on the side. This vibrational structure is approximately repeated on the side of the line at 5420.6Å. The repetition of this structure is more evident on a photographic plate than on a chart record since the intensity becomes too low for the structure to show up on the chart. It is possible to represent the spectrum by the equation:-

$$\nu = 19179 - 730\,k - n_i \nu_i \quad cm^{-1}$$

k = 0,1,2 or 3 (very weak at k = 3)
is a lattice or local mode frequency (see Chapter IV) and has the values 147, 194, 266, 297, 325, 385, 438, 609 cm^{-1}.
Not all are sharp lines but rather bands, especially for $k \geqslant 1$

n_i = 0 or 1 no combinations of the ν_i are apparent but they could occur in the broad background.

FIG. 3.3

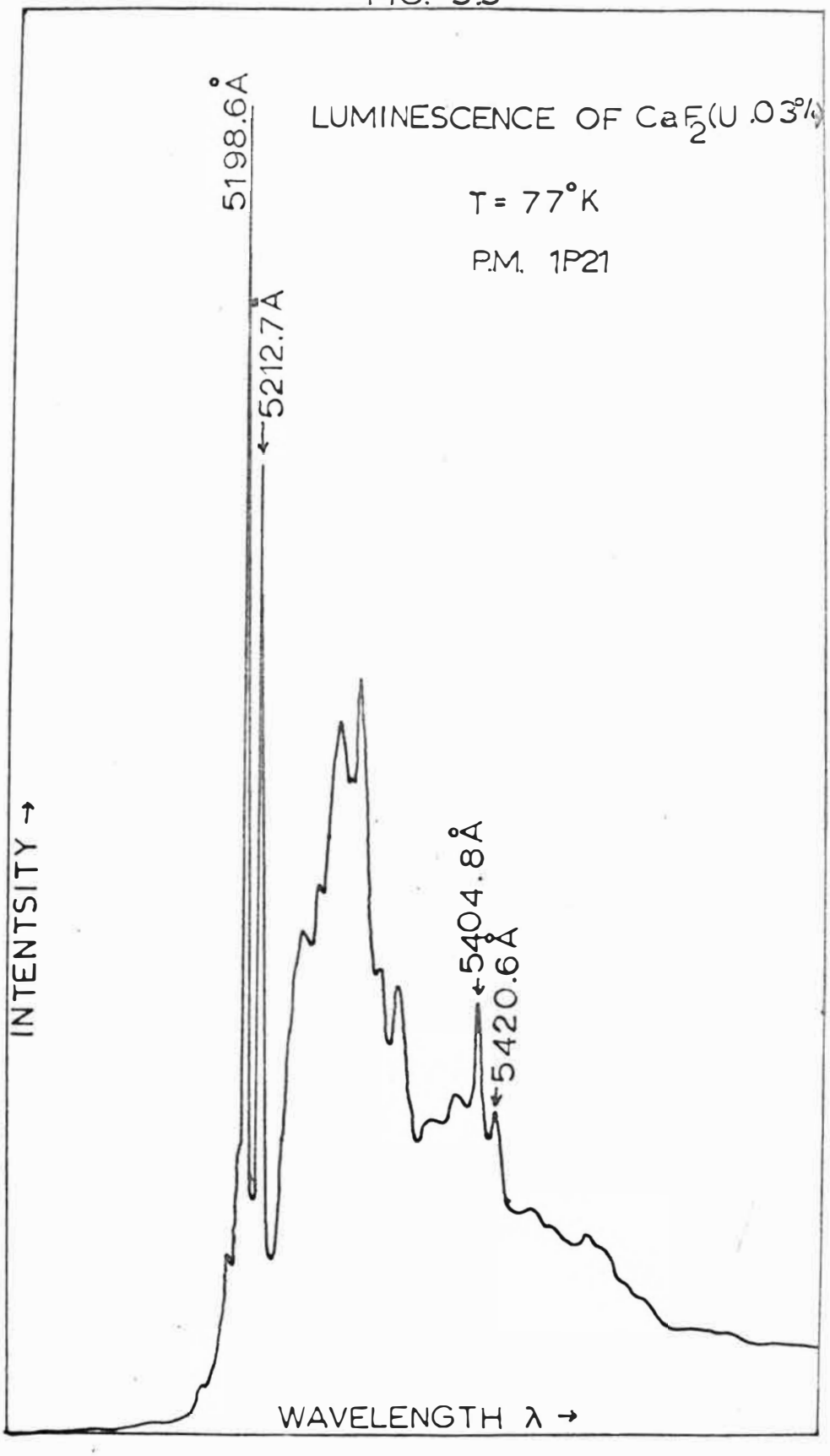
LUMINESCENCE OF CaF_2(U .03%)
T = 77°K
P.M. 1P21
5198.6Å
5212.7Å
5404.8Å
5420.6Å
INTENTSITY →
WAVELENGTH λ →

FIG. 3.4

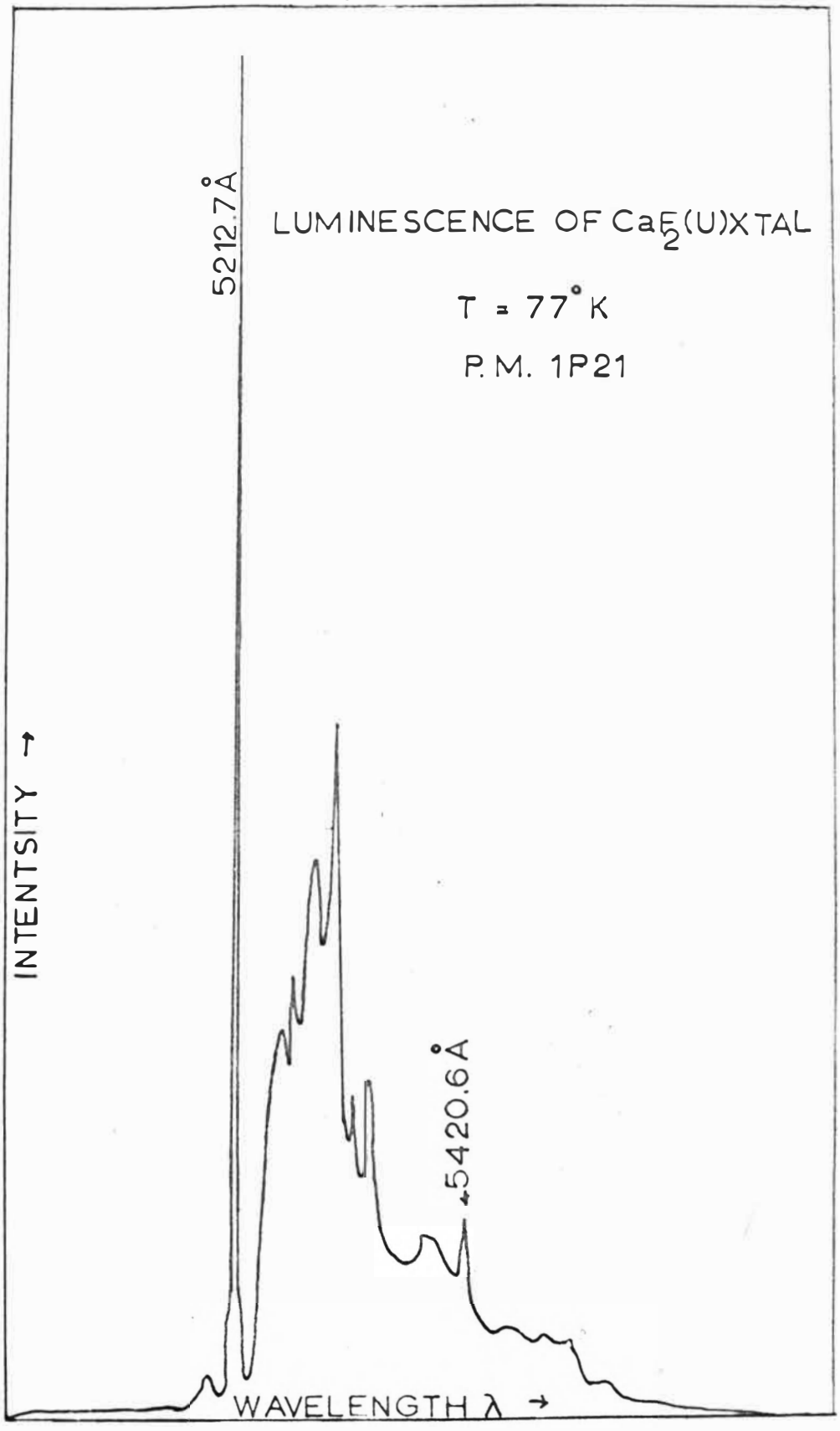
LUMINESCENCE OF CaF_2(U)XTAL
T = 77° K
P. M. 1P21
5212.7Å
5420.6Å
INTENTSITY →
WAVELENGTH λ →

FIG. 3.5

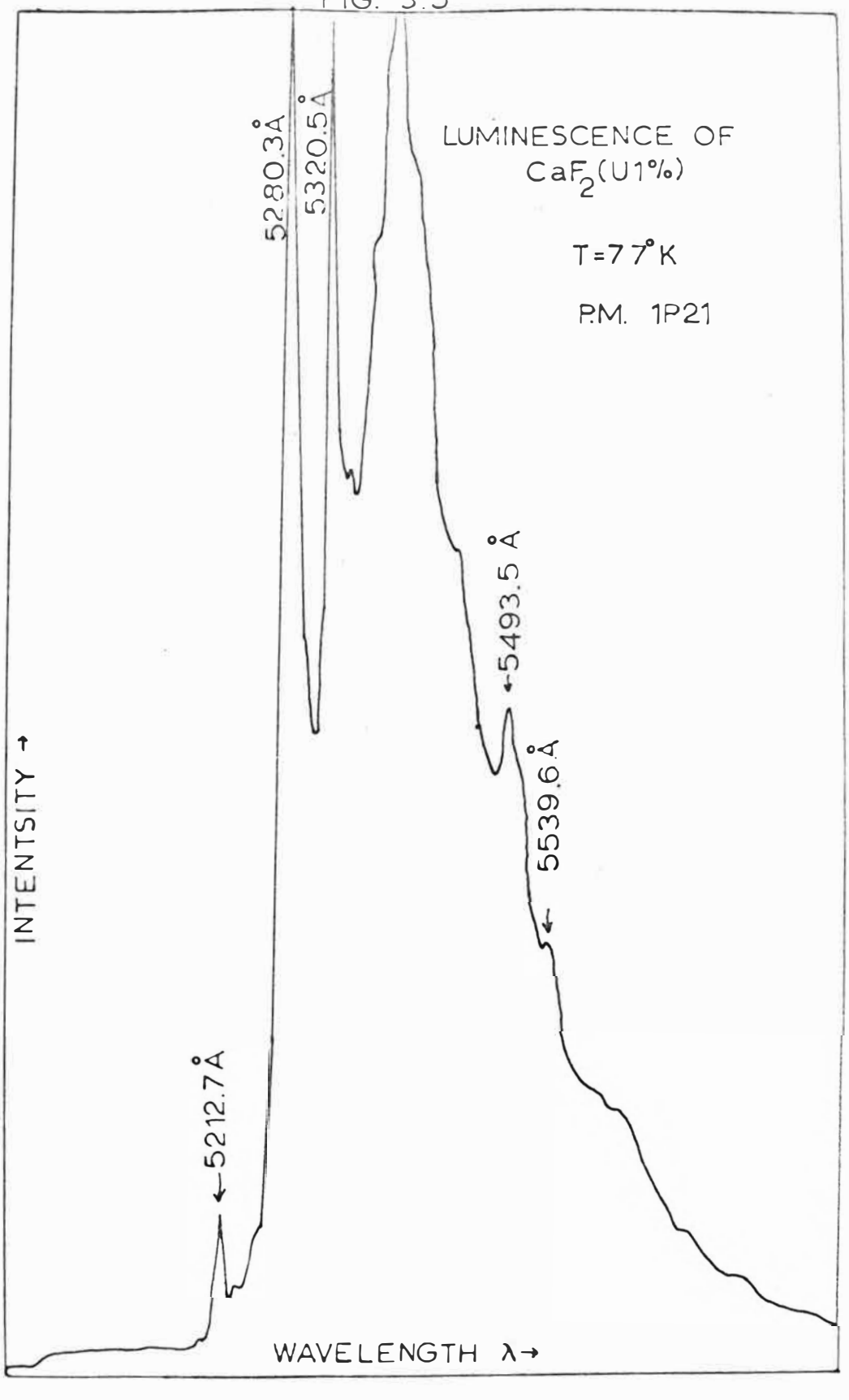
LUMINESCENCE OF
CaF_2(U1%)
T=77°K
P.M. 1P21
5280.3Å
5320.5Å
5493.5 Å
5539.6Å
5212.7Å
INTENTSITY →
WAVELENGTH λ→

FIG. 3.6

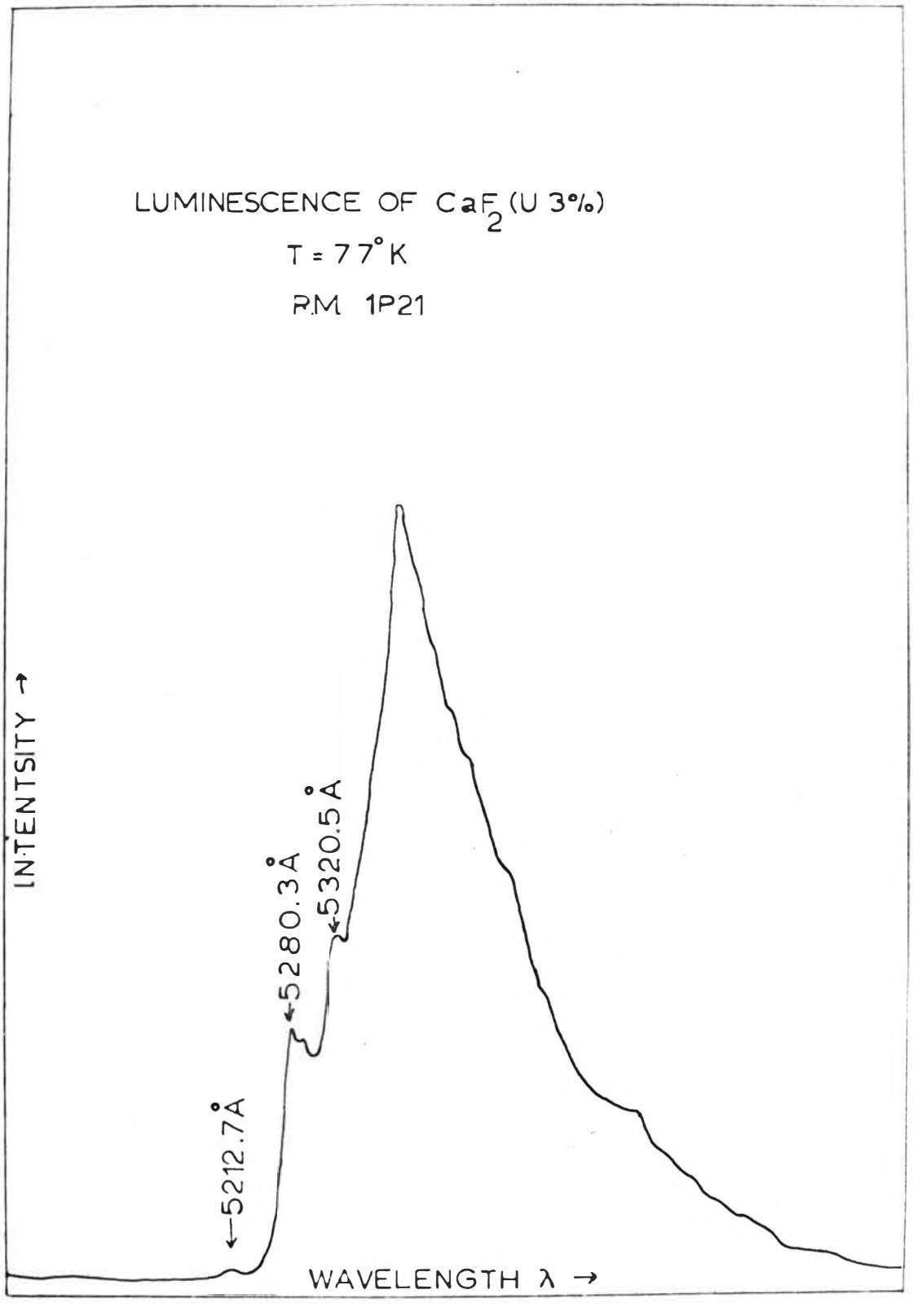
LUMINESCENCE OF CaF_2 (U 3%)
T = 77°K
P.M. 1P21
INTENTSITY →
←5212.7Å
←5280.3Å
←5320.5Å
WAVELENGTH λ →

For most samples as prepared there was an additional no-phonon line at 5198.6Å with a vibrational series, the first line at 5404.8Å i.e. the series could be represented by:-

$$\nu = 19230 - 730k \quad cm^{-1}$$
$$k = 0, 1, 2, \text{ or } 3.$$

There appears to be no values of ν associated with this line. For most crystal samples and reheated powder samples this series of lines is absent or very weak (see Figure 3.4). The intensity of the line is often greater than the no-phonon line at 5212.7Å which will have some reabsorption since it is a resonance line. There appears to be no absorption line corresponding to the 5198.6Å line. Both lines however have almost the same width and also the same temperature dependence for position and width (see Chapter V). Besides this intense "extra" no-phonon line often there are other weaker sharp lines (see spectra in Chapters III and IV) near the 5212.7Å line and these also have the same width and temperature dependence of the intense lines. SrF(U) also has these extra lines but some of them do have an effect on the vibrational structure while for CaF_2(U), if such an effect occurs, it is not obvious.

The origin of these extra lines is not clear and requires further investigation. Variations in the main type of centre seem the most likely origin of these extra lines. Each extra no-phonon line being associated with a different centre which causes an energy shift of the line.

These variations can take the form of lattice defects or even impurities close to the luminescent centre. Another possibility is two or more centres being close to each other and causing some interaction. Heat treatment would give some mobility to these defects so that they could be destroyed or reduced. A well grown crystal would be expected to have little or no defects. This would help explain the

variations due to sample preparation, but does not help to explain the lack of vibrational structure. The fact that there is no structure would imply that very rigid selection rules would apply to these centres. However, the variations in the centre would lower the symmetry and hence would tend to allow more vibronic transitions. Explanations based on a single type of centre with "extra" energy levels (either electronic or vibrational) do not explain the temperature dependence which is almost opposite to that required.

At higher concentrations (i.e. 1%) Type II spectra predominates (see Figure 3.5). This is characterized by two lines (actually they are doublets) at 5280.3Å ($18934\ cm^{-1}$) and at 5320.5Å ($18792\ cm^{-1}$). The line at 5280.3Å occurs in absorption also. There is a band at 5384.7Å (or $366\ cm^{-1}$ from the resonance line). This pattern is repeated with a repetitive frequency of about $740 cm^{-1}$ several times (i.e. the lines at 5493.5Å and 5539.6Å are the start of the second series). As is seen in Figure 3.5 there is other vibrational structure present but the values do not agree with those found in Type I spectra.

As the concentration of uranium is increased from say 0.01% to 10% there is a gradual change in the spectra from Type I to Type II. Type II first appearing at about 0.1%. At high concentrations, only, a band is formed (Figure 3.6) and the samples luminesce weakly at room temperature but become considerably stronger on cooling to 77°K. The interpretation of these concentration changes is that as the concentration of uranium increases the formation of a second type of centre becomes favourable. An absorption band due to Type II centres overlaps the luminescent spectra of Type I so that light emitted by Type I can be absorbed and appear as light emitted by Type II centres. Thus the spectra consists largely of Type II even though there are a considerable

number of Type I centres (as seen from the absorption spectra). As the concentration is increased further some of the Type II radiation must be reabsorbed and the intensity of some lines drops(Figure 3.6). Strong absorption bands (besides weaker lines) can be seen in reflection spectra taken off the powder samples.

On cooling samples giving Type II spectra to 4.2°K the 5212.7Å line is enhanced. No simple explanation can be given of this assuming Type I and Type II spectra arise from the same centre, but different electronic levels. Different centres can explain this, as they will, in general, have different temperature dependence.

The rest of the investigations in this thesis on CaF_2(U) luminescence were made on the low concentration Type I spectra, as crystalline samples of these could be made or obtained (see Chapter II). The origin of Type II spectra requires further investigation and especially to see if crystals containing it can be made.

SECONDARY LUMINESCENCE: Some samples of CaF_2(U) showed a secondary luminescence not dependent on concentration. This luminescence was very weak and only showed up on prolonged exposures. It consisted of two almost identical sets of lines centres at S_1 and S_2 (see Figure 3.7).

Figure 3.7
Secondary Luminescence Lines

Designation	λ Å	ν cm^{-1}	Designation	Å	ν cm^{-1}
β_1			β_2	6509.0	15359
α_1	6042.5	16545	α_2	6514.0	15347
S_1	6049.0	16527	S_2	6521.8	15329
A_1	6061.4	16493	A_2	6534.0	15302

The separation of the two sets of lines is 1,197 cm^{-1}. Very prolonged exposures did not show any other lines. However, lines corresponding to higher energies could be lost in the normal luminescence spectra. The intensity of S_2 was greater than that of S_1 (possibly due to reabsorption, see above under Absorption Spectra).

An explanation of these lines can be made on the basis of an O_2^- ion. J. Rolfe, J. Chem. Phys. 40 1664 (1964) investigated the luminescence of O_2^- ions in alkali halide crystals. These gave a series of lines, the most intense of which were at about 6000Å, separated by a vibrational frequency of about 1,170cm^{-1} (c.f. 1,197 cm^{-1}) corresponding to the known vibrational frequency of O_2^- (Notation used in Figure 3.7 is based on that of Rolfe's). While there is no report of O_2^- luminescence in alkaline earth halides, it is reasonable to assume that it is likely. Normally it would be undetected if it is as weak as it is here. It is thought that due to the large amount of oxygen normally present in preparing samples, some of it entered the lattice as O_2^- ions.

STRAIN EFFECTS: A crystalline sample which had a line width for the 5212.7Å line of about 1Å at 10°K was ground up into a powder. It now gave a line width of 8Å at 10°K. The spectra appeared to be that of a higher temperature (i.e. 150°K instead of 10°K) compared to that of a normal powder sample. Theory shows (see Chapter V) that the line width can be considered as coming from two parts:-

1. a temperature dependent part.
2. a temperature independent part due to local strains.

Strains or dislocations can change the crystal field at the impurity centre and cause small shifts which appear as a statistical broadening of the line. Hence the line width will be that of the temperature independent part until the

temperature is sufficient for the temperature dependent part to become appreciable. Lines from different powders and crystals had different temperature independent line widths. Usually in the range 0.4Å to 1Å and not as great as 8Å.

CHAPTER IV

VIBRONIC SPECTRA

This chapter is mainly concerned with the vibronic spectra and its interpretation. An outline is given of the present theory explaining how the lines observed in the optical spectra are related to the vibrational modes of the crystal lattice. Selection rules are given for the coupling of the vibrational modes (or phonons) to the electronic transition. A comparison is given between measured values of phonons in CaF_2 and the vibronic spectra of CaF_2(U). SrF_2(U) is also considered using CaF_2(U) spectra as a guide since there is less data available on SrF_2.

THEORY OF VIBRATIONAL STRUCTURE:

The problem of vibrational interactions with electronic transitions in solids was treated by M. Lax, J. Chem. Phys. 20 1752 (1952) who derived general moment formulae. However he only applied his method to broad structureless bands. His methods have since been extended by several people to apply to solid state spectra containing detailed structure. The system of interest here has been treated in a general fashion by D.E. McCumber, J. Math. Phys. 5 221 & 508 (1964) Phys. Rev. 135 A1676 (1964) (also see references therein).

Several Russian authors have published work (listed below) on a similar problem using different methods and approximations.

K.K. Rebane & V.V. Khizhnyakev Optics & Spectr. 14 193 & 262 (1963)

E.D. Trifonov Sov. Phys. Doklady 7 1105 (1963)
Sov. Phys. Solid State 6 366 (1964)

M.A. Krivoglaz Sov. Phys. Solid State 6 1340 (1964)

Earlier work on extending Lax's method to systems of trapped electrons (e.g. colour centres) is reviewed by

D.L. Dexter Solid State Physics 6 353 (1958)

This gives some discussion on the approximations often assumed.

E.O. Kane Phys. Rev. 119 40 (1960) derives formula for the spectra in a similar manner to the Russian authors.

Applications to impurity centres of transition metal ions and rare earths (of interest here) is given by:-

A. Kiel Phys. Rev. 126 1292 (1962)
Johns Hopkins University Radiation Labs
Tech. Report AF-93, 1962

D.E. McCumber and M.D. Sturge J. Appl. Phys. 34 1682 (1963)

G.F. Imbusch, W.M. Yen, A.L. Schawlow, D.E. McCumber and M.D. Sturge, Phys. Rev. 133 A1029 (1964)

W.M. Yen, W.C. Scott, and A.L. Schawlow Phys. Rev. 136 A271 (1964)

The theory of the vibronic structure given below is based on the above references, wherein greater detail can be found. (N.B. not all authors seem to agree on the results, though most differences are due to the approximations assumed).

The Hamiltonian for the system of an impurity ion in a crystal and its lattice phonons (or vibrations) is taken as

$$H = He + Hp + H_I \qquad 4.1$$

where He describes the energy $\mathcal{E}$ of an ion in the presence of the crystalline electric field (it is the normal Hamiltonian for crystal field calculations).

Hp represents the phonon system and for a harmonic lattice (assumed here)

$$H_p = \sum_q \hbar \omega_q \left(a_q^+ a_q + \tfrac{1}{2}\right) \qquad 4.2$$

ω_q is the frequency of vibration of the q'th mode. a_q^+ and a_q are the usual phonon annihilation and creation operators

H_I represents the interaction of electron and phonon systems

The interaction H_I is considered to arise from dynamic strains set up by the lattice vibrations. As such it is time dependent and the use of second quartization (in the form of a_q and a_q^+) removes the explicit time dependence. In this chapter, we consider the linear part of H_I

$$H_I' = \psi^+ \psi \sum_q \left(A_q a_q^+ + A_q^* a_q\right) \qquad 4.3$$

where ψ^+ and ψ are similar to a_q^+ and a_q but apply to the electronic state of the isolated impurity ion. (They satisfy the Fermi-Dirac anticommutation relations).

The phonon index ranges over a complete set of lattice vibration modes, and includes those induced by the presence of the impurity ion.

The Aq are coupling coefficients for the coupling of the phonon modes to the electronic level. They are not necessarily the same for each electronic level.

For the transition between two levels, consider a wavefunction of the form $|v_q^a\rangle |u_a\rangle$

$|u_a\rangle$ is the wavefunction for the a 'th electronic level

$|v_q^a\rangle$ is the q' th vibrational wavefunction associated with the a th electronic level.

Hence the total transition probability can be taken as

$$P_{a\to b} = |\langle u_a | p_{ee} | u_b \rangle|^2 \prod_q |\langle v_q^a | v_q^b \rangle|^2 \qquad 4.4$$

where a thermal average is to be also made.

p_{ee} is the appropriate dipole operator for the transition (i.e. electric, magnetic etc.)

(The adiabatic and Franck Condon approximations have been assumed).

Several methods can be used to calculate the spectral distribution function from this (see references). Result for emission from a → b (absorption spectra is similar and involves only a change of sign in some of the equations below) is (neglecting matrix elements for dipole operator)

$$W(\omega) = \frac{1}{2\pi} \int_{-\infty}^{\infty} \exp\left[i\omega t + f(t)\right] dt \qquad 4.5$$

ω is frequency of emitted light

and $$f(t) = \frac{-i\bar{\varepsilon} t}{\hbar} - \gamma + g(t)$$

where $$\bar{\varepsilon} = \varepsilon - \sum_q \frac{|C_q|^2}{\hbar\omega_q}$$

and $$\gamma = \sum_q \frac{|C_q|^2}{(\hbar\omega_q)^2}(1 + 2n_q)$$

$$g(t) = \sum_q \frac{|C_q|^2}{(\hbar\omega_q)^2}\left[(1+n_q)\exp(i\omega_q t) + n_q \exp(-i\omega_q t)\right]$$

average number of phonons $$n_q = \left[\exp\left(\frac{\hbar\omega_q}{kT}\right) - 1\right]^{-1} \qquad 4.6$$

C_q is a coupling parameter related to the Aq

$$\text{e.g.} \quad |C_q|^2 = |A_q^a - A_q^b|^2$$

Therefore equation 4.5 can be expressed as

$$W(\omega)\, e^{\gamma} = \frac{1}{2\pi}\int_{-\infty}^{\infty} \exp\left[i\omega t - \frac{i\bar{\varepsilon}t}{\hbar}\right] \exp[g(t)]\, dt$$

Expanding $\exp[g(t)]$ as a power series and using the integral form for the δ function

$$\delta(x) = \frac{1}{2\pi}\int_{-\infty}^{\infty} e^{ixt}\, dt.$$

we have $$W(\omega)\, e^{\gamma} = \delta\left(\omega - \frac{\bar{\varepsilon}}{\hbar}\right) + \frac{1}{2\pi}\int_{-\infty}^{\infty} g(t) \exp(i\omega t)\, dt$$

$$+ \frac{1}{2\pi}\int_{-\infty}^{\infty} \frac{[g(t)]^2}{2!} \exp(i\omega t)\, dt$$

$$+ \frac{1}{2\pi}\int_{-\infty}^{\infty} \frac{[g(t)]^3}{3!} \exp(i\omega t)\, dt$$

$$+ \text{- - - - - - -}$$

4.7

In equation 4.7 the first term $\delta\left(\omega - \frac{\bar{\varepsilon}}{\hbar}\right)$ corresponds to the "no-phonon" line or 'pure' electronic transition. It is shifted by the phonon interaction by an amount $\sum_q \frac{|C_q|^2}{\hbar\omega_q}$ from that for a static crystal field. This shows that in general the no-phonon line position is not the correct one for crystal field calculations. (From spectral moment the value required is the average frequency for the spectral distribution).

The relative intensity of the no-phonon line is $\exp\left\{-\sum_q \frac{|C_q|^2}{(\hbar\omega_q)^2}(1+2n_q)\right\}$. It is a resonance line (i.e.

occurs in absorption also) and in the approximation here, has zero width. From this expression it can be seen that there are three main factors favouring the appearance of a no-phonon line.

1. Low temperatures.
2. High Debye temperature for the host lattice.
3. Low Stoke's losses. This really implies that $|C_q|^2$ is small or the coupling parameter almost identical for the two states. If they were identical, we would get back to the normal electronic transition.

The other terms in 4.7 give rise to one, two, etc. phonon bands in the vibronic spectra.

For the one phonon band

$$\frac{1}{2\pi}\int_{-\infty}^{\infty} g(t)\exp(i\omega t)\,dt = \sum_q \frac{|C_q|^2}{(\hbar\omega_q)^2}\left\{(1+n_q)\,\delta(\omega - \frac{E}{\hbar} + \omega_q) + n_q\,\delta(\omega - \frac{E}{\hbar} - \omega_q)\right\}$$

This gives lines displaced by the lattice frequencies ω_q from the no-phonon line. These arise from absorption (low energy side) or emission (high energy side) of a phonon accompanying the electronic transition. At low temperatures $n_q \sim 0$ and the emission of phonon is negligible. The band shape on the side of the no-phonon line can be represented by

$$\frac{\rho(\bar{\omega})}{(\hbar\bar{\omega})^2}$$

where $\bar{\omega}$ is the displacement frequency from the no-phonon line

and $\rho(\bar{\omega}) = \sum_q |C_q|^2\,\delta(\bar{\omega} - \omega_q)$ is an effective density of states for the lattice phonons. It is the actual density, $S(\omega)$, weighted by the coupling parameters $|C_q|^2$. For acoustic phonons $|C_q|^2 \sim \frac{\hbar\omega}{2Mv^2}$

where M is mass of crystal

$\bar{v}$ is the average sound velocity

Hence $\rho(\bar{\omega}) \sim \bar{\omega}\ S(\bar{\omega})$ i.e. the one phonon side band has a shape related to $\frac{S(\bar{\omega})}{\bar{\omega}}$. It can be shown from this

that any peculiarities (e.g. a discontinuity) in the phonon spectrum will also occur in the vibronic spectra.

Experimentally it is found that there are marked differences in the vibronic spectra for different impurities in the same host lattice (see for example CaF_2 with Eu^{++} M.V. Hobden Phys. Lett. 15 10 (1965), Ce^{+++} C.W. Struck and F. Herzfeld J. Chem. Phys. 44 464 (1966) and uranium figure 4.7). There are several probable reasons for the differences.

1. Local modes due to different impurity ions will be different. This should only change a few features since the number of local modes is expected to be small.
2. Selection rules may restrict some vibrations from occurring. For instance, parity considerations may prevent odd (or even) parity phonons occurring.
3. Variations in the coupling parameters $|C_q|^2$ Variations of these can influence the intensities of the structure in the vibronic spectra. Many vibronic spectra show lines at the same frequencies but they have quite different relative intensities.

On the high energy side of the no-phonon line, there will be an a proximate mirror image of the vibrational structure, but it will be decreased in intensity by a factor $n_q / 1 + n_q$

For the two phonon band

$$\frac{1}{2\pi}\int_{-\infty}^{\infty} \frac{[g(t)]^2}{2!} e^{i(\omega t)}\, dt = \frac{1}{2}\sum_{qq'} \frac{|C_q|^2 |C_{q'}|^2}{(\hbar\omega_q \hbar\omega_{q'})^2} \Big\{ (1+n_q)(1+n_{q'})\,\delta(\bar{\omega} - \omega_q - \omega_{q'})$$
$$+ (1+n_q)\, n_{q'}\, \delta(\bar{\omega} - \omega_q + \omega_{q'})$$
$$+ n_q (1+n_{q'})\, \delta(\bar{\omega} + \omega_q - \omega_{q'})$$
$$+ n_q n_{q'}\, \delta(\bar{\omega} + \omega_q + \omega_{q'}) \Big\}$$

For $\bar{n}_q \sim 0$ only the combination band $\omega_q + \omega_{q'}$ will be important. The relative intensity of each frequency being

$$\frac{1}{2} \frac{|C_q|^2 \; |C_{q_1}|^2}{(\bar{n}\omega_q \; \bar{n}\omega_{q'})^2}$$

If in general the $|C_q|^2$ are small then the combination band will be very weak compared to the one phonon band. If however, we have a strong δ function vibration, such as a local mode, its coupling parameter may be large so that it appears as an intense sharp line in the vibronic spectra. On the side of this line will be the vibronic structure $A(\omega)/\omega^2$ similar to that for the no-phonon line.

Peaks due to the lattice phonon spectrum will not, in general, show this side structure since they arise not from a single δ function type frequency but rather from a large density of relatively small amplitude δ functions in a small frequency range. It is possible for this effect to occur even if the local mode does not appear as a sharp line, since interactions, not considered here, may cause considerable broadening of it.

If, in general, the vibrational spectrum has several function type singularities in it, then sharp lines will occur at $E/\hbar - \sum_i p_i \omega_i$ in the vibronic spectrum.

where ω_i is the local mode frequency

and p_i is a positive or negative integar.

The relative intensity of the lines is $I_i \prod R_{p_i}$

where $R_{p_i} = \exp\left[-\frac{|C_i|^2}{(\bar{n}\omega_i)^2}(n_i+1)\right]\left(\frac{n_i+1}{n_i}\right)^{\frac{p_i}{2}} I_{p_i}\left(2\frac{|C_i|^2}{(\bar{n}\omega_i)^2}\sqrt{n_i(n_i+1)}\right)$

and $I_p(z)$ is the Bessel function of imaginary argument.

On the side of each δ function singularity will be a vibrational structure related to $\frac{S(\omega)}{\omega}$

Spectral moments for the emission spectrum can be calculated from the correlation function $\exp[f(t)]$
The n ' th order moment being given by

$$\mu_n = \frac{1}{i^n} \frac{d^n}{dt^n} \exp[f(t)]\Big|_{t=0}$$

Zero order moment $\mu_0 = 1$ Therefore, the area under the spectral curve is constant with temperature.
First order moment,

$$\mu_1 = \frac{\bar{E}}{\hbar} + \sum_q \frac{|C_q|^2}{\hbar^2 \omega_q} = \frac{\bar{E}}{\hbar}$$

gives the mean frequency for the spectral band. This corresponds to the value for the static crystal field. The separation of this from the no-phonon lines gives a value of

$$\sum_q \frac{|C_q|^2}{\hbar^2 \omega_q}$$

Second order moment,

$$\mu_2 = \sum_q \frac{|C_q|^2}{\hbar^2 \omega_q} (2n_q + 1)$$

gives the effective width of the emission band and this is temperature dependent.

Higher order moments can be calculated similarly.

In Chapter V further interactions will be considered that make the no-phonon line to have a temperature dependent width and position. Several other interactions and their effects are also discussed.

VIBRATIONAL SPECTRA

Since the phonon spectra are important in the interpretation of the luminescence (or absorption) spectra, some consideration is given below to its structure. The vibrations present in a crystal arise from two more or less distinct cases.

1. Lattice modes due to the host lattice itself. These can be represented by travelling waves extending throughout the whole lattice and hence not greatly effected by the presence of impurities.

2. Local modes due to the impurity ion in the lattice. These modes have an exponential decay away from the impurity centre and hence they are confined to a single centre. Local modes can arise from several causes.

(a) A light impurity can cause a δ function singularity in the frequency spectrum. This normally occurs in a gap of the lattice phonon spectrum.

(b) A heavy impurity will cause a resonance enhancement of the low frequency acoustic modes of the lattice. This will give a peak in the low frequency portion of the spectrum but it is not a δ function singularity.

(c) Internal modes of the impurity itself, if it is a molecular group. These will be just the normal modes for the molecule but influenced by the lattice. They should give some δ function singularities (more likely they will be broadened and will appear as such in the vibronic spectra).

Some discussion on these types of modes and methods of calculation can be found in:

A.A. Maradudin, E.W. Montroll and G.H. Weiss. Solid State Physics. Suppl. 3 (1963)

P.G. Dawber and R.J. Elliott Proc. Roy. Soc. A273 222 (1963)

Singularities in the phonon spectrum $S(\omega)$, can appear as singularities in the vibronic spectrum. These represent easily discernable structure and it is of interest to know the origin or significance of them.

For a lattice in the harmonic approximation, the normal coordinates for the vibrations are plane waves which can be specified by a wave vector q lying inside the first Brillouin zone and by a branch index j. (this also specifies the phonons). For the fluorite (CaF_2) lattice, there are

three acoustic and six optic branches. Figure 4.1 gives the Brillouin zone for the fluorite lattice (which is face centred cubic) and the special points with the usual notation.

To obtain the significance of the structure in the phonon spectrum, the dispersion relations for the vibrational branches need to be considered. Using a suitable model for the crystal lattice (usually either the rigid ion or the shell model is used) these can be calculated. S. Ganesan and R. Srinivasan, Canadian J. Phys. 40 74 (1962) have calculated the dispersion curves for CaF_2 on essentially the rigid ion model. D. Criber, B. Farnoux, B. Jacrot, "Inelastic Scattering of Neutrons in Solids" Vol. II p. 225 I.A.E.A. Vienna 1963, have found the dispersion curves experimentally by neutron scattering for two lattice directions. While their results are not very complete for other than $\underline{q} = 0$, they do show that the work of Ganesan and Srinivasan is essentially correct. Figure 4.2 gives the dispersion curves calculated and the experimental points.

From the dispersion curves for all directions in the lattice it is possible to calculate the phonon spectrum from

$$S(\omega) = 2\omega \frac{v_a}{r} \sum_j \iint \frac{dS}{|\mathrm{grad}_{\underline{q}}\, \omega_j^2(\underline{q})|}$$

where the integration is carried out over the constant frequency surface $\omega^2 = \omega_j^2(\underline{q})$

$S(\omega)$ is the fraction of normal modes in the frequency interval ω to $\omega + d\omega$ for $d\omega \to 0$

v_a = volume of the unit cell (for the direct lattice)

r = number of atoms in the unit cell (3 for CaF_2)

Along certain symmetry directions in $\underline{q}$ space Van Hove singularities occur at frequencies $\omega = \omega_j^c$, where

$$\mathrm{grad}_{\underline{q}}\, \omega_j^2(\underline{q})\Big|_{\omega_j^c} = 0$$

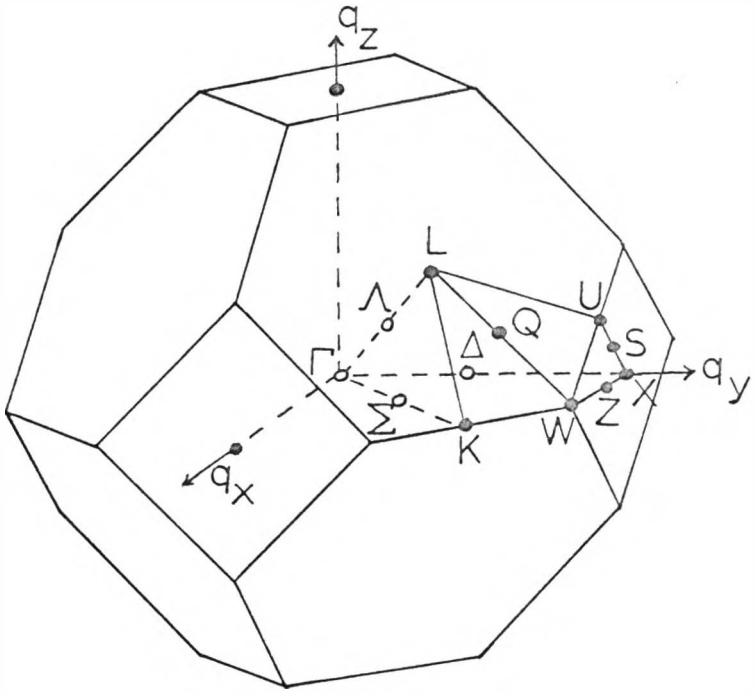

FIG. 4.1 BRILLOUIN ZONE FOR A FACE CENTRED CUBIC LATTICE, m3m, SHOWING SYMMETRY POINTS.

(for notation see G.F. Koster Solid State Physics 5 173 1957)

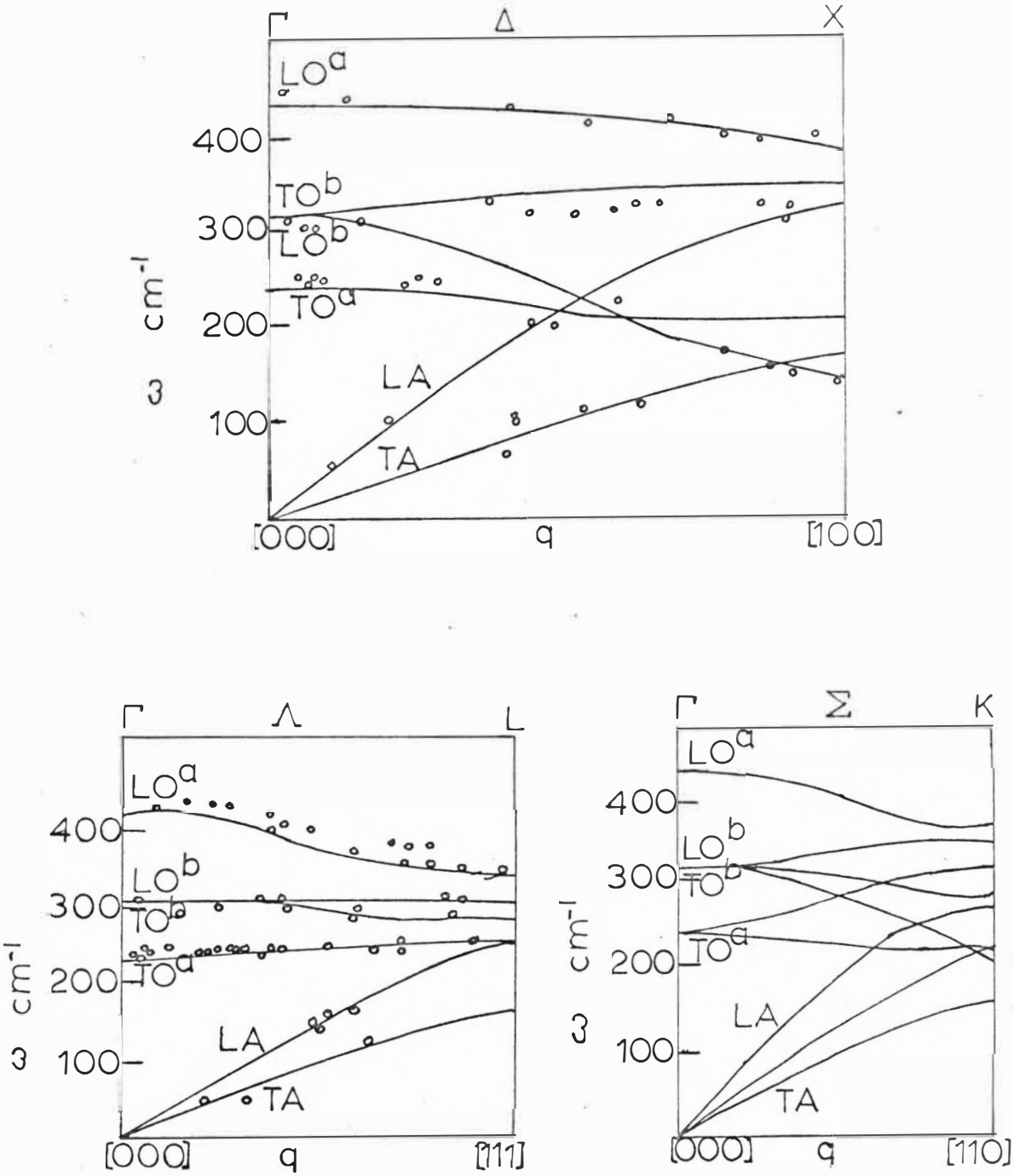

FIG. 4.2 DISPERSION CURVES FOR CALCIUM FLUORIDE

—— Theory ∘ Neutron data

These are referred to as critical points and they cause some form of singularity or discontinuity in $S(\omega)$. Some critical points can arise from considerations of the crystal symmetry to give a symmetry set. Others will come from turning points in the dispersion curves and also cross over points. Not all singularities will of course appear as peaks and some will even appear as dips. The critical points will not necessarily exhaust all the structure in the phonon spectra. It is possible for peaks to arise from accidental causes.

The symmetry set of critical points are those at Γ, L, X and W in the Brillouin zone for CaF_2. (see Figure 4.1) These points have a higher symmetry than a general point in the Brillouin zone and hence there may be selection rules forbidding the phonons at these points from appearing in the vibronic spectra. For lower symmetry points all phonons may couple with the electronic transition. Methods for calculating by group theory which ones will occur are given by R. Loudon, Proc. Phys. Soc. 84 379 (1964).

All the phonons in CaF_2 can be labelled according to the irreducible representation of the space group Fm3m (O_h^5) for the lattice. Phonons at the critical points are labelled by the point group of the point. For the CaF_2 lattice, the point groups associated with symmetry set are

Γ is m3m (Oh) at $\underline{q} = o$

L is $\bar{3}$ m (D_{3d}) at $\left[\frac{1}{2}, \frac{1}{2}, \frac{1}{2}\right]$

X is 4/m m m (D_{4h}) at $[o, o, 1]$

W is $\bar{4}$ 2 m (D_{2d}) at $\left[\frac{1}{2}, o, 1\right]$

Directions of interest are along [111] Λ 3m(C_{3v})

[110] Σ 2mm (C_{2v})

[100] Δ 4mm (C_{4v})

(For notation and group theory see V. Heine "Group Theory in Quantum Mechanics" Pergamon Press 1960).

Figure 4.3 gives the phonon species (irreducible representations) at the symmetry points of possible interest. They are for CaF_2 and are from S. Ganesan and E. Burstein J. de Phys. 26 645 (1965), though the notation is that of Loudon (who gives a different assignment for the point L). It should be noted that for work on the lattice vibrations of CaF_2 there are many discrepancies between various authors on assignments. So while the assignments made here are believed to be correct, they cannot be relied on until an extensive study of the CaF_2 lattice is made.

Figure 4.3

SYMMETRY POINTS AND PHONON SPECIES IN CALCIUM FLUORIDE STRUCTURE

Symmetry Point	Phonon Species
Γ	$2\Gamma_{15}^{-}$ (A, O^a) + Γ_{25}^{+} (O^b)
X	X_1^{+} (LA) + X_5^{+} (TA) + X_2^{-} (LO^b) + X_4^{-} (LO^a) + $2X_5^{-}$ (TO^a, TO^b)
L	$3L_2^{-}$ (LA, LO^a, LO^b) + $3L_3^{-}$ (TA, TO^a, TO^b)
W	$W_1 + W_1' + W_2' + 2W_2' + 2W_3$
Δ	$2\Delta_1$ (LA, LO^a) + $3\Delta_5$(TA, TO^a, TO^b) + Δ_2'(LO^b)
Λ	$3\Lambda_1$(LA, LO^a,LO^b) + $3\Lambda_3$(TA, TO^a, TO^b)
Σ	$3\Sigma_1$(LA, LO^a,LO^b) + Σ_2($TO_1{}^b$) + $3\Sigma_3$(TA_1,$TO^a{}_1$,$TO_2{}^b$) + $2\Sigma_4$(TA_2,TO_2^a)

The phonon species are labelled whether they are longitudinal (L) or transverse (T) acoustic (A) or optic (O) branches. There are two optic branches, one at Γ is infra-red active (O^a) and the other Raman active (O^b). The transverse modes are usually doubly degenerate, but along Σ they split (e.g. TO_1 and TO_2).

Besides Cribier et al. the other main experimental data on CaF_2 is given by:-

W. Kaiser, W.Y. Spitzer, R.H. Kaiser, L.E. Howarth Phys. Rev. 127 1950 (1962) (This gives infra-red data on CaF_2, SrF_2 and BaF_2).

S.J. Fray, F.A. Johnson, J.E. Quarrington "Lattice Dynamics" Ed. R.F. Wallis p. 377 Pergamon Press 1965 (Gives the two phonon infra-red absorption bands for CaF_2, assignments are in doubt.)

J.P. Russell Proc. Phys. Soc. 85 194 (1965) (Raman Spectra, but also spurious effects, see Ganesan and Burstein).

The most accurate values known are those for Γ as this can be assigned fairly well from neutron scattering. Values at the other points are not so well known as the neutron data is not complete there. The values that will be used are taken as a best fit to known infra-red data and the calculated dispersion curves. Values of the phonon frequencies are temperature dependent and most measurements have been taken at room temperature, so that there can be differences at low temperatures.

For CaF_2 at Γ $\quad LO^a = 475\ cm^{-1}$, $TO^a = 258\ cm^{-1}$
$TO^b = LO^b = 322\ cm^{-1}$

For SrF_2 at Γ $\quad LO^a = 374\ cm^{-1}$, $TO^a = 217\ cm^{-1}$
$TO^b = LO^b = 280\ cm^{-1}$

(These values are not so accurate, Raman data from J. Richman Phys. Rev. 133 A1364 (1964)

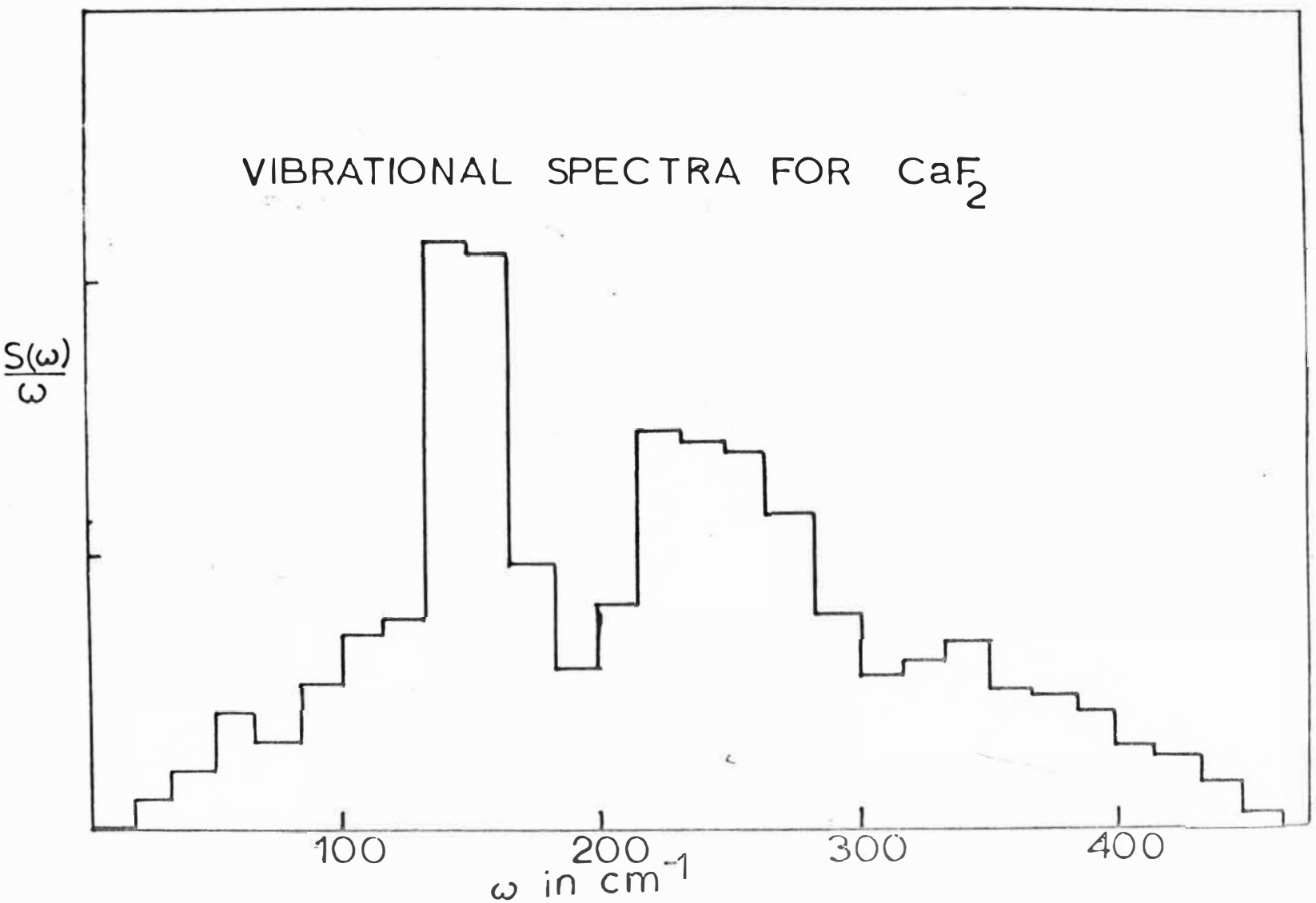
VIBRATIONAL SPECTRA FOR CaF_2
$\frac{S(\omega)}{\omega}$
100
200
300
400
ω in cm^{-1}

Figure 4.4

Figure 4.4 gives a calculated phonon spectrum for CaF_2. It is in the form of a histogram, since the method of calculation requires sampling of $\underset{\sim}{q}$ values in the Brillouin zone. The calculation was made by F.A. Johnson and C.T. Sennett (to be published) and reported by R.J. Elliott, W. Hayes, G.D. Jones, H.F. Macdonald and C.T. Sennett, Proc. Roy. Soc. A289 1 (1965). (This paper compares it to the vibrational structure accompanying an infra-red absorption line due to a local mode phonon of H^- ions in CaF_2. They show a reasonable agreement. The theory for the absorption can be made formally similar to that for the vibronic spectra if ψ^+ and ψ are replaced by b^+ and b, corresponding to the local mode phonon operators). This spectrum appears to be based on the rigid ion model and not the shell model which is usually better and would give quite a different spectrum. The sampling in $\underset{\sim}{q}$ space seems rather coarse to show up any relevant fine structure (see A.M. Karo and J.R. Hardy Phys. Rev. 141 696 (1966) who show that for NaCl rather fine sampling is required). Accurate calculations for the phonon spectrum are required before any unambiguous assignment can be made for the vibronic spectra. Karo and Hardy for NaCl showed that many peaks in the phonon spectrum are associated with critical points not on the zone boundaries.

Comparing figures 4.4 and 4.5, it can be seen that there is little relationship between the two spectra, contrary to that for H^- ions in CaF_2. Also other rare-earth ion spectra in CaF_2 do not show a similar structure. Some form of selection rules must therefore apply, as mentioned above in the last section.

OBSERVED SPECTRA

The luminescent spectra of several samples of CaF_2(U) and for the 'Semi-Elements' crystal of SrF_2(U) was observed at various temperatures from liquid helium to room temperature. Figures 4.5 to 4.16 give a selection of these results. The figures are uncorrected chart recorder traces from the 3.4 m spectrograph and only a portion of the spectrum is shown for

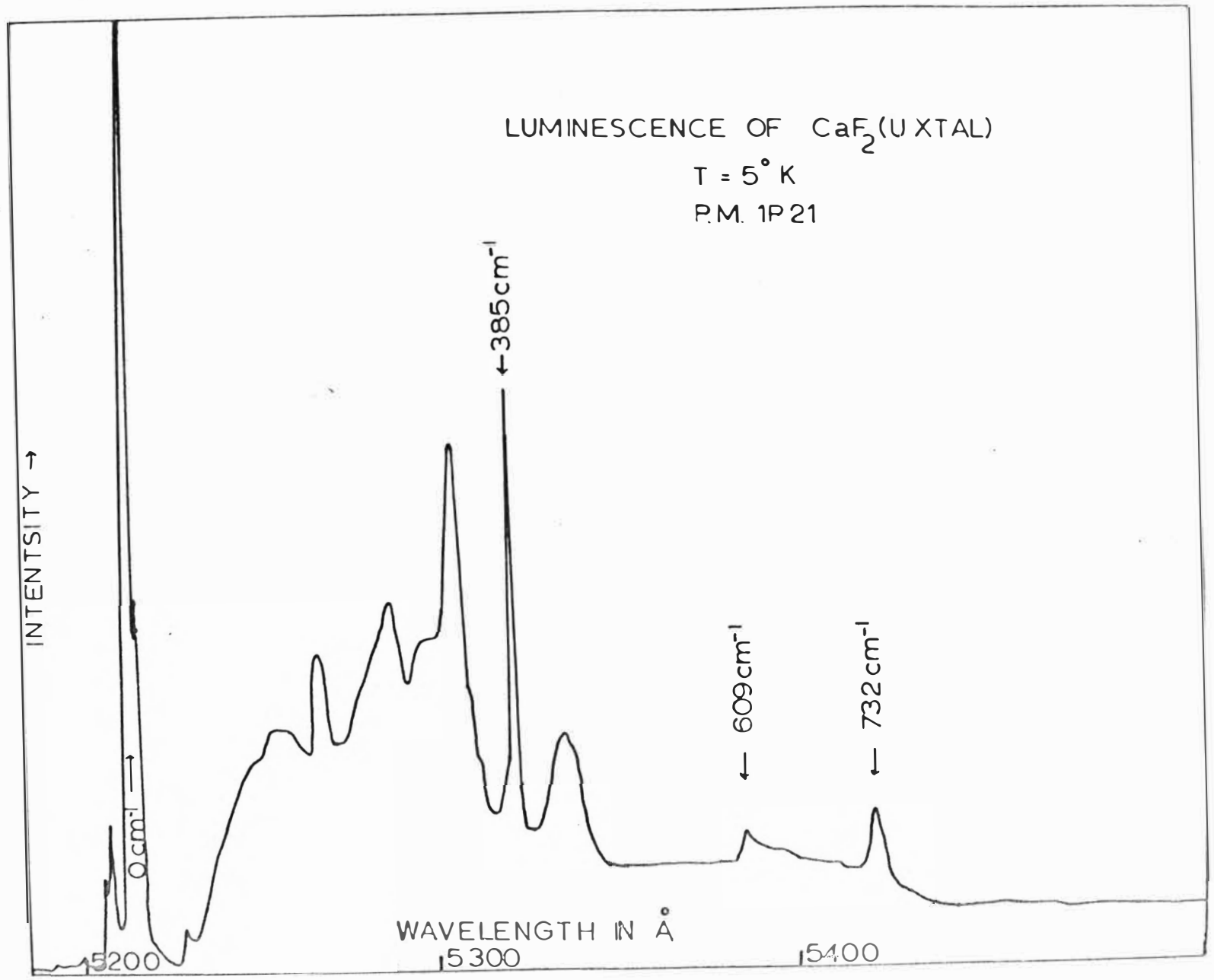
LUMINESCENCE OF CaF_2(U XTAL)
T = 5° K
P.M. 1P21
INTENTSITY →
0 cm⁻¹ →
385 cm⁻¹
609 cm⁻¹
732 cm⁻¹
WAVELENGTH IN Å
5200
5300
5400

Figure 4.5

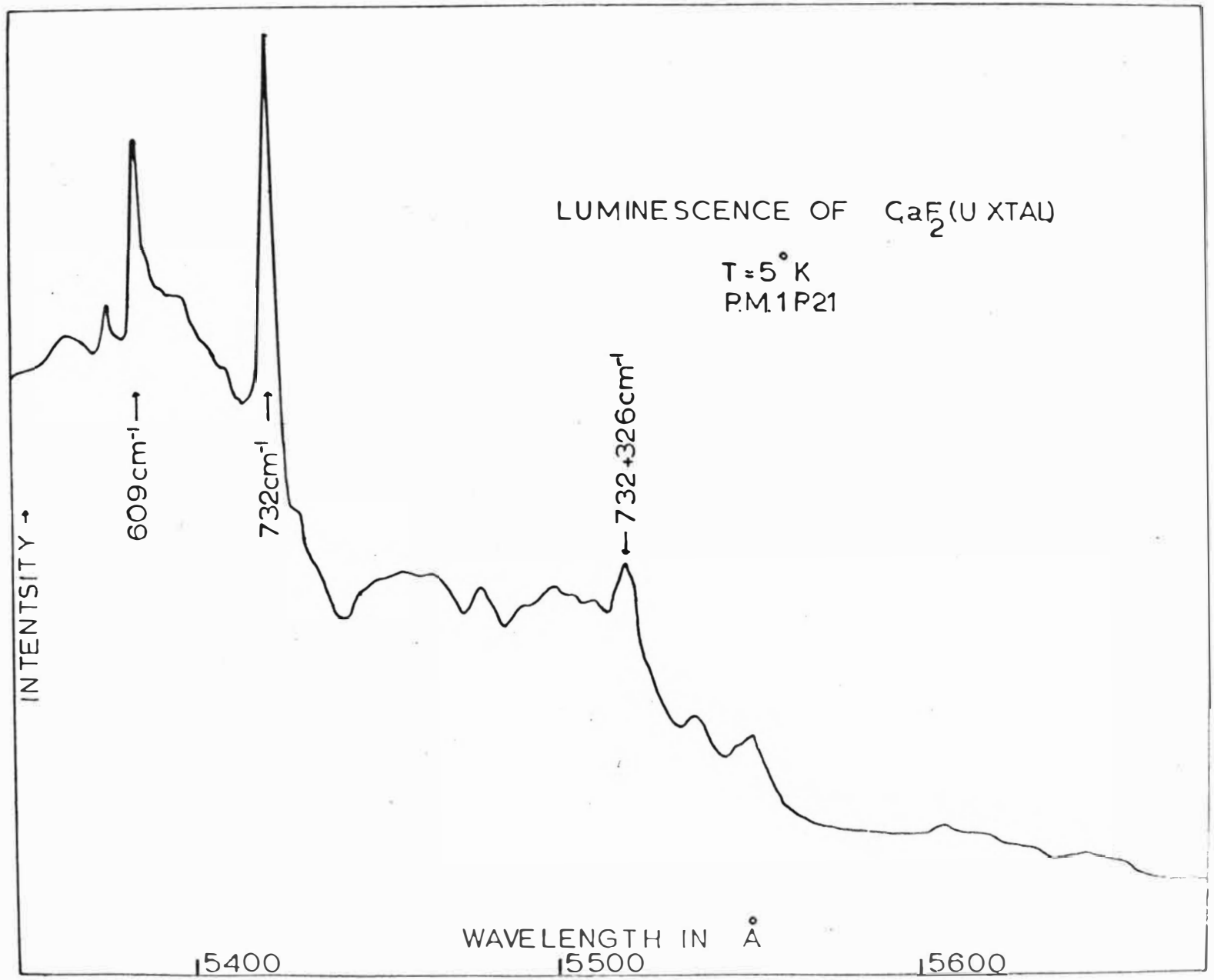
LUMINESCENCE OF CaF_2 (U XTAL)
T = 5° K
P.M.1 P21
609 cm⁻¹
732 cm⁻¹
732 + 326 cm⁻¹
INTENTSITY →
WAVELENGTH IN Å
5400
5500
5600

Figure 4.6

LUMINESCENCE OF CaF_2(U·01%)
T = 11° K
P.M. 1P21
INTENTSITY →
-51cm⁻¹
0cm⁻¹
147cm⁻¹
194cm⁻¹
266cm⁻¹
297cm⁻¹
325cm⁻¹
385cm⁻¹
438cm⁻¹
609cm⁻¹
682cm⁻¹
732cm⁻¹
WAVELENGTH IN Å
5200
5300
5400

Figure 4.7

Figure 4.8

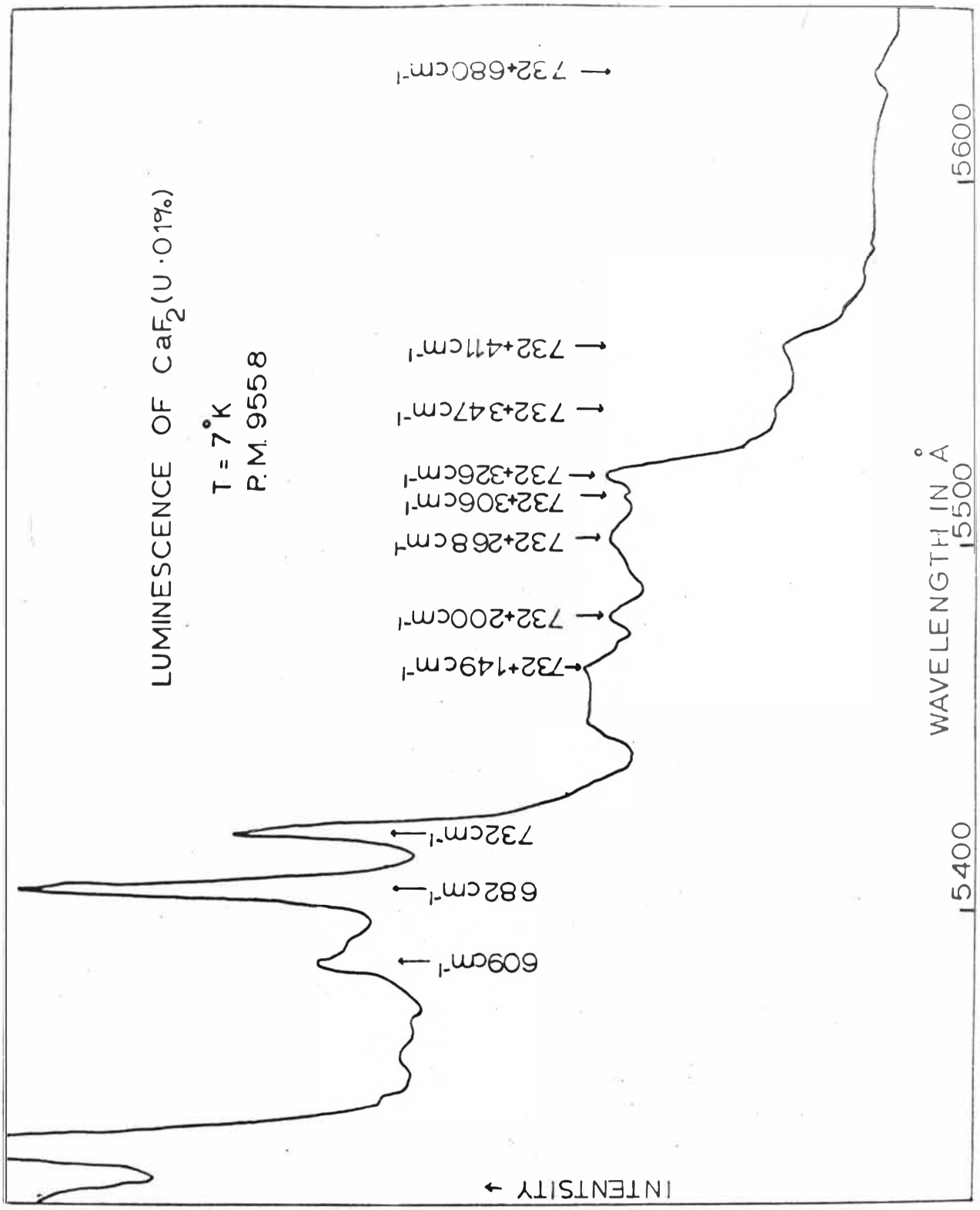
LUMINESCENCE OF CaF_2(U·01%)
T = 7°K
P.M. 9558
INTENSITY →
WAVELENGTH IN Å
15400
15500
15600
609cm⁻¹
682cm⁻¹
732cm⁻¹
732+149cm⁻¹
732+200cm⁻¹
732+268cm⁻¹
732+306cm⁻¹
732+326cm⁻¹
732+347cm⁻¹
732+411cm⁻¹
732+680cm⁻¹

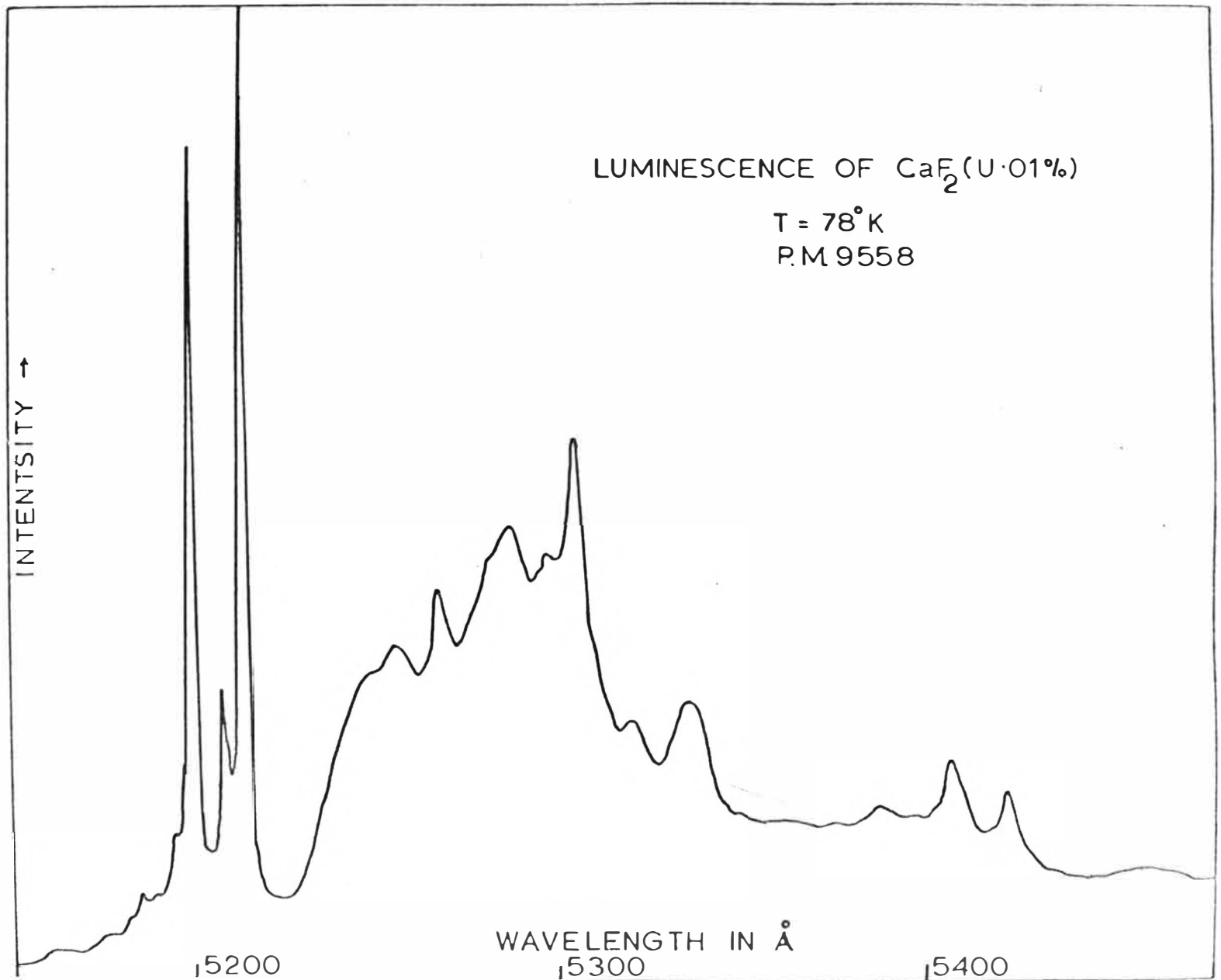
LUMINESCENCE OF CaF_2 (U·01%)
T = 78°K
P.M 9558
INTENTSITY →
WAVELENGTH IN Å
5200
5300
5400

Figure 4.9

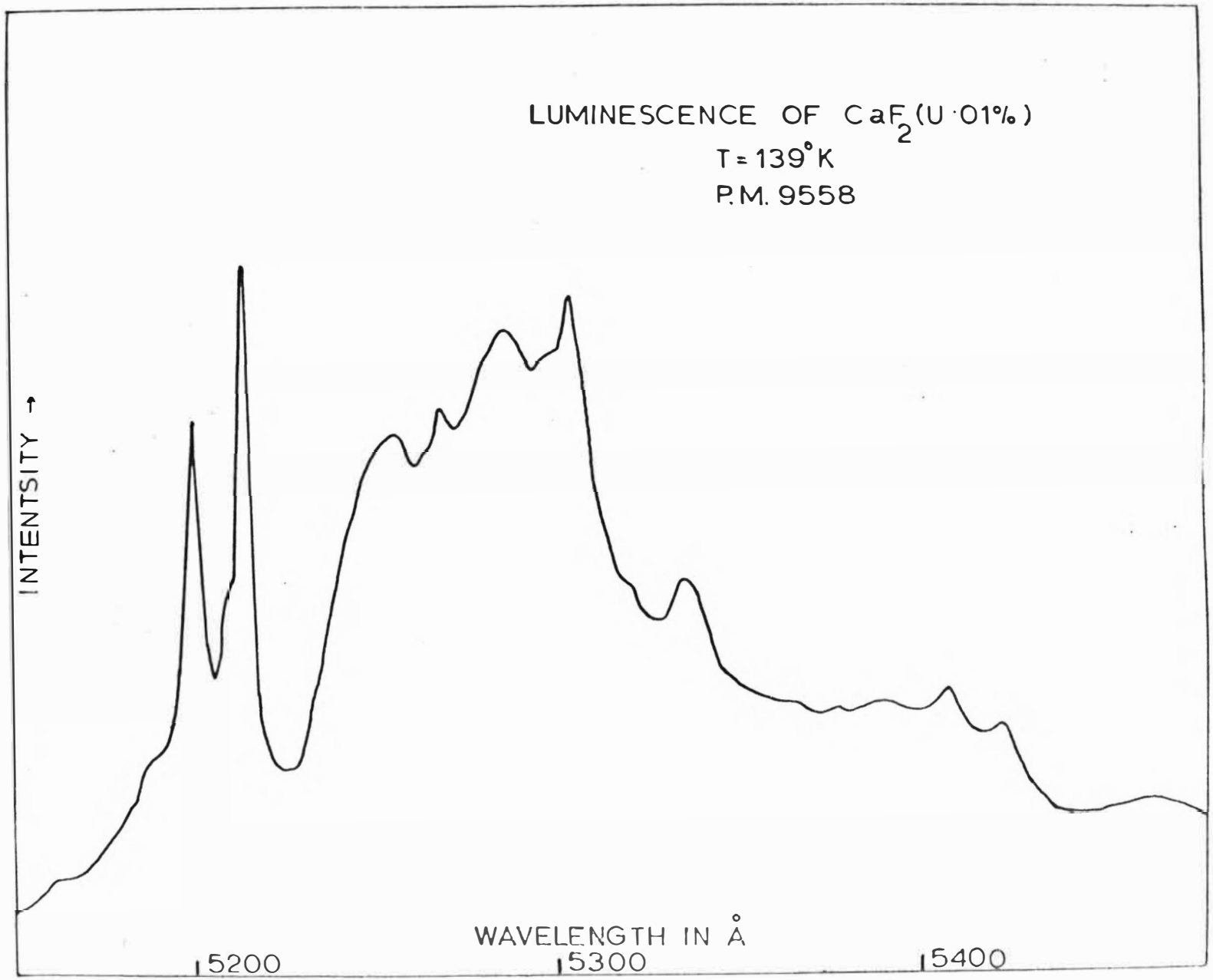
LUMINESCENCE OF CaF_2 (U·01%)
T = 139°K
P.M. 9558
INTENTSITY →
WAVELENGTH IN Å
5200
5300
5400

Figure 4.10

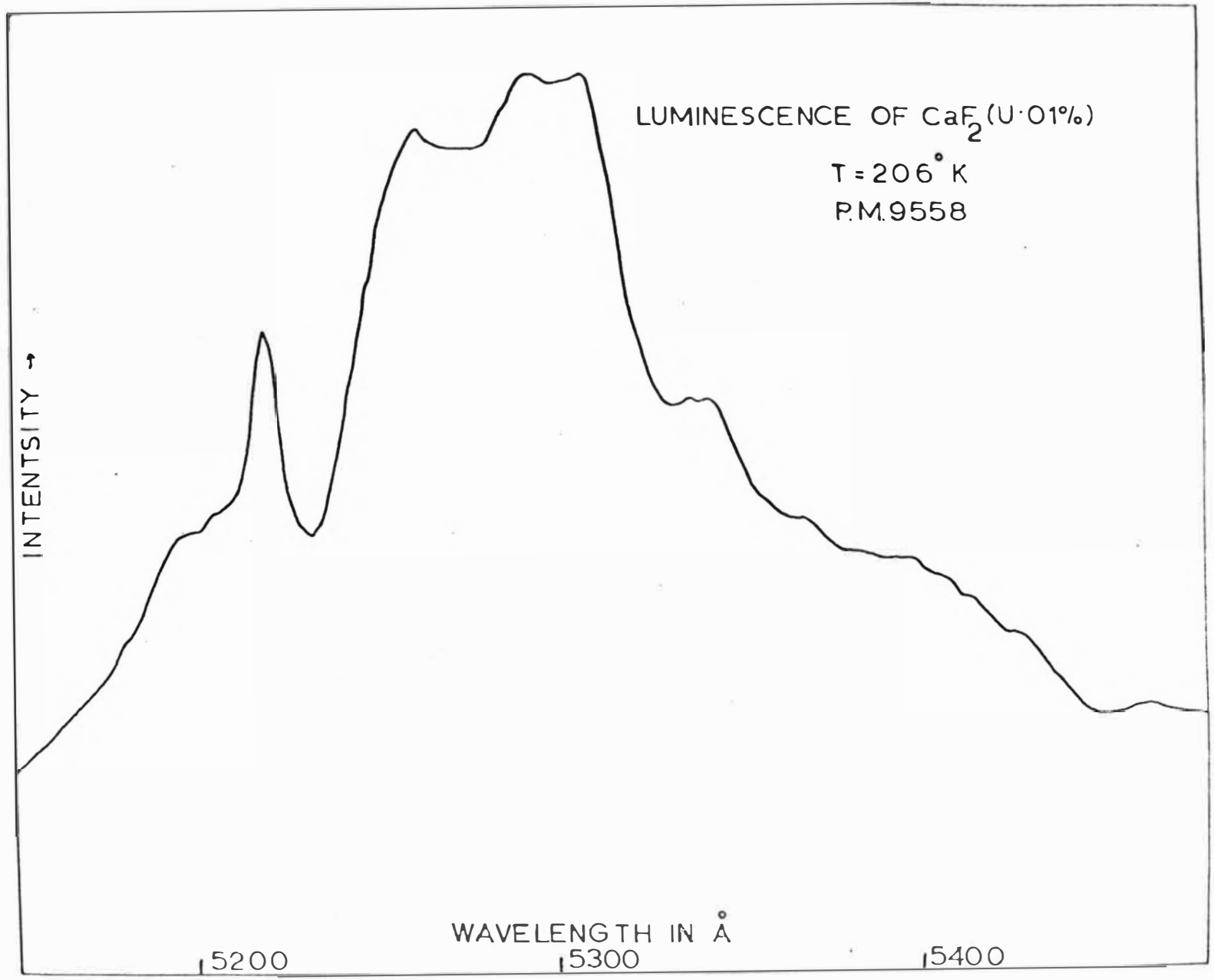
LUMINESCENCE OF CaF_2 (U·01%)
T = 206° K
P.M.9558
INTENTSITY →
WAVELENGTH IN Å
5200
5300
5400

Figure 4.11

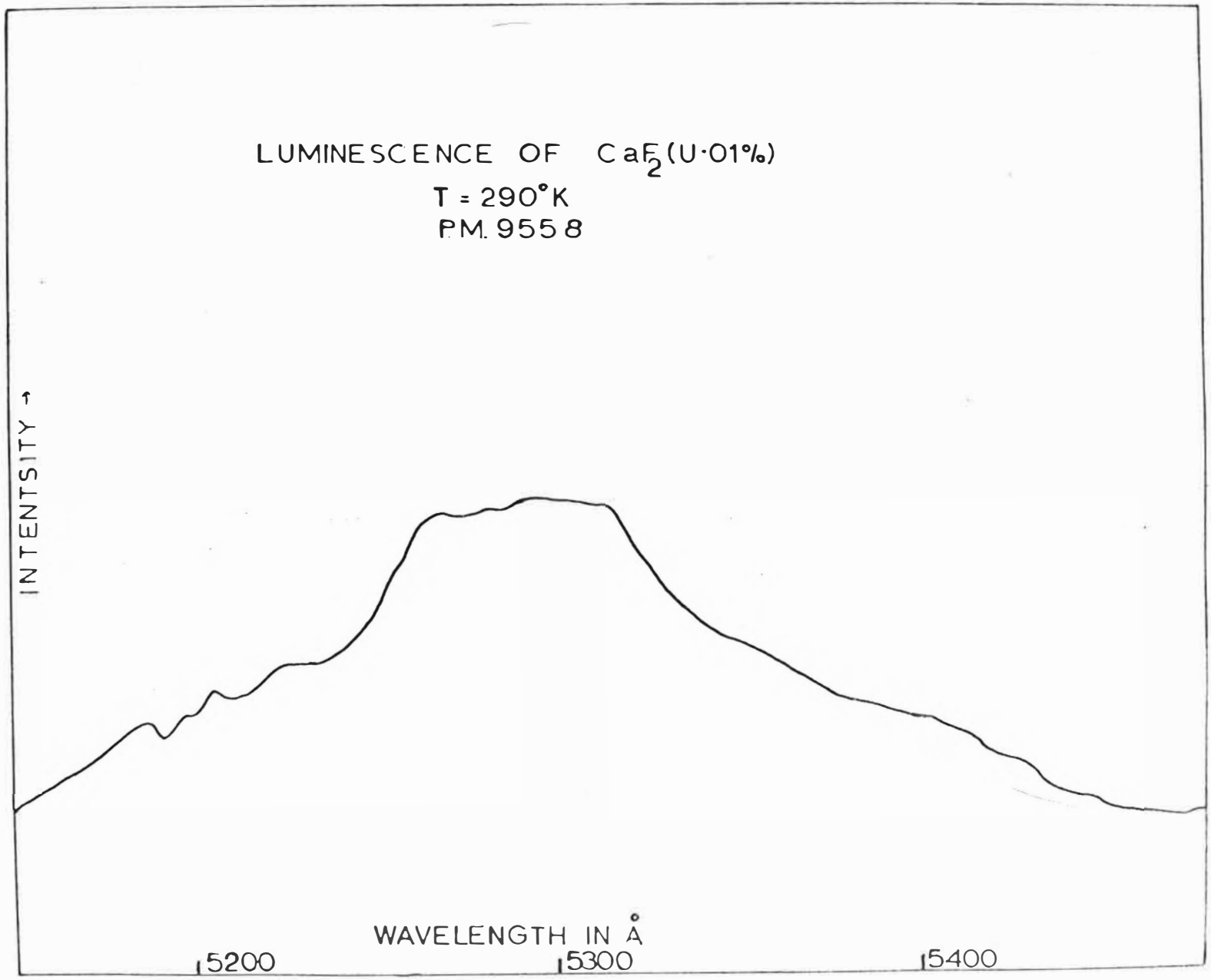
LUMINESCENCE OF CaF_2 (U·01%)
T = 290°K
P.M. 9558
INTENTSITY →
WAVELENGTH IN Å
5200
5300
5400

Figure 4.12

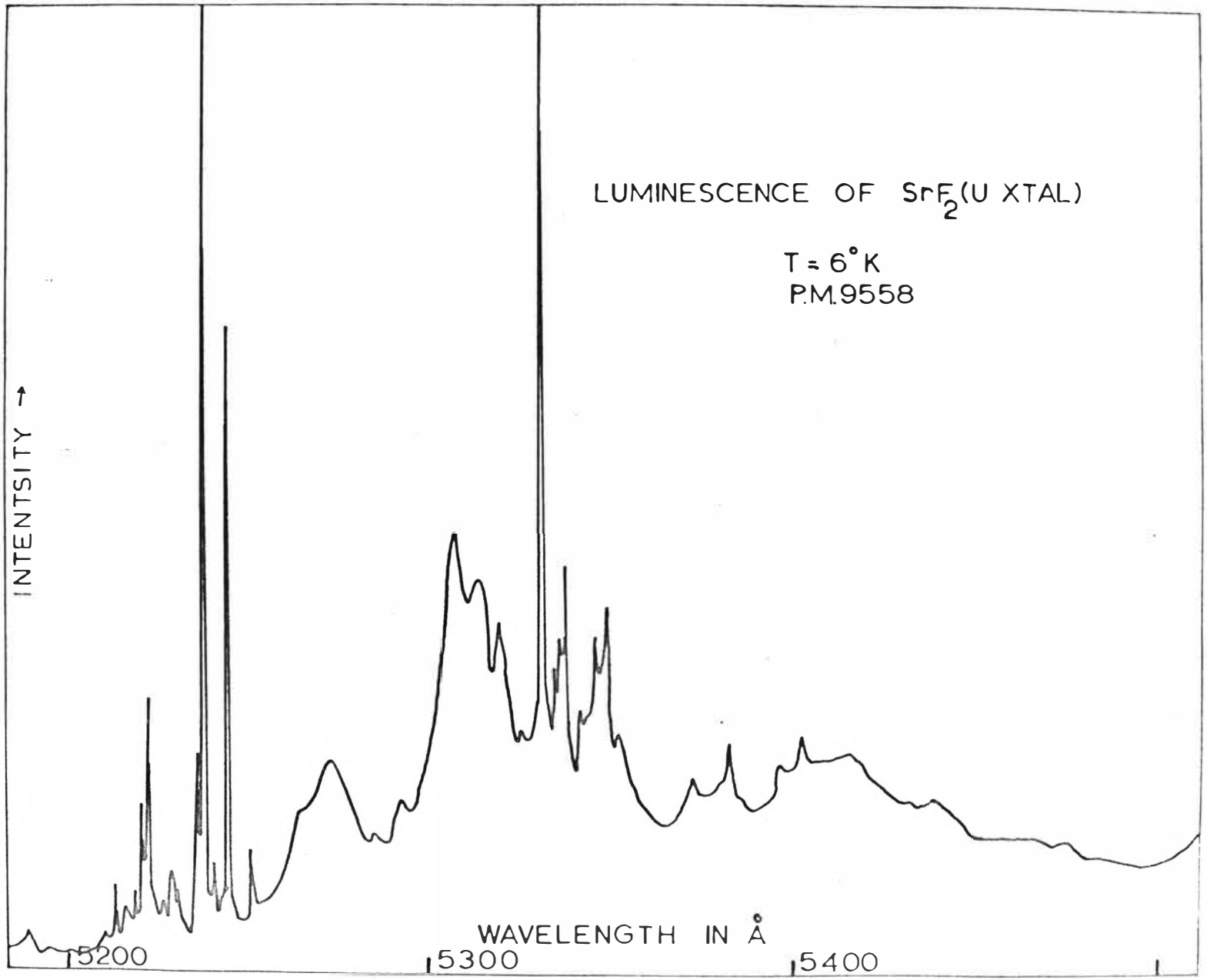
LUMINESCENCE OF SrF_2(U XTAL)
T = 6°K
P.M.9558
INTENTSITY →
WAVELENGTH IN Å
5200
5300
5400

Figure 4.13

LUMINESCENCE OF SrF_2(U XTAL)
T = 79° K
P.M. 9558
INTENTSITY →
0 cm⁻¹
125cm⁻¹
167cm⁻¹
198cm⁻¹
250cm⁻¹
292 cm⁻¹
330cm⁻¹
391cm⁻¹
510cm⁻¹
702cm⁻¹
702+121 cm⁻¹
702+250cm⁻¹
WAVELENGTH IN Å
5200
5300
5400

Figure 4.15

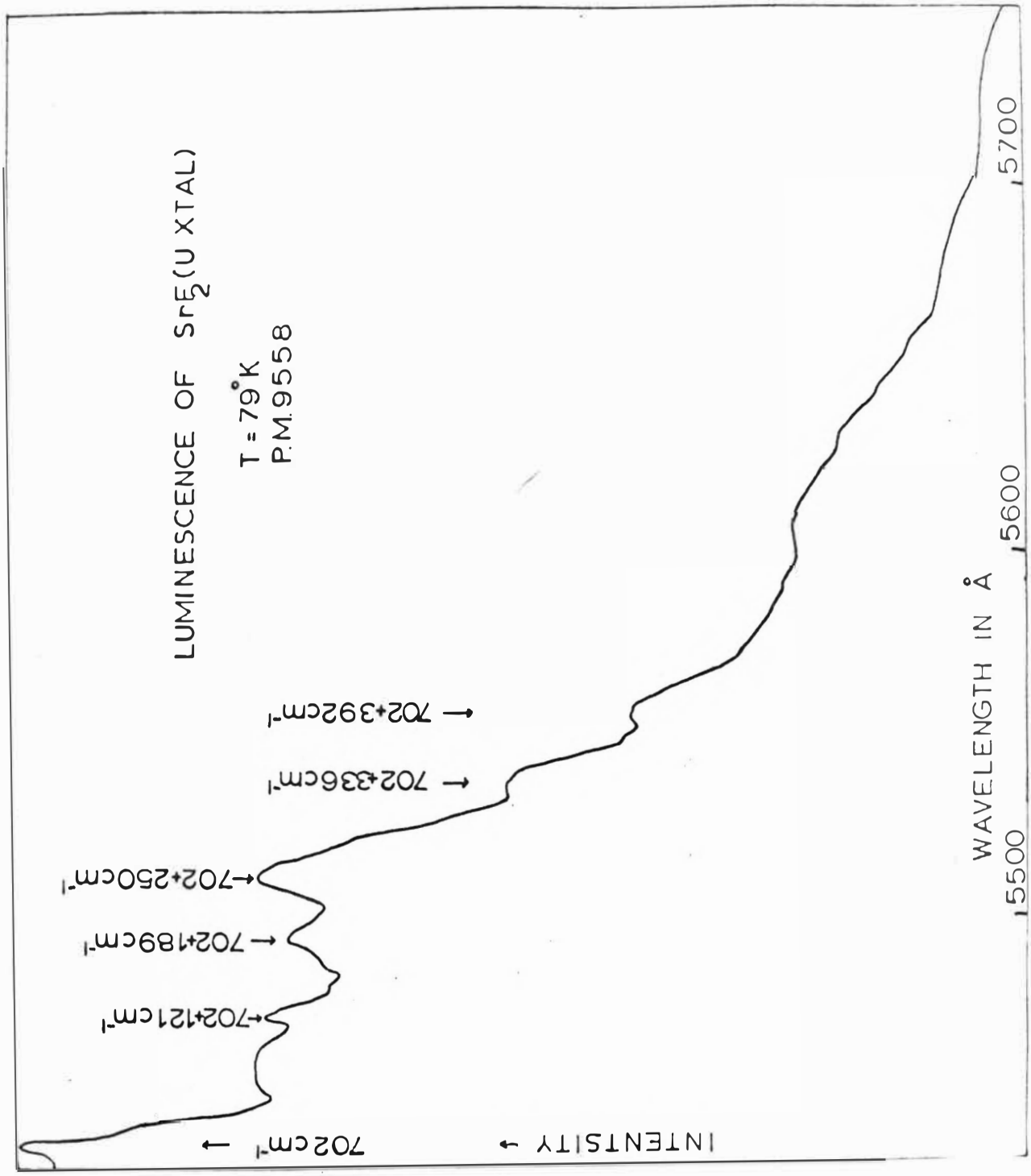
LUMINESCENCE OF SrF_2(U XTAL)
T = 79°K
P.M.9558
INTENTSITY →
WAVELENGTH IN Å
5500
5600
5700
702 cm⁻¹ →
← 702+121cm⁻¹
← 702+189cm⁻¹
← 702+250cm⁻¹
← 702+336cm⁻¹
← 702+392cm⁻¹

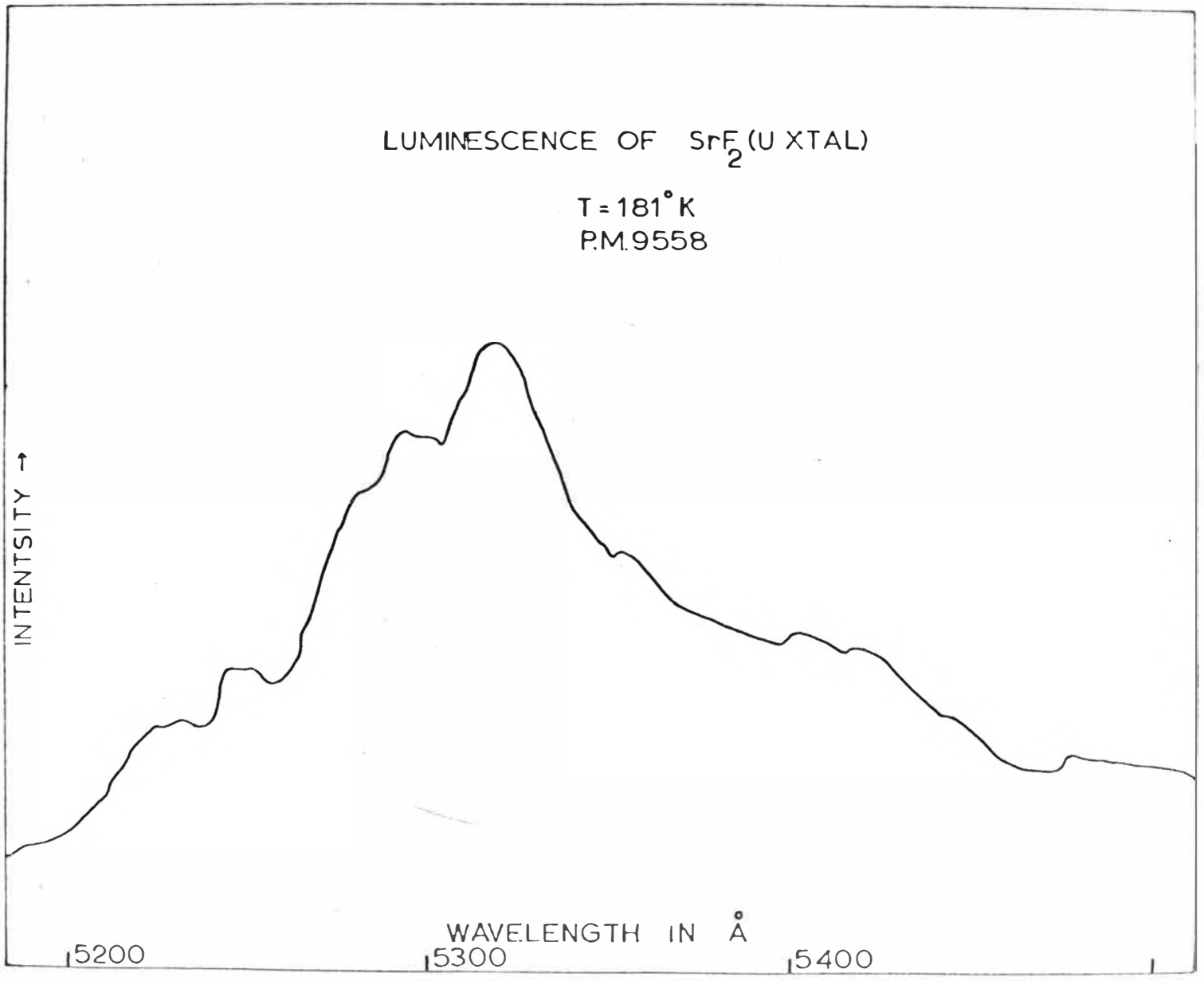
LUMINESCENCE OF SrF_2 (U XTAL)
T = 181° K
P.M. 9558
INTENTSITY →
WAVELENGTH IN Å
5200
5300
5400

Figure 4.16

each to give some idea of the vibrational structure occurring with the no-phonon lines. (These have been cut off to fit the figure on the page without losing some of the detail). The gain settings for each spectra is generally different (though known) so figures do not give a direct comparison of intensities. Some discussion of intensity relationships is given in Chapter V. For correcting the intensity, the photo-multiplier (P.M.) used is specified (from Figure 2.1 this requires the red end to be increased).

The CaF_2(U ·01%) is a powder sample made up with this concentration of uranium. CaF_2 (UXtal) refers to a crystalline sample (see Chapter II) whose concentration of uranium would be between 0·01% and 0·1%. The SrF_2 (U Xtal) refers to the treated crystal from 'Semi-Elements' (see Chapter II) and should have a uranium concentration of 0·01%.

Vibrational frequencies marked in some figures refer to energy differences, in cm^{-1}, from the no-phonon line (taken as 0 cm^{-1}). The appropriate no-phonon line is clear for CaF_2(U) but not so for SrF_2(U) where the stronger one has been taken. Figures 4.6, 4.8 and 4.15 give an enlarged view of the two phonon combination bands. These are assigned as combining with the repetitive vibrational frequency of 730cm^{-1} for CaF_2 and 702cm^{-1} for SrF_2. The pattern is fairly obvious on a photographic plate and the fit on the chart is fairly good considering the extra broadening of the lines. The repetitive frequency is most probably an internal mode belonging to the uranium centre (most likely from uranium oxygen bonds).

For CaF_2(U) (Figures 4.5 - 4.8) two different samples are shown to illustrate the variation in intensities of various lines in the spectra between the samples. This illustrates quite markedly the effect of the extra no-phonon line. In the crystal sample, there is also a considerable enhancement of the 385cm^{-1} line at 5°K, though on increasing the temperature, its intensity drops relative to the other lines. Figures 4.9 - 4.12 show the higher temperature spectra which illustrate the

typical broadening of the lines and a general shift of the spectra, shown by all samples. At about room temperature (approximately half the Debye temperature 510°K), the no-phonon lines are no longer obvious. The spectrum has now broadened out considerably.

For SrF_2(U) (Figure 4.13 - 4.16), only the crystal sample was investigated. This in some ways is similar to CaF_2(U) but has some marked differences. Some of these differences will be due to the different vibrational spectra for the SrF_2 lattice, and cannot be evaluated until this is known. However, it is not thought that this could explain all the differences.

The two no-phonon lines both appear to have similar vibrational structure on the side of them as many lines occur their separation ($23cm^{-1}$). One line being weaker is not so dominant and lines thought due to it are not indicated in the figures. As can be seen from Figures 4.13 and 4.14, there is a very marked difference on going from 6°K to 79°K for which there is no counterpart in the CaF_2(U) luminescence. The main features of this effect are the weakening (for decreasing temperatures) of a group of lines at about $180cm^{-1}$ (also the combination with $702cm^{-1}$), while a group of lines at $330cm^{-1}$ to $390cm^{-1}$ increases considerably (also the combination with $702cm^{-1}$). The $330cm^{-1}$ line (at 5330.7Å) is very sharp and has the same width as the no-phonon line. This, with its temperature dependence (see Chapter V) suggests that it is due to another electronic level of the centre. It could possibly be due to a new centre forming similar to that for CaF_2(U). However, further results are required on this as only one sample of SrF_2(U) was investigated and it is not known if this behaviour is typical.

The higher temperature spectra show a similar broadening to that of CaF_2(U) though the no-phonon lines are gone at 181°K (which is approximately half the Debye temperature 380°K).

Comparison with the results of D.L. Wood and W. Kaiser Phys. Rev. 126 2079 (1962) on Sm^{++} in CaF_2, SrF_2 and BaF_2 is

interesting. They found that the luminescence of Sm^{++} in CaF_2 and SrF_2 had the same order of magnitude in intensity while that for BaF_2 was down by a factor of 1,000. This is similar to that for uranium in CaF_2, SrF_2 and BaF_2. Also the spectra of Sm^{++} in SrF_2 and BaF_2 showed many extra electronic transitions compared to that for CaF_2. A similar effect appears to occur here for SrF_2(U). Wood and Kaiser considered the differences to come from a change in the electronic transition from electric dipole to magnetic dipole.

SELECTION RULES

Using different models for the luminescent centre, it is possible to calculate selection rules for the vibronic spectra along the lines used by Loudon (Proc. Phys. Soc 84 379 (1964). Generally selection rules allow nearly all vibrations to combine with the electronic transition but as already noted, some form of selection rules must operate for the CaF_2 lattice (even if only weakly) since the vibronic spectra for various impurities vary. Hence it is worthwhile to see if some model can be made to fit the data. For the uranium centre, there is an additional difficulty in not knowing what the electronic transition is. Hence it is hoped that using the vibronic spectra and a suitable centre, some information can be obtained on this.

The values of the phonons at Γ were given above and comparing with the vibronic spectra (Figure 4.7) there appears to be no evidence of these phonons occurring. (Possibly $TO^b = LO^b$ does, but it is not definite). Selection rules based on the conservation of momenta normally only allow phonons at or near Γ to occur, and the effect of an impurity is to breakdown some of the so-called forbidden transitions. Hence to prevent phonons at Γ to appear, some fairly restrictive selection rules apply. From this it is possible to obtain some information on the luminescent centre and the electronic transition.

The symmetry points of interest are X and L since these

have high enough symmetry for selection rules to be restrictive. Point W, in general, is not expected to give any peaks in the phonon spectrum, but rather discontinuities (c.f. Karo and Hardy on NaCl). Points along Σ however may give rise to several peaks but they have too low a symmetry for any restrictions to occur.

Usual selection rules (see Loudon) state that only those phonons whose transformations, under the site group, that occur in the product $\Gamma_i \times \Gamma_t \times \Gamma_f$ will appear.

Where Γ_i = symmetry of initial electronic state

Γ_f = symmetry of final electronic state

Γ_t = symmetry of appropriate dipole operator

Figure 4.3 gives the representations of the phonons under the space group, and these representations have to be reduced under the operations of the site group of the centre. Loudon gives a table to do some of these. Here the restriction placed on the non-occurrence of phonons at implies that products giving Γ_{25}^+ or Γ_{15}^- (or their reduction on site group of lower symmetry) are not allowed. (N.B. notation used here is based on Loudon's version of G.F. Koster, Solid State Physics 5 173 (1957) where character tables can be found).

If the model of the centre is taken of the oxygen ions symmetrically replacing the fluorine ions around the uranium (see Figure 4.17) the site symmetry is $\bar{4}$ 3 m(Td). The restriction on Γ_{25}^+ and Γ_{15}^- now means the representation P_4 cannot occur. However here $\Gamma_t = P_4$ for magnetic and electric dipole transitions. By building up a multiplication table for $\bar{4}$ 3 m, it is found that the only product satisfying

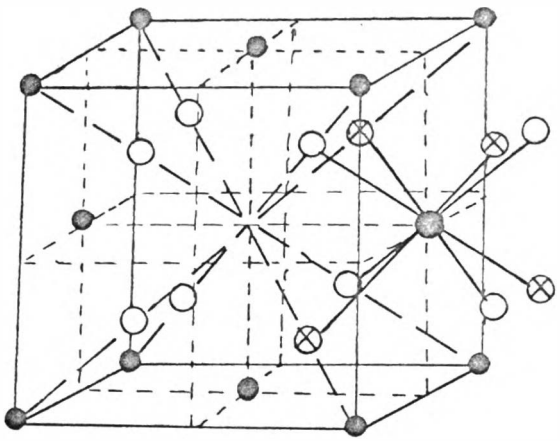

FIG. 4.17 MODEL OF THE SYMMETRICAL CENTRE, $\bar{4}3m$, FOR $CaF_2(U)$.

● Ca^{++} O F^-

● U^{6+} ⊗ O^{--}

the required conditions is $P_2 \times P_4 = P_5$. This means that only phonons with representation P_5 can occur. Also, it requires $\Gamma_i \times \Gamma_f = P_2$ which implies $\Gamma_i = P_1$ and $\Gamma_f = P_2$. Since the transition $P_1 \Rightarrow P_2$ is not normally allowed, the transition must be a forced electric dipole one, due to phonons of symmetry type P_5. Decay time measurements are in accord with this.

The phonons of P_5 type at X and L are:

$$X_4^+ \ , \ X_5^+ \ , \ X_3^- \ , \ X_5^-$$

and $$L_2^+ \ , \ L_3^+ \ , \ L_1^- \ , \ L_3^-$$

Comparing with Figure 4.3 the phonons which occur are

$$X_5^+ (TA) \ , \ X_5^- (TO^a, TO^b)$$

and $$L_3^- (TA, TO^a, TO^b)$$

As can be seen only transverse modes occur (i.e. doubly degenerate ones) and no longitudinal ones.

Another possible centre with high symmetry is one where the calcium replaced by an uranyl ion, with its oxygen atoms taking intersitial positions in the lattice. This gives a site symmetry of 4/m mm (D_{4h}) (same as point X). Here Γ_t is M_1^- and M_5^- for electric dipole transitions and M_4^+ and M_5^+ for magnetic dipole transitions. These are also the symmetry representations which are not allowed to occur. By constructing the multiplication table for 4/m mm it is found that there are no allowed products. This is too restrictive and even phonons at lower symmetry would not be allowed. Even allowing the Raman active phonons to occur, M_4^+ and M_5^+ still does not allow any products. This would suggest that the centre is unlikely if the restriction on phonons at Γ is valid.

Assuming that the restriction at Γ is valid, the symmetrical centre can be taken as the model of the luminescent centre. The phonon frequencies should agree with those from the vibronic spectra. Figure 4.18 lists those for CaF_2(U) with a possible assignment based on values from the dispersion curves (Figure 4.2). Some caution is needed in applying the comparison at this stage as the phonon frequencies are not known sufficiently accurate enough for an unambiguous assignment. As can be seen from Figure 4.2 there are special points along Σ which are quite capable of explaining most of the vibronic spectra. Until more extensive neutron scattering data is available, the assignments are only tentative.

FIGURE 4.18

Vibronic Frequency	Assignment	Other Vibronic Spectra*
147 cm^{-1}	TA (X) = 150 cm^{-1}	
194 "	TO^a (X) = 217 "	Ce^{+++}, Sm^{++}, Eu^{++}, Tm^{++}
266 "	TO^a (L) = 270 "	
297 "	TO^b (L) = 300 "	Ce^{+++}
325 "	TO^b (X) = 327 "	Ce^{+++}
385 "	? LO^a (Σ) = 370-380 cm^{-1}	Ce^{+++}, Eu^{++}, Sm^{++}, Tm^{++}
435 "		Ce^{+++}
609 "		
732 "	Internal mode.	

* From data in M.V. Hobden Phys. Litt. 15 10 (1965)
C.W. Struck and F. Herzfeld, J. Chem. Phys. 44 464 (1966)

The third column in Figure 4.18 lists rare earth ions whose vibronic spectra in CaF_2 give the same frequencies (or ones

very close to them).

Of all the allowed phonons at X and L, only TA(L) = 175 cm^{-1} is not apparent in the vibronic spectra. The fit for $TO^a(X)$ is not good but more accurate data may give a closer fit. This frequency of 190 - 200 cm^{-1} occurs in many other vibronic spectra (see Figure 4.18) and so it must be a feature of the phonon spectrum for calcium fluoride. The agreement for the other assignments is very good, being within a few cm^{-1}.

The peaks at 385 cm^{-1} and 435 cm^{-1} must belong to the calcium fluoride lattice as they occur for rare earth ions also. The assignment for the 385 cm^{-1} is given as likely only as no neutron data exist for the Σ direction. The 435 cm^{-1} line could also come from LO^a but it may be an accidental peak in the phonon spectrum.

Values for longitudinal modes at X and L are not evident in the vibronic spectra (as expected from selection rules) though some values of LA and LO^b are close to those for transverse modes and may not be distinguishable. For LO^a there is no appropriate value (neutron scattering is fairly accurate here).

Other kinks and bumps in the vibronic spectrum may be identifiable when accurate data on the calcium fluoride phonon spectrum is available. A kink at about 100 cm^{-1} in the vibronic spectra may come from a local mode due to the presence of a heavy impurity ion (uranium). For Tm^{++} there appears to be one at 95 cm^{-1}. (B.Z. Malkin Sov. Physics J.E.T.P. 21 1101 (1965). On the mass difference alone, this would put the local mode for uranium at 70 cm^{-1}. However, the presence of oxygen bonds (these would be stronger than uranium-fluorine bonds) would upset the force constants so that the frequency would increase.

Some of the higher vibrational structure may be due to two (or three) phonon processes but it is not expected to be very marked.

Local modes for the luminescent centre are assumed responsible for the 609 cm^{-1} and 732 cm^{-1} (and possibly others) lines. As seen from Figures 4.6 and 4.8, the lattice phonons appear in combination with 732 cm^{-1}. This is most probably due to vibrations of a uranium-oxygen bond (in analogy with the uranyl ion). If the centre is taken as an octahedral UO_4F_4 molecular complex of symmetry 4 3 m its modes of vibration can be found. The irreducible representations of these are $2P_1 + 2P_3 + 4P_4 + 2P_5$. Since there are two P_5 type modes, these can occur in the vibronic spectrum and the values 609 cm^{-1} and 732 cm^{-1} are assigned to them. There does not appear to be vibrational structure associated with the 609 cm^{-1} line as there is for the 732 cm^{-1} line.

On the basis of the assignments for $CaF_2(U)$ the vibronic spectrum of $SrF_2(U)$ can also be assigned. This gives values of the phonons as:-

TA (X) = 125 cm^{-1} $\quad$ TO^a (X) = 198 cm^{-1}

TO^a(L) = 250 cm^{-1} $\quad$ TO^b (L) = 268 cm^{-1}

TO^b(X) = 292 cm^{-1} and internal mode at 702 cm^{-1}

The presence of the no-phonon line at 5330·7Å complicates the spectra so that any further assignment is difficult and would be unreliable.

As has been seen, one model for the luminescent spectra can give rise to selection rules which can explain the spectra fairly well. Variations of these centres could occur by the oxygens taking up other positions around the uranium. There are two other fairly symmetrical centres of symmetry $\bar{3}$m and 4/m m m, and of course several of lower symmetry. Some of these centres may be similar to that

for NaF(U) in that the uranyl ion may fit into lattice positions, with the other oxygens at varying positions. This would give a variety of centres and hence variations in the spectra of which this is not much, apart from the 'extra' no-phonon lines. Selection rules would also break down and the explanation of the vibronic spectra would have to be made in terms of variations in the Aq. Further work, however, is required to test the model for the centre and also the assumed selection rules.

CHAPTER V

TEMPERATURE DEPENDENCE

In Chapter IV a theory for the vibronic spectra was developed. This was quite adequate for explaining the main features of the spectra. However, several features, which are experimentally observable, were not explained. These are mainly temperature dependent effects, the main one being the shift and broadening of the no-phonon lines. (None was predicted previously.) They are examined in this Chapter and no essential modification of the results of Chapter IV are required. The references given there will also be relevant to this chapter.

PERTURBATION TERMS

In the last chapter, the interaction Hamiltonian (equation 4.2) was

$$H_I' = \psi^+\psi \sum_q \left[A_q a_q^+ + A_q^* a_q \right]$$

This corresponded to phonons being either emitted or absorbed during the electronic transition, and it is linear in the a_q and a_q^+. Higher order terms of products of a_q and a_q^+ can be considered next. Terms involving $a_q^+ a_q$ will correspond to the simultaneous emission and absorption of a phonon during an electronic transition and give rise to broadening of the no-phonon line (so called Raman broadening). These terms represent the scattering of a phonon from $\underline{q}$ to $\underline{q}'$ by means of the impurity, thus changing the crystal state from one of zero crystal momenta to one of momentum $-\underline{q} + \underline{q}'$ while at the same time, it is possible to conserve energy.

Equation 4.2 is effectively a generalization of the dynamic lattice strain

$$\epsilon = \sum_q \left(\frac{\bar{h}\ w_q}{2M\bar{v}^2}\right)^{\frac{1}{2}} (a_q - a_q^+)$$

The interaction Hamiltonian H_I can be considered as being expanded as a power series of ϵ hence the next term is taken as

$$H_I'' = \psi^+\psi \sum_{qq'} B_{qq'} (a_q^+ - a_q)(a_{q'}^+ - a_{q'}) \qquad 5.1$$

where $|B_{qq'}| \sim |A_q|^2$

If H_I'' is applied as a first order correction to the transition, it can be shown that there is a temperature dependent width, $\Gamma(T)$ and a shift $\Delta\omega(T)$ of the no-phonon line given by

$$\Delta\omega(T) = \alpha_1 \int_0^\infty \frac{d\bar{w}}{2\pi}\ \rho(\bar{\omega})\ n(\bar{\omega}) \qquad 5.2$$

and

$$\Gamma(T) = \bar{\alpha}_1 \int_0^\infty \frac{d\bar{\omega}}{2\pi}\ \left[\rho(\bar{\omega})\right]^2 n(\bar{\omega})\left[1 + n(\bar{\omega})\right] \qquad 5.3$$

α_1 and $\bar{\alpha}_1$ are appropriate constants.

The effective density of states $\rho(\bar{\omega})$ is identical to that of Chapter IV if $|Bqq| = |A_q|^2$ This correction has little effect on the rest of the spectra and gives the no-phonon line a Lorentz shape.

If the lattice phonon spectrum can be approximated by a Debye spectrum for acoustic phonons, where

$$|A_q|^2 = \frac{\hbar\omega}{2\rho_m V \bar{v}^2}$$

and $$\rho(w) = \frac{\hbar w^3}{2 \rho_m \bar{v}^5} \quad \text{for } o \leq \omega \leq \omega_D$$

$$\frac{\hbar \omega_D}{k} = \Theta_D \text{ an effective Debye temperature}$$

$\bar{v}$ is an average sound velocity for the crystal

ρ_m is the mass density of the crystal lattice

Hence $$\Delta\omega(T) = \alpha \left(\frac{T}{\Theta_D}\right)^4 \int_o^{\frac{\Theta_D}{T}} \frac{x^3 dx}{e^x - 1} \qquad 5.4$$

and $$\Gamma(T) = \bar{\alpha} \left(\frac{T}{\Theta_D}\right)^9 \int_o^{\frac{\Theta_D}{T}} \frac{x^6 e^x}{(e^x - 1)^2} dx \qquad 5.5$$

where $$x = \frac{\hbar\omega}{kT}$$

and α and $\bar{\alpha}$ are proportionality constants.

The integrals occur in specific heat theory and have been evaluated, see "Handbook of Mathematical Functions" Ed. by M. Abramowitz and I.A. Stegun, N.B.S. (1964) and J.M. Ziman, Proc. Roy. Soc. A226, 436 (1954). (Some of the values used in this thesis were obtained from S. Johnson, Standford University, private communication).

Since α and $\bar{\alpha}$ are effectively only scaling parameters, the temperature dependence of the no-phonon line width and shift is to be fitted by one parameter Θ_D. This is now not

necessarily the same as the Debye temperature from specific heats but it is related to the real phonon spectrum (see discussion on Θ_D's in M. Blackman, Handbuch der Physik VII/I 325, (1955)). Θ_D is not necessarily the same for equations 5.4 and 5.5 if the phonon spectrum is not a Debye one.

From experimental data on ruby it has been found that a single value of Θ_D can fit the line widths and shift very well. This would be expected as properties involving a Debye temperature are usually insensitive to the fine structure of the phonon spectrum. The Debye temperature can usually give a good fit to specific heat data even though the Debye temperature shows some temperature dependence (less than 5% variation for calcium fluoride over most of the temperature range). A better fit to the experimental data of line shifts and widths can come from taking $\rho(\omega)$ from the observed vibronic spectra and using it in equations 5.2 and 5.3.

ZERO TEMPERATURE LINE WIDTH

Theory so far predicts a zero width for the line at $T = 0^{\circ}K$. In fact, there is found a residual line width at low temperatures and this is not greatly temperature dependent (some dependence has been reported though no proper investigation made).

This residual line width presumably results from random static strains in the crystal (the phonon interaction comes from dynamic strains). If the strains are "microscopic" and randomly distributed, the line shape at $T = 0^{\circ}K$ should be Gaussian. This is found for many lines. However, deviations from Gaussian are found (e.g. see figure 5.5) and this results probably from macroscopic strains. (There appears to be some experimental evidence for the effect of residual strains (see Chapter III) not only for uranium in calcium fluoride but also for ruby crystals).

Isotope effects can also produce a non-Gaussian broaden-

ing (due to small line shifts) but this should be quite small for uranium.

At any temperature the line shape is a convolution of a Gaussian and a Lorentzian line (known as a Voigt profile). At high temperatures, the Lorentz width predominates and the line appears Lorentzian, and at low temperatures it is Gaussian. Since the Gaussian width is considered constant, it can be readily subtracted out to leave only the temperature dependent Lorentz part (even if Gaussian part is variable, it is still possible to subtract it out). Methods and tables for doing this are given by H.C. Van de Hulst and J.J.M. Reesinck, Astrophys J. 106 121 (1947) and D.W. Posener Aust. J. Phys. 12 184 (1959).

Subtraction out is a bit more difficult if the line shape is not a Voigt profile, so generally the line shape is approximated to one.

Another important experimental factor which can effect the line shape is the effect of reabsorption. This, for luminescence, can be important for powders where many reflections can occur. If the emitting and absorbing centres had exactly the same line shape, the resulting line would be the same. However, the different centres can have different line shapes or more likely different positions due to local static strain effects. The Gaussian shape observed is really only a statistical average over the shifts for a large number of centres. This would complicate the line shape and the uranium luminescence observed will have some reabsorption effects.

ANHARMONIC EFFECTS

While the perturbations H_I' and H_I'' are themselves essential anharmonic effects, there are other ones which can affect the spectra.

The lattice Hamiltonian Hp was taken for a harmonic lattice. However, most lattices are strictly anharmonic, though an-

harmonicities usually cause variations of only a few per cent (for most crystals of interest). Lattice expansion as a function of temperature is one of these effects. Providing the temperature is somewhat less than the Debye temperature, the lattice anharmonic effects can be ignored. Most of the effects on the vibronic spectra can be accounted for by assuming a different $\rho(\omega)$ for each temperature. The vibronic spectra may show some changes such as loss of structure besides the effect of temperature dependence in Chapter IV.

Another anharmonic effect is the change in frequency between the local modes associated with the ground state and the excited state of the impurity ion. Since lattice modes extend over the whole crystal they are not greatly affected by the impurity for low concentrations. Changes in frequency will contribute to a temperature dependent line shift and width. Apart from this, the frequency changes do not upset the general results. The importance of these shifts and widths has not yet been tested as equations 5.2 and 5.3 seem adequate explanations for this. Rebane and Khizhnyakov suggest that under the right conditions, the frequency changes can cause the sharp lines due to local modes or the no-phonon lines to have components, but no direct experimental confirmation of this has been given.

OTHER ELECTRONIC LEVELS

Considerations so far have been given largely on the assumption of a transition between two isolated electronic levels. The presence of other electronic levels can complicate the issue by mixing in with the one associated with the transition.

Radiationless transitions will compete with the emission of light if general mixing of states occurs. This mixing can be due to vibrations and hence it will be temperature dependent (mixing is caused by thermally excited single or multiple phonons). Luminescent lifetimes will become

shorter with increasing temperature (as found) and the intensity will fall off until the luminescence is 'quenched'.

For a group of electronic levels which form a multiplet, with no mixing with other states, many of the essential features remain. No-phonon lines will occur with vibrational structure as before but now it may overlap that of other lines in the multiplet. The phonon interaction H_I will now be represented by a matrix which can couple levels of the multiplet. Line broadening can also be caused now by the absorption or emission of a phonon changing the system to another electronic level in the multiplet (which will be typically separated by energies in the phonon spectrum).

Other energy levels can have effect on the higher perturbation terms. If H_I is taken in second order perturbation for line widths and shifts, the factor $E_b - E_i$ enters into the denominator (E_b is energy level from which the transition occurs, and E_i is any other level). Usually $E_b - E_i$ is large and the effect on the spectra is small. Here terms due to H_I'' dominate. However, if $E_b - E_i$ is small, these perturbations will become important.

EXPERIMENTAL LINE SHIFTS

Figures 5.1 and 5.2 give the measured shifts of the no-phonon lines as a function of temperature, compared with the theoretical values. Figure 5.1 gives the shifts for the CaF_2 (U .01%) sample using the two no-phonon lines indicated (see Figures 4.7 - 4.12 for general spectra). Similarly Figure 5.2 gives those for SrF_2 (U Xtal) (see Figures 4.13 - 4.16). No error range is indicated but it is expected to be of the order of 1 cm^{-1} (see Chapter II), though with the care taken in the measurements, it could be smaller. This puts the low temperature values (of the order of 0.1 cm^{-1}) very much in doubt, so any fit with

Figure 5.1

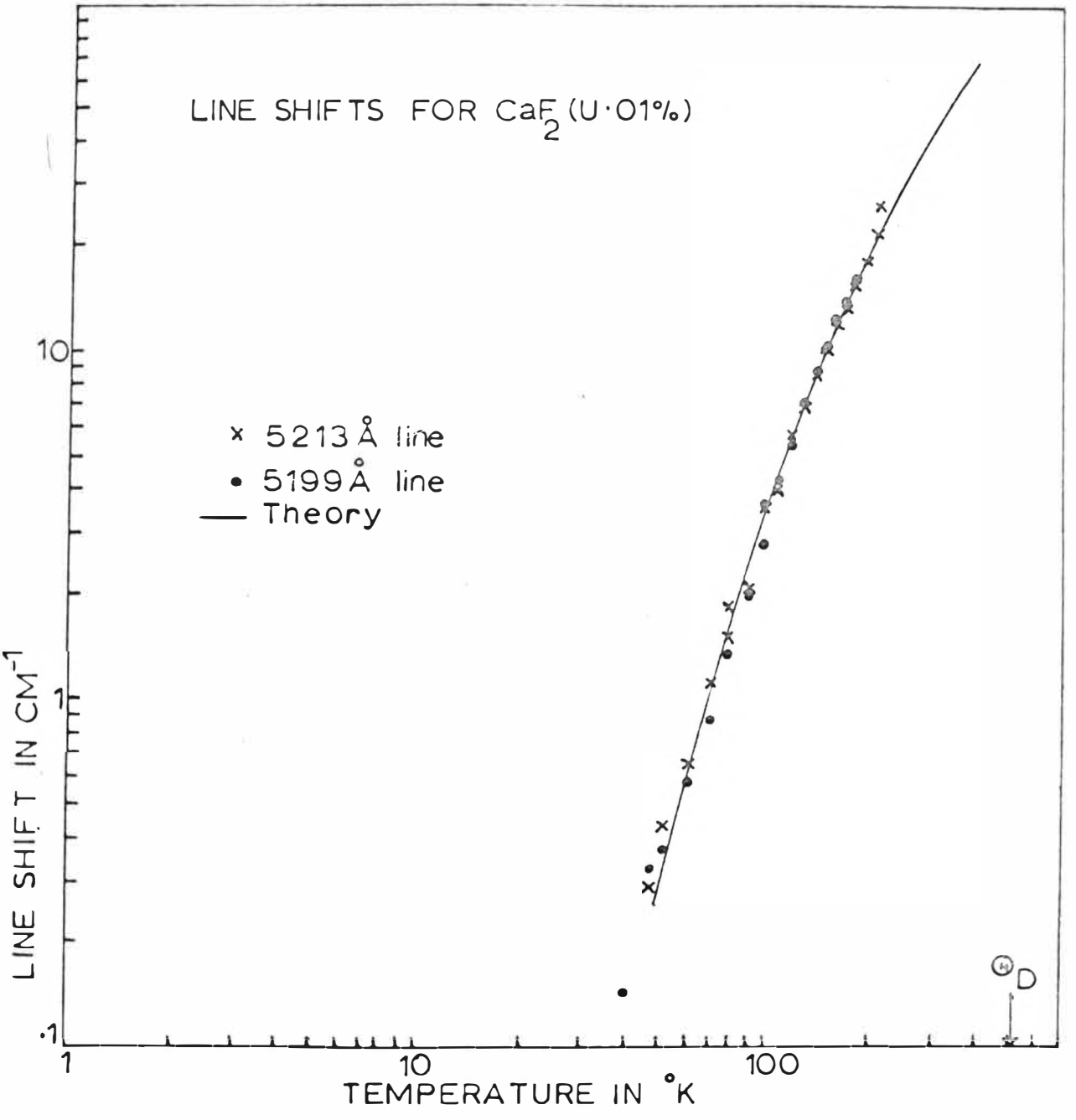
LINE SHIFTS FOR CaF_2 (U·01%)
× 5213 Å line
• 5199 Å line
— Theory
LINE SHIFT IN CM^{-1}
10
1
·1
1
10
100
TEMPERATURE IN °K
Θ_D

Figure 5.2

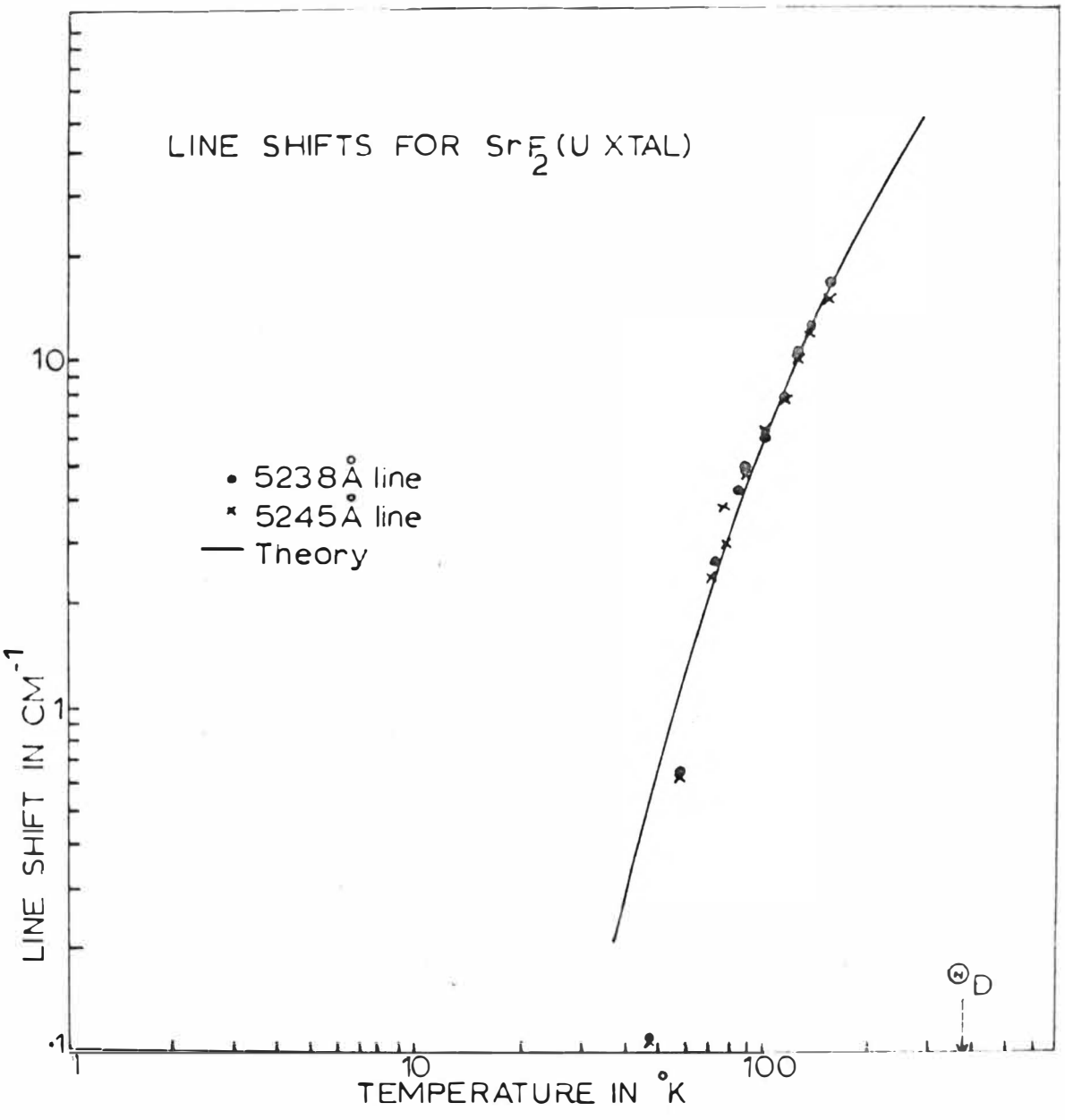
LINE SHIFTS FOR SrF_2 (U XTAL)
• 5238Å line
× 5245Å line
— Theory
LINE SHIFT IN CM^{-1}
10
1
.1
1
10
100
TEMPERATURE IN °K
D

theory in this region may be accidental. As can be seen the two no-phonon lines for each sample have almost identical temperature shifts (any differences are in the range of measurement error).

The theoretical curves are drawn using equation 5.4. Known values of Θ_D were used and α chosen to fit with experiment. Values used are:

for CaF_2 (U ·01%) $\alpha = -430\ cm^{-1}$

and for SrF_2 (U Xtal) $\alpha = -310\ cm^{-1}$

(accuracy about ± 10%)

A $\Theta_D = 510^oK$ (at 0^oK) for calcium fluoride was taken on the basis of D.R. Huffman and M.H. Norwood, Phys. Rev. 117 709 (1960). They showed values of Θ_D from both specific heat data and elastic constants agreed within experimental error. For strontium fluoride a value of $\Theta_D = 380^oK$ (at 0^oK) was determined from elastic constant data by D. Gerlich, Phys. Rev. 136 A1366 (1964). (No specific heat data appear to exist). If strontium fluoride is similar to calcium fluoride, this value should be close to the specific heat value.

A possibly better fit for the data in Figures 5.2 and 5.3 may come from a lower value for Θ_D. For calcium fluoride where Θ_D is known as a function of temperature, it is more like 490^oK over the temperature range of interest. For ruby, $MgO(Cr^{3+})$ and $MgO(V^{2+})$ values of Θ_D substantially lower than that from specific heat data were necessary. Specific heat data depends on all phonon modes while for the shift (and also width) it may be that only some of the modes are effective. For H^- ions in calcium fluoride which has a vibrational structure (Elliot et al. Proc. Roy. Soc. A289 1 (1965)) a $\Theta_D = 425^oK$ is required to fit the line shift data (S.S. Mitra and R.S. Singh, Phys. Rev. Litt. 16 694 (1966)

and this value also gives a reasonable fit to the data in Figure 5.1.

For the 5330.8Å no-phonon line in SrF_2(U) the temperature shift was opposite (e.g. α is positive) to that for the other two no-phonon lines in Figure 5.2. As the intensity of this line dropped very rapidly with temperature only a few measurements of the shift could be made. The maximum overall shift measured relative to the other two lines was 1 cm^{-1} (up to 80°K). While this is inside the errors in measurement, the difference is thought to be real, since all the shifts measured were positive while all those for the other lines were negative. The width of the line is within experimental error the same as for the other two no-phonon lines. These facts suggest that the 5330.8Å line arises from another electronic level. If the transition belongs to the same centre, some account of it should be made in the perturbation calculation (see above, this would effect the width more, as the effect on the shift is to give a similar temperature dependent shift).

EXPERIMENTAL LINE WIDTHS

While the width of a line can be measured more accurately than its position, there can be however considerable error in finding the half-height (at which the width is measured). Nearby lines overlap the no-phonon lines (these are often weak no-phonon lines) and at higher temperatures, the two phonons lines are broad enough to overlap each other. There is also a general background which increases with temperature. In the measurements taken, an estimation was made of these effects in determining the half-height. Figures 5.3 and 5.4 give the width of the lines for CaF_2(U•01%) and SrF_2 (U Xtal) at half-height as a function of temperature. Because of the overlapping lines, it was not possible to extend the results to higher temperatures. As can be seen, the two no-phonon lines have the same widths within the experimental accuracy.

Figure 5.3

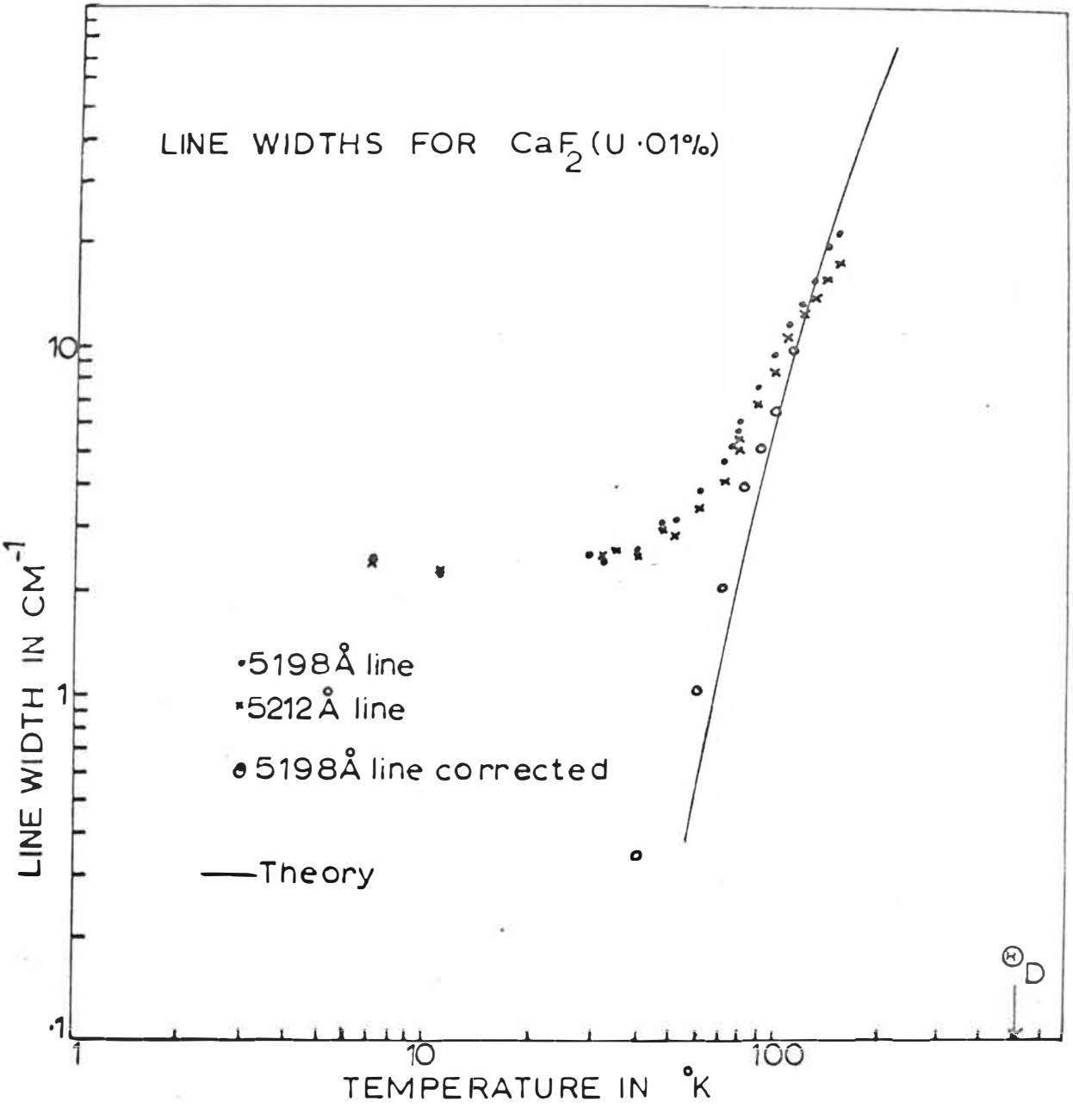
LINE WIDTHS FOR CaF_2 (U ·01%)
10
1
·1
LINE WIDTH IN CM^{-1}
·5198Å line
·5212Å line
o 5198Å line corrected
——Theory
Θ_D
1
10
100
TEMPERATURE IN °K

Figure 5.4

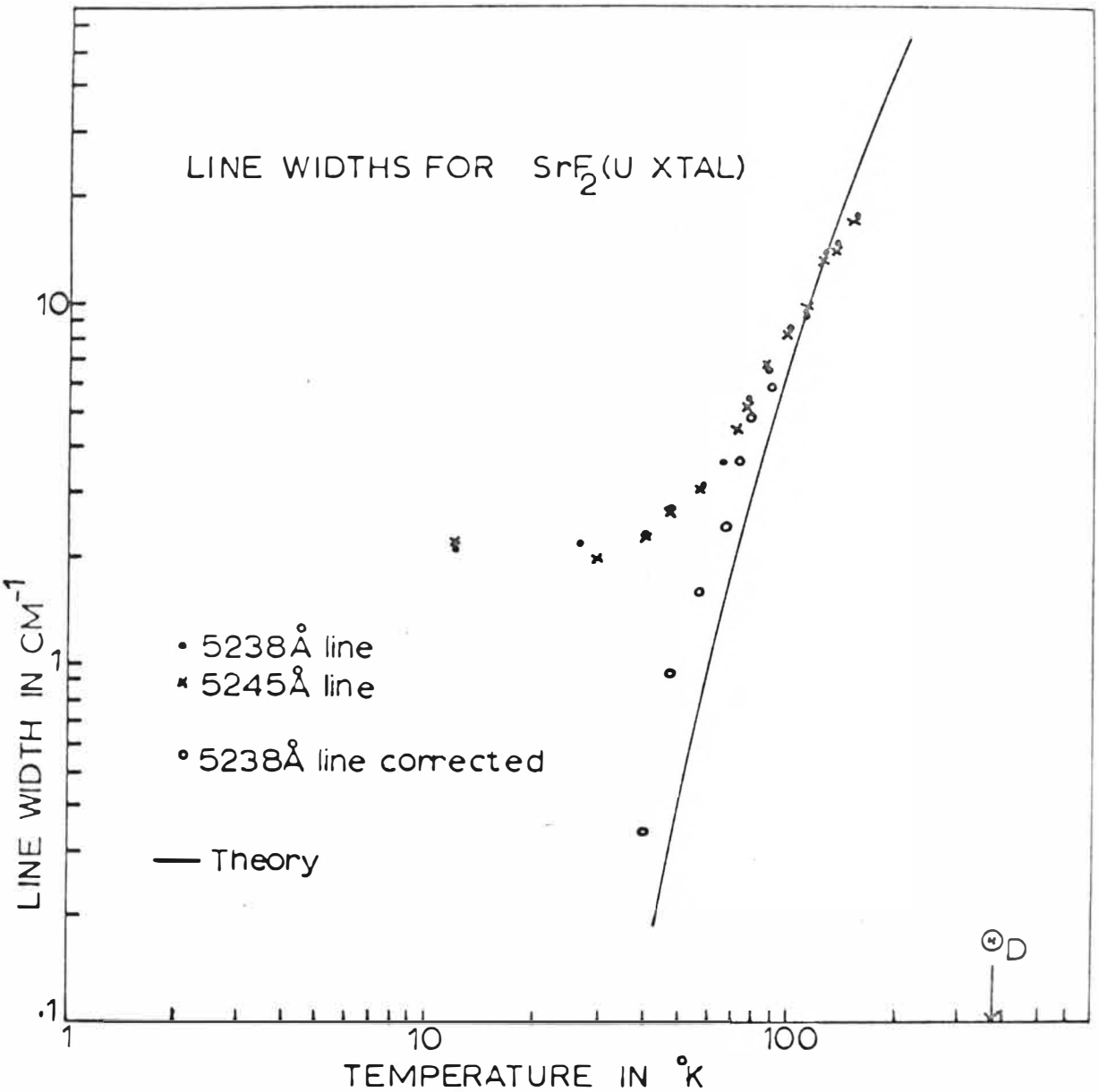
LINE WIDTHS FOR SrF_2 (U XTAL)
10
1
.1
LINE WIDTH IN CM^{-1}
• 5238Å line
× 5245Å line
° 5238Å line corrected
— Theory
Θ_D
1
10
100
TEMPERATURE IN °K

The corrected points for the 5198Å and 5238Å lines were calculated assuming a zero temperature line width due to static strain broadening of 2.4 cm^{-1} and 2.1 cm^{-1} respectively. Values for the other no-phonon lines will follow the same general trends as they have almost the same line widths. A Gaussian shape was assumed for the strain broadening, and the line shape was assumed to be a Voigt profile. Using tables, the Lorentz part was found and the value for this is plotted as the corrected points. At higher temperature the line shape is almost Lorentzian (to at least 90%) and no correction was made.

In practice the line shape, especially for the lower temperatures, often did not fit to a Voigt profile. For SrF_2(U), the low temperature line shape approximated fairly well to a Gaussian line, except for the wings which were more like a Lorentz line. CaF_2(U) however, gave an almost Lorentz shape at low temperatures (see Figure 5.5) and this does not have a Gaussian part.

Even though experimentally it appears invalid, the Gaussian width was removed as this is what would be expected from theory. This enables a comparison to be made with the theoretical curve which does not allow for a zero temperature line width. The curve is drawn from equation 5.5 with the same Θ_D as above.

The values of $\bar{\alpha}$ used

for CaF_2 (U .01%) $\bar{\alpha}$ = 2760 cm^{-1}

and for SrF_2 (U Xtal) $\bar{\alpha}$ = 1070 cm^{-1}

The fit with theory is within the possible experimental error, considering the approximations used for the corrected points and in determining the higher temperature half widths. However, both SrF_2(U) and CaF_2(U) show the same systematic tendencies which may suggest that the fit is not very good. By varying Θ_D and $\bar{\alpha}$ it is possible to obtain a better fit

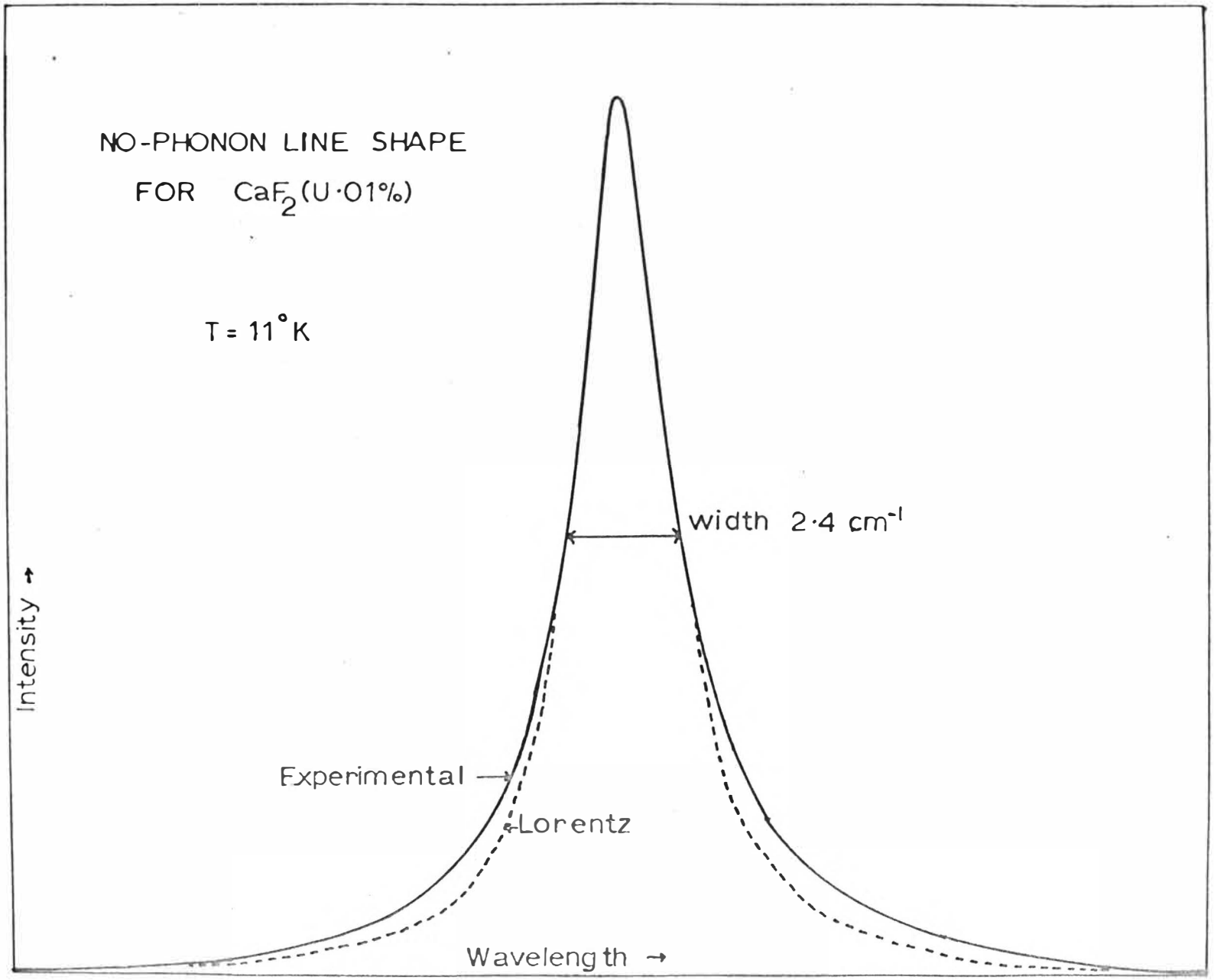
NO-PHONON LINE SHAPE
FOR CaF_2(U·01%)
T = 11°K
width 2·4 cm⁻¹
Intensity →
Experimental
Lorentz
Wavelength →

Figure 5.5

for a value of Θ_D of approximately half the normal one.

A different value of Θ_D is permissible for equations 5.4 and 5.5 since these are considered approximations to equations 5.2 and 5.3 respectively. Widths, as has been mentioned, are more sensitive to another electronic level and this may cause the difference (assuming $CaF_2(U)$ has a second electronic level similar to $SrF_2(U)$. Another possible explanation is that not all modes contribute to the Raman broadening. If only the transverse acoustic branch contributed its cut off frequency would correspond to the Debye temperature. The value for this is 175 cm^{-1} which corresponds to $\Theta_D = 250^oK$ (i.e. approximately half the normal value). This idea would require all modes to contribute to the line shift (since it has a normal Θ_D) but only one for the width.

However, any explanation based on equation 5.3 for the line width must remain tentative, as the line shapes observed are not those expected. If crystals can be grown with a smaller residual line width, they may give a better fit to the theory as the present residual width appears to be too large. For ruby it is possible to obtain a residual width of about 0.1 cm^{-1} (c.f. 2 cm^{-1} here). This suggests that there are other broadening processes applying here, such as due to macroscopic static strain. Hence any definite conclusions must be made on better crystals.

ANTI-STOKES LINES

These are down in intensity by a factor $n_q/1 + n_q$ to the lines on the low energy side (Stokes' lines) of the no-phonon line. At high temperatures when $n_q/1+n_q$ becomes appreciable, the vibrational structure becomes lost (e.g. see Figure 4.11) and it is difficult to see if the Stokes' and Anti-Stokes' bands have the same structure.

To compare these, low temperatures are required, but also that means very low intensity. Prolonged exposure at 77°K, using plates, managed to show the Anti-Stokes' lines (for a region of about 250 cm^{-1}) and these proved to be an exact mirror image of the Stokes' lines.

SPECTRAL MOMENTS

The total intensity of the luminescence was monitored by a separate photomultiplier (1P21) during the spectral run and this is essentially a measurement of the zero order moment μ_0. This was found to vary very little for CaF_2(U) until about 150°K when it slowly fell off. As the spectra then is also starting to broaden out rapidly with temperature, the intensity change will be due (at least in part) to the photomultiplier's spectral response. It is not so sensitive to red (see Figure 2.1) and this is the end of the spectra which has considerable enhancement at higher temperatures. Hence it can be said that μ_0 is approximately independent of temperature. At high temperatures, fall off can be expected due to non-radiative transitions.

Other spectral moments were not taken since the re-absorption process will enhance the vibronic lines at the expense of the no-phonon line. This would upset the moments since they depend more on the shape of the spectra.

CHAPTER VI

SUMMARY AND CONCLUSION

This thesis has been mainly concerned with the luminescent system of powder samples of uranium in calcium fluoride (and partly on that in strontium fluoride). The only features known previously of the luminescence were:-

1. Oxygen was required before the green luminescence would occur. This was assumed used for charge compensation and a symmetrical centre was postulated.
2. Wavelengths of some of the luminescent lines had been measured.
3. The decay time of the luminescence was known.

In this thesis these further facts on the luminescent system are established:-

1. The presence of an absorption spectra. Several lines have been found and ascribed to the luminescent centre. In particular, a resonance line was found which appears to show vibrational structure similar to the luminescent spectra.
2. A second luminescent centre has been shown to exist and is favoured in higher concentration samples. No model was however proposed for this.
3. It has been possible to give some assignment to the luminescent lines. These have been interpreted as a no-phonon line with its accompanying vibrational structure. Bands in the vibrational structure have been assigned to lattice vibrations. Combination bands with an internal mode (similar to the uranyl luminescence) have been shown to exist.

4. Selection rules have been considered in testing a model of the centre. This favoured the earlier proposed centre though it is not conclusive. Some symmetry assignment for the electronic levels was also possible.

5. Temperature dependent effects have been investigated. The line shifts and widths follow the temperature dependence for a no-phonon line. It was shown that the normal Debye temperature could give an adequate explanation for the line shifts. Line widths did not give such an agreement, as lines were not the shape expected (may be due to sample preparation).

Besides the luminescence of uranium in calcium fluoride, the following were also reported:-

1. A detailed luminescent spectra of uranium in strontium fluoride is given. This was found to be similar to that for uranium in calcium fluoride except for a second electronic transition which did not seem to have a counterpart in $CaF_2(U)$.

2. Luminescence of O_2^- ions in calcium fluoride was considered to occur to explain some additional luminescent spectra observed.

Extension of the investigations is required before an adequate explanation for the luminescent system of uranium in calcium fluoride (or strontium and barium fluoride) is known. The main obstacle is in the preparation of samples. This thesis has been concerned largely with powder samples to obtain preliminary useful information on the luminescence. If suitable, clear, strain free crystal samples can be made, an extension of the work would be worthwhile.

Crystals would enable polarization and stress spectra to be obtained and this should enable the nature of the centre to be determined (as has been done for LiF(U) and NaF(U)). From this, it will be then possible to determine the electronic nature of centre (using that of the uranyl ion, if known, as a guide).

A more detailed investigation of the vibrational interaction can then be made. Comparison with other impurity ions in calcium fluoride should also be made to explain the differences in the vibronic spectra. This would require accurate information of the phonon spectrum of calcium fluoride. Spectra in strontium and barium fluorides can then be compared and possibly information obtained on their phonon spectra.